

Diogo Miguel José Carregosa

BsC Biochemistry

**Design, synthesis and biological evaluation of new
derivatives of phenolic metabolites**

Dissertation for obtaining a Master Degree in
Biochemistry for Health

Supervisor: Rita Ventura, Ph.D, ITQB-NOVA
Co-supervisor: Cláudia Nunes dos Santos, Ph.D, iBET/ ITQB-NOVA

September 2018

Diogo Miguel José Carregosa
BsC Biochemistry

Design, synthesis and biological evaluation of new derivatives of phenolic metabolites

Dissertation for obtaining a Master Degree in
Biochemistry for Health

Supervisor: Rita Ventura, Ph.D, ITQB-NOVA
Co-supervisor: Claudia Nunes dos Santos, Ph.D, iBET/ ITQB-NOVA

Jury:

President: Doctor Pedro Matias
Examiner: Doctor Ana Petronilho
Vogal: Doctor Margarida Archer

**Instituto de Tecnologia Química e Biológica- António Xavier –
Universidade Nova de Lisboa**

September 2018

Copyright

Este documento, intitulado *Design, synthesis and biological evaluation of new derivatives of phenolic metabolites*, foi escrito por Diogo Miguel José Carregosa e todos os direitos de cópia, *copyright*, encontra-se de acordo com os termos propostos por ITQB-NOVA. O Instituto de Tecnologia Química e Biológica António Xavier e a Universidade Nova de Lisboa têm o direito, perpétuo e sem limites geográficos, de arquivar e publicar esta dissertação através de exemplares impressos reproduzidos em papel ou de forma digital, ou por qualquer outro meio conhecido ou que venha a ser inventado, e de a divulgar através de repositórios científicos e de admitir a sua cópia e distribuição com objetivos educacionais ou de investigação, não comerciais, desde que seja dado crédito ao autor e editor.

Acknowledgment

Para começar gostaria de agradecer às entidades que tornaram este projeto possível nomeadamente a Universidade Nova de Lisboa, mais concretamente o Instituto de Tecnologia Química e Biológica (ITQB-NOVA) e ao Instituto de Biologia Experimental e Tecnológica (iBET). De seguida gostaria de agradecer à minha orientadora Rita Ventura e à minha co-orientadora Cláudia Santos, por me terem aceite para este projeto e me terem recebido de braços abertos e por terem participado nas minhas ideias malucas. Obrigado por me terem dado tanto espaço para crescer, por me terem ensinado tanto, pela oportunidade de apresentar este trabalho numa convenção e num workshop e pela confiança que depositaram em mim.

Gostaria de agradecer as todas as pessoas do laboratório da minha orientadora (*Bioorganic Chemistry lab.*) e também do grupo do professor Christopher Maycock com o qual partilhamos o espaço, mas muito mais do que isso. Assim gostaria de deixar um agradecimento especial a: Miguel Bernardo, Márcia (chão) Rénio, João (o liberal) Cascão, Bárbara Rebelo, ao próprio professor Christopher Maycock, à Eva Lourenço, Osvaldo Ascenso e Saúl Silva. Obrigado por terem tornados todos os dias diferentes e felizes. Gostaria ainda de deixar grande, grande Obrigado à Vanessa Miranda, por ter sido a colega de bancada que precisava e uma pessoa espetacular que me recebeu e me ensinou muito desde o primeiro dia, dentro e fora daquilo que é o trabalho de laboratório. Gostaria ainda de deixar uma menção à Filipa Almeida, com quem eu estive pouco tempo, mas que me incentivou a escolher este projecto.

Gostaria de agradecer as todas as pessoas que estão e que passaram pelo laboratório da minha co-orientadora (*Molecular Nutrition and Health Lab.*), e dos quais nunca irei esquecer, assim sendo, um abraço enorme à Ana Tavanéz, Carolina "Das Moscas", Carolina Palma Santos, Melanie Matos, Regina Menezes, Rita Ramos, Rafael Carecho. Um carinho especial às pessoas que estão comigo desde o primeiro dia, que são uns amores de pessoa e que ainda assim reuniram forças para me aturar todos os dias, um agradecimento especial à M. Inês Bento e à Andreia Gomes, que tenho a dizer, se fores tão boa mãe como foste pessoa para mim, vais ter o(a) filho(a) mais feliz do mundo. Queria ainda mencionar de forma especial o nome Ana Filipa Raimundo com quem passei pouco tempo mas "é como se tivéssemos ido à escola juntos". Gostaria ainda de deixar um carinho enorme pela Inês Figueira, com o qual o tempo que tive foi o suficiente para deixar muitas saudades, apesar de que sei, ainda nos iremos encontrar muitas vezes: obrigado pela tua energia, boa disposição, por partilhares os teus conhecimentos de uma forma tão inspiradora e claro pelo trabalho nas HBMEC. Joana Pereira, apesar do curto espaço de tempo que tivemos juntos, gostaria de te agradecer tal como agradeci à Filipa Almeida, por me ajudares a escolher este projeto, e obrigado por me mostrares as LUHMES.

Aos meus colegas desde o primeiro mês da faculdade, que permanecem até hoje, e que são a grande ancora para me manter afastado do trabalho quando preciso, dos *brainstorms* aos churrascos, obrigado por estarem lá todos os dias: Miguel Bernardo, Ricardo Barras, Catarina Barbosa, Sérgio Torres, Cláudia Freitas, Ruben Guerreiro.

Agradeço à minha família me viu trabalhar todos os dias que conseguia, que me viu menos do que gostava mas que mesmo assim me apoiou e sempre me ofereceu tudo o que precisei, quando precisei.

Catarina Pereira Loureiro, obrigado pelo apoio, pelos conselhos, pelos dias que cheguei tarde e lá estavas há minha espera, por manteres a minha sanidade mental, obrigado por Tudo

A quem eu me possa ter esquecido, foi um ano longo, mas se estás a ler isto é porque te preocupas e mereces um Obrigado!

Abstract

Multiple (poly)phenolic compounds, related with the consumption of dietary products have been described to modulate microglial cells, influencing the inflammatory response in the brain and microglia-mediated neuronal apoptosis. However, low amounts of information is available about small compounds, present in human blood circulation after the metabolization of (poly)phenols. Previously we have shown some of these small metabolites, capable of crossing the blood brain barrier at physiological concentrations, and be neuroprotective.

To improve the effect observed by these small compounds in reducing neuroinflammatory markers in microglia cells, we have synthesized a library of compounds to understand and elucidate, the chemical structural features leading to the decrease of these inflammatory markers. To achieve this goal while keeping the focus on physiologically relevant metabolites, sulfate and glucuronic acid conjugates, the most common type of human phase II metabolites present in circulation, were chemically synthesized. The impact of the synthesized compounds on reducing neuroinflammation was evaluated by microglia release of one of the major hallmarks of inflammation: Tumor necrosis factor alpha ($TNF\alpha$), in a model of microglia cells stimulated with bacterial lipopolysaccharides.

Addressing a pharmacological approach, the synthesis and biological evaluation of the compounds was made through a cycle, meaning that, following the synthesis and biological evaluation of the first group of compounds, a second group, based upon the structure of compounds with highest bioactive potential would be synthesized and tested.

Our results demonstrated that two compounds were able to considerably reduce neuroinflammation at physiologically relevant concentrations. Furthermore, while evaluating multiple compounds with small structural differences we have unveiled a core structure necessary for the activity of the compounds. Moreover, these two compounds were tested for their ability to cross an *in vitro* model of human brain permeation, recreating the blood brain barrier.

A selection of compounds was also evaluated in differentiated SH-SY5Y neuronal cells exposed to a oxidative insult. Results showed three compounds and their corresponding sulfate metabolites having a significant increase in cell viability. Finally, all compounds were evaluated by a *in silico* model of permeation in order to evaluate their ability to cross the BBB.

Together, our results elucidate the effects of small dietary metabolites and derivatives in mitigating neuroinflammation, deciphering their role in the prevention of neurodegenerative diseases such as Alzheimer's and Parkinson's disease.

Keywords: Neuroinflammation; Neuroprotection; (Poly)phenols; Chemical derivatives; Blood Brain Barrier

Resumo

Múltiplos compostos (poli)fenólicos, relacionados com o consumo de produtos alimentares encontram-se descritos pela sua capacidade de modular microglia, influenciando a resposta inflamatória e a morte neuronal intermediada pela microglia. Contudo, pouca informação se encontra disponível sobre pequenos compostos, presentes em na corrente sanguínea em humanos, após a metabolização de (poli)fenóis. Anteriormente, mostrámos que alguns destes pequenos metabolitos são capazes de atravessar a barreira hematoencefálica a concentrações fisiológicas e são neuroprotectores.

De modo a melhorar os efeitos observados nestes pequenos compostos, em reduzir a marcadores de neuroinflamação em células de microglia, sintetizámos uma biblioteca de compostos, com a esperança de entender e elucidar a estrutura química relacionada com a diminuição destes marcadores inflamatórios. De modo a atingir este objetivo, e mantendo um foco nos metabolitos de relevância fisiológica, conjugados de sulfatos e ácido glicurónico, os derivados mais comuns da metabolização de fase II em humanos, foram quimicamente sintetizados. O impacto dos compostos sintetizados em reduzir a inflamação foi avaliado através da libertação de um dos maiores marcadores de inflamação em células de microglia: o fator de necrose tumoral alfa, num modelo de microglia estimulada com lipopolissacarídeos provenientes de bactéria.

O nosso trabalho focou-se numa abordagem farmacológica onde a síntese e avaliação biológica dos compostos foi realizada através de um ciclo, ou seja, após a síntese e avaliação biológica dos primeiro grupo de derivados, um segundo grupo, ou iteração, de compostos foi sintetizado, com base nos resultados do primeiro grupo e avaliado.

Os nossos resultados demonstraram que dois compostos são capazes de reduzir consideravelmente a inflamação a concentrações fisiologicamente relevantes. Além do mais, ao avaliar a biblioteca de compostos com pequenas variações estruturais, nós desvendámos um possível núcleo estrutural, necessário para a atividade dos compostos. Estes compostos foram ainda avaliados quanto à capacidade de atravessar a barreira hematoencefálica num modelo *in vitro* de permeabilidade em células da barreira hematoencefálica humana.

Um conjunto de compostos foi avaliado em neurónios SH-SY5Y diferenciados e expostos a um insulto oxidativo, resultando na descoberta de três compostos, e os correspondentes sulfatos, capazes de aumentar significativamente a viabilidade celular. Finalmente, todos os compostos foram avaliados por um modelo *in silico* de permeabilidade, de modo a avaliar a sua capacidade de atravessar a barreira hematoencefálica de forma passiva.

De um modo geral, os nossos resultados elucidam os efeitos de pequenos compostos fenólicos e derivados metabólicos em mitigar a neuroinflamação, decifrando assim o seu papel na prevenção de doenças neurodegenerativas tais como a doença de Alzheimer e Parkinson

Palavras Chave: Neuroinflamação; Neuroproteção; (Poli)fenóis; Derivados químicos, Barreira Hematoencefálica

Contents

Abreviatures	xxi
Objectives	xxiii
1 State of the art	1
1.1 Microglial cells: The brain (over)protector	1
1.1.1 Microglia, the immune innate cells of the central nervous system	1
1.1.2 Cell markers and inflammatory pathways	2
1.1.2.1 Nuclear factor kappa B (NF- κ B)	2
1.1.2.2 Mitogen-activated protein kinases pathway (MAPK)	3
1.1.2.3 Nuclear factor of activated T cells (NFAT)	3
1.1.2.4 Cytokine and chemokines: A focus on TNF- α	4
1.1.3 Microglia and Neurodegenerative diseases	5
1.1.3.1 Microglia-TNF α relationship	5
1.1.3.2 Microglia (dys)function and aging	5
1.2 (Poly)Phenols impact on Neuroinflammation	7
1.2.1 (Poly)phenols are grouped in different families	7
1.2.2 Natural compounds and neuroinflammation	8
1.2.2.1 The interest on natural compounds	8
1.2.3 (Poly)phenol metabolism and the role of microbiota	8
1.2.4 Compound ability to cross the BBB	9
1.2.4.1 Gut-Brain axis	9
1.2.5 Mechanism of action of (poly)phenolic metabolites	10
1.3 Neuroprotection	12
2 Materials and Methods	13
2.1 Chemical Synthesis	13
2.1.1 Synthesis of First Iteration Compounds	15
2.1.2 Synthesis of Second Iteration Compounds	21
2.2 Biological Evaluation	23
2.2.1 Cell culture	23
2.2.2 Anti-inflammatory potential of synthesized compounds	23
2.2.3 Membrane permeation	24
2.2.4 Neuroprotective effects in SH-SY5Y	25
2.3 Statistical analysis	25
3 Results	27
3.1 Synthesis of chemical derivatives- First Iteration derivatives	27
3.1.1 Synthesis of catechol and pyrogallol (metabolic) derivatives	27
3.2 Biological evaluation of the synthesized compounds	31
3.2.1 Pyrogallol-2-sulfate, the isomer present in higher concentration in blood stream, showed increased protection over pyrogallol-1-sulfate	31
3.2.2 Two derivatives showed promising results in the modulation of TNF α release	32
3.3 Synthesis of chemical derivatives- Second Iteration derivatives	34
3.3.1 Synthesis of 4-methylpyrogallol and phloroglucinol sulfate derivatives	34
3.4 Biological evaluation- Second Iteration derivatives	34
3.4.1 Resorcinol-sulfate a second iteration derivative elucidates a possible main core structure	34
3.4.2 Incubation of cells with different concentrations indicates the results are dose dependent	37

3.5	Blood Brain Barrier permeability	39
3.5.1	<i>In silico</i> membrane permeability model shows the ability of compounds to cross various membrane including the BBB	39
3.5.2	HBMEC permeation results	39
3.6	Compounds with ability to protect neurons from oxidative insult	42
4	Discussion	45
4.1	First Iteration Compounds	45
4.1.1	Synthesis of First Iteration Compounds	45
4.1.2	Choosing pyrogallol-2-sulfate as the compound of reference	46
4.1.3	Two compounds from the initial library of compounds revealed an increase protection over pyrogallol-O-2-sulfate	47
4.2	Second Iteration Compounds	47
4.2.1	Synthesis of Second Iteration Compounds	47
4.2.2	Biological evaluation of second iteration compounds	48
4.2.3	The activity of the compounds appear to be dose-dependent	49
4.2.4	Compound mechanism of action could be related with GPR35	49
4.2.4.1	G-protein coupled receptor 35	49
4.2.5	Compound transport across the BBB	52
4.2.5.1	<i>In Silico</i> assay	52
4.2.5.2	HBMEC evaluation of permeation	52
4.2.6	Compounds ability to protect SH-SY5Y	53
5	Conclusions	55
	References	57
A	Annex A - Glossary of compounds	67
B	Annex B- Toxicity effect of second iteration compounds in microglia cells	73
C	Annex C - Determination of t-BHP LD50 in SH-SY5Y	75
D	Annex D - Evaluation of compounds in SH-SY5Y	77
E	Annex E - Evaluation of Neuronal Differentiation	79

List of Figures

1.1	Microglia role, function and behavior are dependent on differential gene expression that correlate to various phenotypes rather than the classical M1/M2 phenotypes. Arrows reaching from surveillance microglia represent up-regulated genes that lead to the corresponding phenotype. Arrows leading out of each phenotype represent the up-regulation of cytokines, chemokines and receptors due to the specific phenotype. Adapted from <i>Nature Reviews Neurology</i> ¹⁰	1
1.2	NF- κ B canonical and non-canonical activation pathway. Canonical activation of NF- κ B is dependent on TNF α , IL-1 or TLR activation and culminates in the activation of RelA/p50. Non-canonical activation of this pathway is dependent on CD40L receptor activation, involves NIK and activates RelB/P52 transcription. Adapted from Lawrence et. al. ¹⁶	3
1.3	Simplified representation of the MAPK pathway. Activation begins in the cell membrane through TNF α , LPS or TGF β . The signaling cascade culminates in the activation of MKKs and consequent P38, ERK and JNK kinase activation. These kinases lead to the formation of the C-fos-jun dimer (AP-1) that migrates to the nucleus and acts as a transcription factor. Adapted from Murshid et al. ²²	4
1.4	Main classes of (Poly)phenols with representative structures. Examples are given in italic, and food sources are shown below. ^{75,74}	7
1.5	Small benzoic and phenolic compounds shown in circulation are dependent of human and microbiota metabolism. A , Pyrogallol and catechol are formed from the unspecific hydrolysis of the ester bound in (-)-epicatechin-3-O-gallate. B , Microbiota conversion of cyanidins into small phenolic compounds present in blood, urine and feces. C , Different metabolites are formed in different areas of the gastrointestinal track. Adapted from Del Rio et al. 2013 ^{74,101}	10
2.1	Structures of compounds used for the synthesis of conjugate derivatives.	13
2.2	Synthesis of 4-methylpyrogallol (7) from 2,3,4-trihydroxybenzaldehyde (14)	15
2.3	Synthesis of 4-(hydroxymethyl)catechol (5) from protocatechuic acid (16)	15
2.4	General scheme for the synthesis of sulfate derivatives.	15
2.5	Structures of sulfate derivatives (obtained as sodium salts)	16
2.6	Synthesis of benzyl syringate (10b) from syringic acid (10)	17
2.7	Specific anomeric carbon deacetylation of the methyl glucuronate resulting in the correspondent 2,3,4-tri-O-acetyl-D-glucuronate methyl ester (18)	18
2.8	Synthesis of 2,3,4-tri-O-acetyl-1-O-trichloroacetimidoyl- α -D-glucuronate (19)	18
2.9	Glycosylation reaction - Synthesis of glucuronide derivatives using BF ₃ .OEt ₂	19
2.10	Glycosylation reaction - Synthesis of glucuronide derivatives using TMSOTf	19
2.11	Synthesis of the deacetylated glucuronides	19
2.12	Synthesis of the glucuronide	19
2.13	Structure of glucuronide derivatives	20
2.14	Synthesis of methoxyphloroglucinol (11) from phloroglucinol (3)	21
2.15	Synthesis 4-(hydroxymethyl)pyrogallol (13) from 2,3,4-trihydroxybenzaldehyde (14)	21
2.16	Synthesis of 2,3,4-trihydroxybenzoic acid (15) from 2,3,4-trihydroxybenzaldehyde (14)	22
2.17	Structure of compounds used the synthesis of second iteration sulfate conjugates	22
3.1	Chemical structures of the synthesized compounds. The ratios present in case of a mixture of isomers is shown in the figure. Further information is included in tables 3.1 and 3.2	28

3.2	Evaluation of the effects of (un)sulfated compounds in the release of TNF α by microglia cells. A Chemical structures of the compounds found in circulation (compound 1S, 2S1 and 2S2) and their corresponding (un)sulfated structures (compounds 1 and 2). B Comparison between the effect of (un)sulfated compounds and each of the isomers as well as the mixture of pyrogallol-sulfate isomers. C Schematic overview of the division between the two groups and consequent subgroups of compounds. Statistical differences are denoted as ***p<0.001, **p<0.01 and *p<0.05 relatively to LPS insult and as # # # p<0.001, # # p<0.01 and # <0.05 relatively to untreated cells. Data are presented as means \pm SD, n=3.	31
3.3	Evaluation of the effects of (un)sulfated compounds in the release of TNF α by microglia cells. A, C Chemical structures of the two subgroups of compounds, evaluated in B and D respectively. B, D Evaluation of the ability of the compounds to reduce the release of TNF α from microglial cells stimulated with LPS. Statistical differences are denoted as ***p<0.001, **p<0.01 and *p<0.05 relatively to LPS insult and as # # # p<0.001, # # p<0.01 and # <0.05 relatively to untreated cells. Data are presented as means \pm SD, n=3.	32
3.4	A , Atoms numbers relative to the cyclic benzenic aromatic ring. B The relative position of the different chemical groups on the benzene ring and the corresponding release of TNF α was designed in order to analyze the structure-activity relationship. C, D Based on the structural features and the effects observed, chemical derivatives of compounds 3 and 7 , were selected and synthesized.	33
3.5	Chemical structures of second iteration derivatives. All further information is included in table 3.3	34
3.6	A Chemical derivatives based on compounds 3 and 7 were synthesized. B Biological evaluation of second iteration derivatives showed that three compounds 2S2 , 3SM and 12S have a significant activity in reducing TNF α released by microglia. Compounds marked in B with a represent compound derivatives of compound 3 , and b derivatives of compound 7 . C Structure activity relationship of the compounds was represented in a heatmap, showing the structurally significant core for the activity of these molecules. D Chemical groups associated with increased activity are highlighted with color. The information was extracted from C . Green chemical groups represent a group necessary for an increase in 10% in protection, blue represent an cumulative increase of 20%, and red represent a further increase of 10 to 20 %. Statistical differences are noted as ***<0.001 relative to LPS stimulated cells and # # # <0.001 relatively to control cells.	36
3.7	A The levels of TNF α were evaluated after 6 hours of incubation, without LPS. No statistical significance was detected. B The levels of TNF α were evaluated while using different concentrations of the compounds. Compounds were incubated for 6 hours followed by incubation with LPS for 24 hours. Statistical differences are noted as ***<0.001 relative to LPS stimulated cells and # # # <0.001 relatively to control cells.	38
3.8	A selection of compounds were evaluated in SH-SY5Y upon oxidative insult with t-BHP. Three compounds and the corresponding sulfates showed a high capacity to prevent cell death. Cytotoxic effects were assessed by measuring ATP content A and cell metabolic capacity C . Statistical differences are noted as *p<0.05 relatively to control. Neuroprotective effects were also measured by these two methods B, D . Statistical differences are noted as ***p<0.001, **p<0.01 and *p<0.05 relatively to t-BHP insult. To further increase the understanding on neuron viability, apoptosis was measured using annexin V, while dead cell were measured using propidium iodide through flow cytometry. Statistical differences are denoted as ***p<0.001 relatively to the percentage of dead cells present in t-BHP insulted cells and as # # # p<0.001 relatively the percentage of viable cells present in t-BHP insulted cells.	43
4.1	Compound 4S , 5S and 6S only showed one sulfated conjugate	45
4.2	Compounds 4 and 6 have multiple tautomers that are in equilibrium in solution, thus reducing the reactivity of the phenol. 4 : 2,4,6-trihydroxyacetophenone; 6 : 4-hydroxy-catechol.	46
4.3	A The chemical Structures of pyrogallol (2) and 4-methylpyrogallol differ only on a methyl group (7). B 2,3,4-Trihydrobenzaldehyde (14) can serve as basis for the synthesis of compound 13 and 15	48

4.4	Other classes of compounds, like compound 21 , could be synthesized based upon the structure of pyrogallol (2) and 4-methylpyrogallol (7) and of known neurotransmitters like dopamine (20)	49
4.5	Kynurenic acid is a metabolite of tryptophan that can to activate GPR35. A , tryptophan metabolic pathway. B , GPR35 subunits and cascade of events ¹⁵¹	50
4.6	Hypotetic <i>mus musculus</i> GPR35 inflammatory pathway based on the analysis of KEGG pathways: mmu04010-MAPK; mmu04062- chemockine; mmu04151-PI3K-Akt; mmu04064-NF-kB. Pathway was built using Pathvisio 3.3 (2018) ¹⁵⁷	51
5.1	Structure of the compounds that showed the highest activity in: A the reduction of the inflammatory cytokine TNF α , in microglia cells, upon exposure to LPS; B in the reduction of cytotoxic effects, in neurons, upon oxidative insult. 3SM - phloroglucinol-mono-sulfate; 12S - resorcinol-O-sulfate; 1 - catechol; 2 pyrogallol; 9 - 3-methylcatechol.	56
B.1	Cell metabolic capacity was evaluated in microglia cells, in order to verify if toxic effects were evident from compound incubation. No statistical significance was found between the compounds and the control, non-incubated cells.	73
C.1	The LD50 or 50% lethal dose for SH-SY5Y using t-BHP was calculated using celltiter blue and celltiter glo. Dose response curves were created with the same protocol as for the model used for the evaluation of compound neuroprotective capability. For the calculation of LD50, t-BHP logarithmic concentration was plotted vs the measured fluorescence in the case of celltiter blue, and luminescence in case of celltiter glo(in percentage). An exponential curve was plotted and the value of LD50 obtain for a inhibition of 50% relative to control cells. The values of LD50 were 20.38 A and 19.80 B . A concentration of 20 μ M was used as a compromise between both extrapolations.	75
D.1	The toxic effects of eighteen compounds were evaluated in SH-SY5Y neurons using Celltiter Blue (B) and celltiter Glo (A). Statistical differences are noted as ***p<0.001, **p<0.01 and *p<0.05 relatively to t-BHP insult	77
E.1	Microscopy images of SH-SY5Y obtain in a Leica DM6 microscope. Cell morphology and neurite growth was visually inspected along the time of differentiation. A,B SH-SY5Y undifferentiated cells at the end of 7 days. C,D Differentiated cells at the end of 7 days with all-trans retinoic acid. E Live cell imaging of neurons at 7 days of differentiation, the image showed the formation of neuronal networks upon differentiation. F, G, H Morphology, neurite growth and viability was verified at the end of 7 days of differentiation using calceunurin, for cell viability, Hoechst 33258 for nucleus stain and propidium iodide for staining dead cells. F Live cell imaging of undifferentiated SH-SY5Y, the image showed the presence of epithelial-like population of SH-SY5Y cell line. G Differentiated cells showed the formation of long neurites with no signs of dead population. H Positive control for dead cells using 20 μ M t-BHP for 16h after cell differentiation.	79

List of Tables

1.1	List of natural compounds present in dietary food products and able to modulate inflammatory markers	8
1.2	Neuroprotective effect of (poly)phenol metabolites on neuronal cell model of SH-SY5Y . . .	12
2.1	List of phenolic compounds commercially acquired for the synthesis of chemical derivatives	14
2.2	List of phenolic compounds previously synthesized by the Bioorganic Chemistry lab. ¹²⁸ . . .	14
2.3	Phenolic compounds commercially acquired for the synthesis of second iteration derivatives	21
3.1	List of chemical synthesized compounds (compounds are numbered in the order by which they were evaluated)	29
3.2	List of chemical synthesized compounds (compounds are numbered in the order by which they were evaluated)- Continued	30
3.3	Synthesized and tested compounds- Second iteration	35
3.4	<i>In silico</i> calculations of membrane permeation for the tested compounds	40
3.5	<i>In silico</i> calculations of membrane permeation for the tested compounds (Continued) . . .	41
4.1	Selection of agonistic compounds of GPR35. EC ₅₀ were obtain through dynamic mass redistribution assay ^{152,148}	50
A.1	List of chemical compounds acquired commercially	68
A.2	List of chemical synthesized compounds (compounds are numbered in the order they were evaluated)	69
A.3	List of chemical synthesized compounds (compounds are numbered in the order they were evaluated)	70
A.4	List of chemical synthesized compounds (compounds are numbered in the order they were evaluated)	71

Abreviatures

Asyn	Alpha Synuclein
AB	Amyloid Beta
AD	Alzheimer's Disease
ALS	Amyotrophic Lateral Sclerosis
APT	Attached Proton Test
BBB	Blood Brain Barrier
CaN	Calcineurin
CCL	Chemokine Ligand
CD	Complex of Differentiation
CNS	Central Nervous System
COMT	Catechol-O-methyl Transferase
COSY	Correlation Spectroscopy
COX	Cyclooxygenase
DAT	Dopamine Active Transporter
DBU	1,8-Diazabicyclo(5.4.0)undec-7-ene
DCM	Dichloromethane
DMAP	4-Dimethylaminopyridine
DMF	Dimethylformamide
DMSO	Dimethyl sulfoxide
EtAc	Ethyl Acetate
ELISA	Enzyme-linked Immunosorbent Assay
ERK	Extracellular signal-regulated Kinase
GPCR	G Protein Coupled Receptor
GPR35	G Protein Coupled Receptor 35
HBMEC	Human Brain Microvascular Endothelial Cells
Hex	Hexane
HMQC	Heteronuclear Multiple-Quantum Correlation
IBD	Inflammatory Bowel Disease
IFN	Interferon
IL	Interleukin
JNK	c-Jun N-terminal Kinases

LPH	L actase P hloridzin H ydrolase
LPS	L ipopolysaccharides
LT	l ymphotoxin
MAPK	M itogen- a ctivated P rotein K inase
MCP1	M onocyte C hemoattractant P rotein 1
MetOH	M ethanol
MPTP	1 - m ethyl- 4 - p henyl- 1,2,3,6 -tetrahydropyridine
MS	M ultiple s clerosis
NFκB	N uclear F actor K appa B
NFAT	N uclear F actor of A ctivated T cells
NMR	N uclear M agnetic R esonance
NTT	N eurotransmitter T ransporter
PD	P arkinson's D isease
SULT	S ulfotransferase
TGF	T ransforming G rowth F actor
THF	T etrahydrofuran
TH	T yrosine H ydroxylase
TLR	T oll-like R eceptor
TMSOTf	T rymethylsilyl trifluorosulfate
TNF	T umor N ecrosis F actor
TNFR	T umor N ecrosis F actor R eceptor
UGT	U ridine-5-diphosphate g lucuronosyltransferases

Objectives

The main goal of this project was to develop synthetic analogues, based upon a selection of phenolic compounds present in the blood stream. These compounds were described to reduce the release of inflammatory markers, in the brain, such as NO and Tumor necrosis alpha. As such, the primary objective consisted in synthesizing compounds with increased activity, meaning further decreasing the levels of present inflammatory markers.

In order to complete our main objective, several key steps were considered: 1) Synthesizing the above mentioned synthetic analogues by selecting the appropriate starting materials (phenolic compounds), containing different methyl and hydroxyl groups. From those, the corresponding sulfate esters and glucuronide conjugates were also chemically synthesized; 2) The library of compounds synthesized previously was then tested in a brain inflammatory cellular model composed of microglia stimulated with lipopolysaccharides. Inflammatory markers such as the above mentioned Tumor necrosis alpha were evaluated; 3) Based upon the results other chemical modifications such as the introduction of alkyl groups or the acquisition of other starting materials were considered and further analogues were synthesized; 4) Second iteration compounds (synthesized in 3) were then re-evaluated in microglia cells.

Two parallel objectives relevant for our work were also considered: The ability of compounds to cross the blood brain barrier (BBB), and the impact of the most interesting compounds in neuronal cells.

Compound ability to cross the BBB was evaluated through an *in silico* model of brain permeation. The two compounds with the highest activity were also evaluated in a cellular model of brain permeation composed of Human Brain Microvascular Endothelial Cells.

A selection of compounds were evaluated in a neuronal model exposed to an oxidative insult. These compounds were selected based on their activity in microglia cells and their structural correlation with other chemical molecules known to act on neuronal cells. The capability of such compounds to prevent toxic effects was considered through cell viability assays, mainly cell metabolic capacity assays and markers of apoptosis.

1. State of the art

1.1 Microglial cells: The brain (over)protector

1.1.1 Microglia, the immune innate cells of the central nervous system

Microglia are the monocellular brain-resident, myeloid innate immune phagocytic cells of the central nervous system (CNS).^{1,2,3} These cells are distributed broadly across the brain and spinal cord, and constitute in humans, depending on region, 0.5% to 20% of the total number of glial cells.^{4,5,6} During development these cells modulate proliferation, differentiation, metabolism and formation of neuronal networks and synapses, and during injury they are responsible for microglia mediated apoptosis and phagocytosis of dead cells, protein aggregates and pathogens. Microglia are able to modulate themselves, neurons, astrocytes and other cells of the CNS through the release of chemokines and cytokines, thus modulating the environment, and inducing proliferation, survival or cell death⁷.

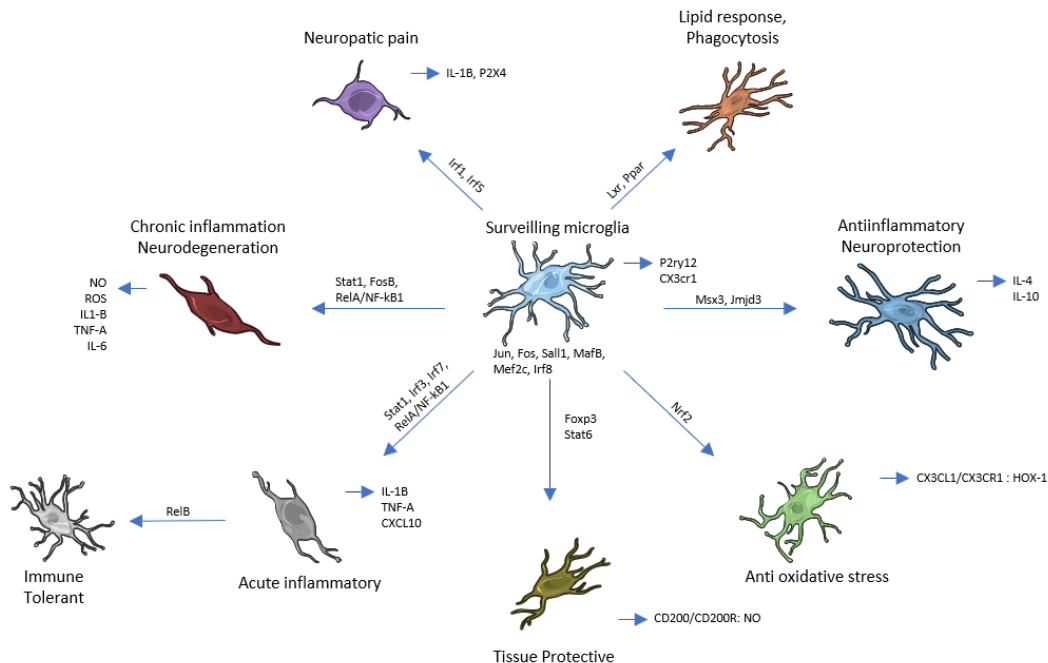


Figure 1.1: Microglia role, function and behavior are dependent on differential gene expression that correlate to various phenotypes rather than the classical M1/M2 phenotypes. Arrows reaching from surveillance microglia represent up-regulated genes that lead to the corresponding phenotype. Arrows leading out of each phenotype represent the up-regulation of cytokines, chemokines and receptors due to the specific phenotype. Adapted from *Nature Reviews Neurology*¹⁰

Classically, microglia functions have been divided into two opposing phenotypic states, M1 and M2, following the same model used for macrophages. This bi-polar definition is still controversial and was adapted from *in vitro* observations which may or may not be reproducible in physiological conditions. Nevertheless, this model is still of great value to facilitate our understanding of the role and potential function of microglia *in vivo*. M1 phenotype corresponds to a proinflammatory and neurotoxic state typically characterized by the expression of major histocompatibility complex class II molecules, activation of interferon γ (IFN γ) and tumor necrosis factor α (TNF α) pathways and consequent release of inflammatory cytokines like TNF α , interleukins (IL) such as IL-5 and IL-1 β and chemokine ligands (CCL) such as CCL2⁸. M2, the contrasting phenotype, relates to anti-inflammatory and healing state induced by

IL-4, IL-13 and IL-10. Normally this involves the activation of pathways related with the release of IL-10 and Transforming growth factor β (TFG β) as well as increased levels of arginase 1. M2 microglia is also responsible for the release of brain-derived neurotrophic factor, insulin-like growth factor I and glial cell-derived neurotrophic factor.⁹

Recently, new information indicates that a vast number of phenotypes exist that depend on the environment, mainly hormones, chemokines, neurotransmitters, cytokines and small interference RNA, and also, long range stimuli like calcium and glutamate waves¹⁰. Some of these phenotypes are described in figure 1.1.^{10,9}

From the different phenotypes shown in figure 1.1 those that more resemble the classical M1/M2 model also represent the mostly studied examples: chronic inflammation through the activation of NF- κ B pathway and anti-inflammatory phenotype through the transcription of *Msx3* and *Jmjd3* genes and the release of anti-inflammatory cytokines like IL-4 and IL-10. On the other hand, evidences of wide range of phenotypes and not a bi-polar system opens the doors for explaining some roles and mechanisms still partially unknown. For example, *lipid response* had received a increased interest due to the relationship between lipids and cholesterol, diabetes and Alzheimers disease, although much is still to be translated to an *in vivo* scenario¹¹. Other phenotypes like *Neuropathic pain* represent one of the most complex systems and are related with several neurotransmitters receptors on microglia and the possible control these cells exert over neurons¹². The role of microglia-neuron communication system CD200/CD200R was also unknown until recently. New data demonstrates that this receptor system is essential for neuron recognition by microglia and is also involved in modulating chronic inflammation.¹³

1.1.2 Cell markers and inflammatory pathways

Overall, microglia like other cells from the immune innate system, represent a complex and dynamic system in order to archive balance between neurotoxic and neuroprotector effects upon inflammatory response.¹⁴ Several molecular pathways are known to be directly implicated with the inflammatory system, and although they cannot be seen as completely separated systems, each is responsible for the release of different molecules that control this balance, mediating cell processes of survival, proliferation and apoptosis.¹²

1.1.2.1 Nuclear factor kappa B (NF- κ B)

Nuclear factor kappa B (NF- κ B) is a transcription factor responsible for a complex system of networks that culminate in cell survival and proliferation¹⁵. NF- κ B pathway in immune cells is also linked to the first responses upon pathogen recognition and the consequent release of cytokines mediating the activation of other pathways and recruitment of immune specialized cells such as lymphocytes.^{15,16}

The NF- κ B pathway is divided into the canonical and non-canonical activation pathways, both of which are present in microglia cells.¹⁷

Activation of the canonical NF- κ B pathway is dependent on activation of TNF α receptor 1A, IL-1 receptor 1 or toll-like receptors (TLR) coupled with CD14 in the case of LPS. Upon the receptor-stimuli specific signaling cascade, this activation pathway culminates with the activation of I κ B kinase also denominated IKK complex. In the canonical activation pathway NF- κ B is composed of three subunits: I κ B, RelA and p50. The activated IKK will then phosphorylate the I κ B subunit, marking this subunit for ubiquitination and leaving RelA and p50 free and capable of migrating into the nucleus, leading to the transcription of a vast number of genes, with predictions of above 135 activated genes.¹⁸ Examples of such genes include cytokine production: *CCL17*, *CXCL3* (fractalkine), *IFNG* (interferon gamma), *IL1A*, *IL1B*, *IL2*, *IL6*, *IL17*, *LTA* (lymphotoxin A), *TNF*; non-canonical NF- κ B pathway genes: *TNFSF13B* (B-cell activating factor or BAFF), *CD40*, *NFKB1* (NF- κ B p100 subunit); NF- κ B regulatory genes: *LBP8* (also known as CD14 Lipopolysaccharides receptor), *NLRP2* (NF- κ B pathway inhibitor); adhesion factors such as *FN1* (fibronectin); regulation of other inflammatory pathways such as MAPK and NFAT and apoptotic factors: *FOS* (c-fos), *MYC* (c-myc), *BCL2*, *NPY1R* (neuropeptide Y-Y1 receptor); growth factors such as *BDNF* (brain-derived neurotrophic factor) and many more.

In the case of the non-canonical activation of the NF- κ B pathway, it is achieved through lymphotoxin beta receptor, CD40 ligand receptor or B-cell activating factor (BAFF) activation in the case of B lymphocytes. Both lead to the activation of an alternative IKK complex composed of NF- κ B inducing kinase (NIK). In the non-canonical pathway NF- κ B is composed of the p100 and RelB. Upon activation, IKK phosphorylates p100 leading to its ubiquitination. The p100 subunit is then cleaved and transformed into p52 that together with RelB is transported into the nucleus where it is responsible for the transcrip-

tion of genes such as *CXCL12*, *CXCL13*, *CCL19*, *CCL21* and *TNFSF13B*, responsible for the production of cytokines linked to inflammatory cell recruitment, differentiation, and B lymphocyte survival.¹⁹

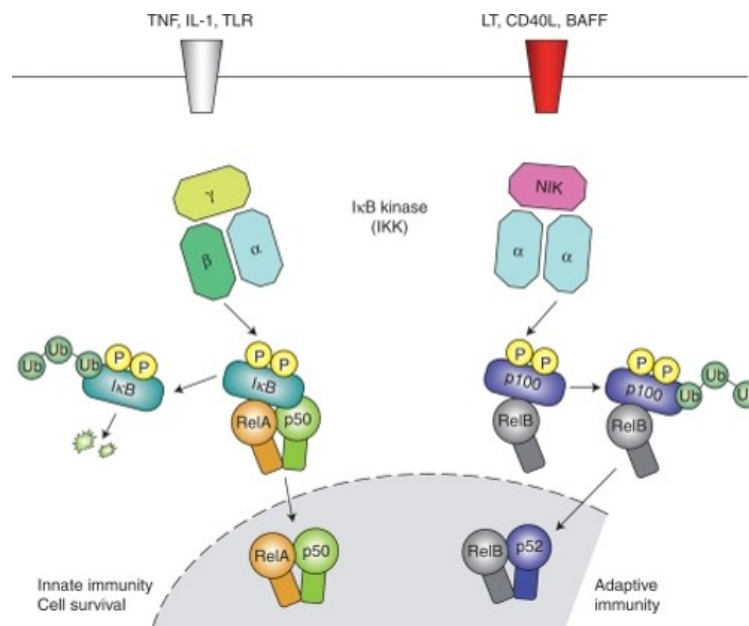


Figure 1.2: NF- κ B canonical and non-canonical activation pathway. Canonical activation of NF- κ B is dependent on TNF α , IL-1 or TLR activation and culminates in the activation of RelA/p50. Non-canonical activation of this pathway is dependent on CD40L receptor activation, involves NIK and activates RelB/P52 transcription. Adapted from Lawrence et. al.¹⁶

1.1.2.2 Mitogen-activated protein kinases pathway (MAPK)

Mitogen-activated protein kinases (MAPK) belong to the family of serine kinases and are associated with differentiation, proliferation and apoptosis. The MAPK pathway is composed by a series of proteins that are mainly induced by receptors in the cell membrane culminating in the regulation of three major kinases: extracellular signal-regulated kinase (ERK), p38, and c-Jun NH2-terminal kinase (JNK).²⁰ These kinases coordinate the formation of a C-fos, C-jun dimer designated activator protein 1 (AP-1) that is internalized into the nucleus and acts as a transcription factor for a series of cytokines and growth factors responsible for: heat shock, oxidative, osmotic stress and finally inflammatory response (fig.1.3)^{20,21}.

MAPK, just like NF- κ B can be activated by tumor necrosis alpha through TNFR or by a toll-like receptor together with CD14 for the activation via lipopolysaccharides. Nevertheless, other activators of this pathway exist although they are commonly represented by growth factors such as T cell growth factor (TGF).

The relation between MAPK and NF- κ B is however a much more complex network of regulations. Both pathways can be activated simultaneously through the same stimuli. However NF- κ B can not only express MAPK activators like TNF α but also regulate its intensity since NF- κ B is responsible for the expression of *FOS* (C-fos) as stated previously.

1.1.2.3 Nuclear factor of activated T cells (NFAT)

NFAT is an inducible transcription factor, responsible for the expression of pro-inflammatory cytokines such as TNF α and lymphotoxin- β ²³.

Activation of NFAT is mediated by the activity of calcium/calmodulin-activated protein phosphatase: calcineurin (CaN), and thus is highly dependent on the presence of intracellular calcium and efflux pumps present in the membranes²⁴. Once activated, NFAT is translocated from the cytoplasm to the nucleus where it becomes active and initiates the transcriptions of various genes related with inflammation²⁵. Moreover, NFAT pathway was also, in the past, related with the regulation of microglia phenotypes as well as the expression of monocyte chemoattractant protein-1 (MCP-1)²⁶.

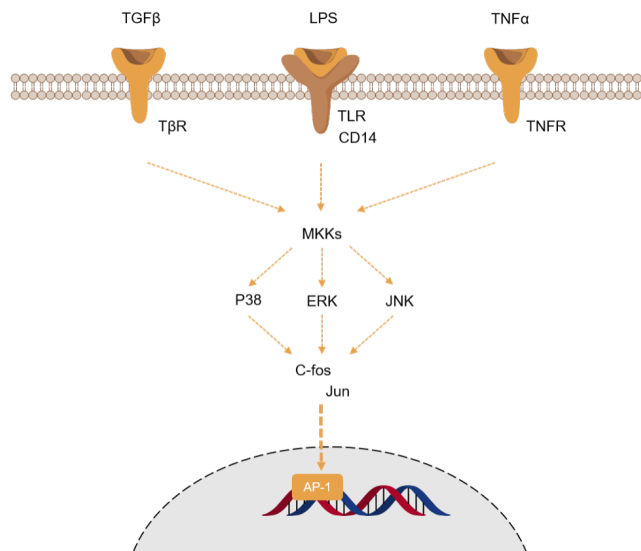


Figure 1.3: Simplified representation of the MAPK pathway. Activation begins in the cell membrane through $\text{TNF}\alpha$, LPS or $\text{TGF}\beta$. The signaling cascade culminates in the activation of MKKs and consequent P38, ERK and JNK kinase activation. These kinases lead to the formation of the C-fos-jun dimer (AP-1) that migrates to the nucleus and acts as a transcription factor. Adapted from Murshid et al.²²

1.1.2.4 Cytokine and chemokines: A focus on $\text{TNF}\alpha$

Cytokines and chemokines act as the main vehicle for microglia cells to transmit a specific message, and thus are of great importance for modulating their own function but also the surrounding environment, including: neurons, astrocytes and endothelial cells^{27,28}. Various types of messages could be sent through different cytokines or different combinations thereof. These messages include cell proliferation, differentiation, apoptosis, phagocytosis, cell attraction, migration and many others²⁹.

Cytokines involved with inflammation have been categorized into pro and anti inflammatory. Pro-inflammatory or just inflammatory cytokines are essential in triggering inflammatory pathways, starting the inflammatory process and resolving a specific insult, either from pathogens or the accumulation of toxic proteins excreted by neurons. Examples of inflammatory cytokines include $\text{IL-1}\beta$, $\text{TNF}\alpha$, IL-6 , IL-15 , IL-17 and IL-18 .³⁰ Anti-inflammatory cytokines like IL-4 , IL-10 and IL-13 represent the main cellular response against increased inflammation and are crucial in order to restore homeostasis of the system³⁰.

Tumor necrosis alpha ($\text{TNF}\alpha$) is without doubt one of the most important cytokines and one of the most cited with more than ten thousand items in PubMed in 2017 alone. $\text{TNF}\alpha$ gained this status due to its ability to modulate a vast set of cell activities (proliferation, differentiation, apoptosis), depending on the concentration present in the extracellular matrix. It is rapidly produced after trauma, infection or exposure to bacterial lipopolysaccharides, and represent one of the most abundant cytokines in the development of the inflammatory process³¹. $\text{TNF}\alpha$ plays a very critical role in activating various pathways including the before mentioned MAPK and $\text{NF-}\kappa\text{B}$, and, by doing so, is able to modulate the expression of other cytokines and other inflammatory markers such as prostaglandins, platelet activating factor and Cyclooxygenase-2 (COX-2) expression^{32,33,34}. $\text{NF-}\kappa\text{B}$ in particular is very important for the understanding of the complex inflammatory system, since this particular pathway is able to produce $\text{TNF}\alpha$ and at the same time be activated by this cytokine, creating an auto-activation mechanism that must be under tight control in order to maintain balance. Several pathologies are directly related with $\text{TNF}\alpha$ dysfunction like inflammatory bowel disease (IBD), ischemia and type 2 diabetes mellitus^{35,36,37}.

In the CNS, neurons are a great example of the importance of the balance and tight control necessary for this cytokine. Neurons, like almost every other mammalian cells express $\text{TNF}\alpha$ receptor one and two (TNFR1 and TNFR2) and are modulated by the action of this cytokine³⁸. Observations indicate that lower concentrations are essential for cell survival while at high concentrations cell apoptosis and necrosis is inevitable³⁹. However, in contrast with other mammalian cells, mature neurons are locked in G0 division state, meaning they do not replicate. As such, neuronal health and survival is essential for the overall function of the brain. Various evidences suggest the direct implications of $\text{TNF}\alpha$ in neurological diseases like Alzheimer's disease (AD), Parkinson's disease (PD) and Multiple sclerosis (MS).^{40,41,42}

Studies have demonstrated that $\text{TNF}\alpha$ is able to cross the BBB and migrate in and out of the

brain^{43,44}. Nevertheless, the main producers and regulators of this cytokines in the brain are microglia cells, and thus they are main player responsible for maintaining healthy levels of $TNF\alpha$ in the environment and directly impact neuron viability. In the case of imbalance they are also responsible for recruiting specialized cells from the adaptive immune system in order to archive homeostasis.

1.1.3 Microglia and Neurodegenerative diseases

1.1.3.1 Microglia- $TNF\alpha$ relationship

Microglia, the innate immune cells of the central nervous system are the main cells responsible for the expression and release of tumor necrosis factor alpha in the brain, although other cells like astrocytes and some classes of neuron populations are also able to constitutively release lower levels of $TNF\alpha$ ^{45,46}. Microglia, on the other hand, produce and release $TNF\alpha$ based on the extracellular concentration of $TNF\alpha$ and based on gradients are able to decrease its production and start producing anti-inflammatory cytokines or jump to a inflammatory response. Depending on further stimuli microglia will adapt to different phenotypes as shown in figure.1.1. For example, increased levels of $TNF\alpha$ together with high levels of glutamate are known to be associated with a neuropathic pain and chronic inflammation phenotype (fig.1.1).^{47,48}.

Exposure to high levels of $TNF\alpha$ is associated with microglia acute inflammatory response. This response is essential for the development of the immune response, production of cytokines and specialized cell recruitment. Discrete but constant exposure and consequent activation of microglia, specially with age, is associated with immune tolerance and the inability to respond in case of tissue damage and infection that may lead to tissue loss and death⁴⁹. Constant exposure to $TNF\alpha$ is associated with chronic inflammation, the presence of increased and constant levels of this cytokine lead to an overactivation of the phagocytosis process, culminating in the phagoptosis of viable or damaged but viable neurons, instead of the usual cell repair mechanisms in place by microglia, like neurite pruning⁵⁰. Increased levels of apoptotic factors and number of cells demonstrating a phagocytic phenotype leads to an abnormal decrease in the number of neurons. This factor demonstrates to be critical and associated with various pathological conditions and neurodegenerative diseases such as Alzheimer's, Parkinson's and Multiple sclerosis.⁵¹

1.1.3.2 Microglia (dys)function and aging

With age, the number and intensity of inflammatory triggers is increased together with microglia response, which may be caused by a priming effect⁵². Studies focusing on old age microglia of mouse have uncovered that 25% of microglial cells expressed MHC-II receptor in opposition to 2% in young adult mice⁵³. MHC-II is a class of receptors present in lymphocytes and other antigen presenting cells although they can be observed in other dendritic cells upon chronic exposure to Interferon gamma⁵⁴. Receptors were not the only overexpressed proteins, pro-inflammatory cytokines like $TNF\alpha$, $IL-1\beta$ and anti-inflammatory cytokines $IL-19$ and $TGF\beta$ were also upregulated in aged microglia⁵⁵. The overexpression of pro and anti inflammatory markers with age is associated with the loss of balance of the immune system and chronic inflammation⁵⁶. This age-like phenotype was observed in a matter of days with primary cultures.⁵⁷

Morphology was another factor modulated by age. Reduced ramification of microglia has been detected in old age human brains and in patients with Parkinson's disease.⁵⁸ Morphologic changes in dystrophic (senescence) microglia have been linked to age-dependent degeneration. Interestingly, the presence of dystrophic elements was found to a much higher extent in old age subjects (68-year-old), than in younger age subjects (38-year-old), which seems to be correlated with sporadic Alzheimer's disease.⁵⁹

The two most common neurodegenerative diseases, Alzheimer's and Parkinson's, both share a common risk factor: age. Both diseases are associated with pathological features like neuron apoptosis but also necrosis, synaptic loss, neurofibrillary tangles and accumulation of protein aggregates. These factors are directly or indirectly related with glial, specially microglial activation and function, and a variety of recent studies relate microglia and $TNF\alpha$ with these diseases.^{51,60}

In AD, microglia seem to be responsible for the phagocytosis of proto fibrillar Amyloid- β ($A\beta$) one of the major hallmarks of the disease, protecting neurons against its neurotoxic effects, although, in aged microglia, phagocytosis seems to be impaired.⁶¹ Recently in an APP23 model of AD, over-activation of microglia and alterations in cell cytoskeleton were observed and considered likely to contribute to further neurodegeneration.⁶²

In PD, mouse models using neurotoxins replicating disease mechanisms and symptoms, such as 1-methyl-4-phenyl-1,2,3,6-tetrahydropyridine (MPTP) or rotenone have been used in order to evaluate the contribution and the role of microglia. However, few studies have focused on aged microglia.⁶³ Another study in monkeys also demonstrated an increased and persistent microglia reactivity after exposure to MPTP.⁶⁴ Other models using non-aggregated α Synuclein have demonstrated their ability to trigger TLR-mediated immune responses.⁶⁵ Interestingly, recent evidence has shown that microglia of adult mice display phagocytic impairment of α Syn oligomers associated with an enhanced TNF α secretion.⁶⁶

1.2 (Poly)Phenols impact on Neuroinflammation

1.2.1 (Poly)phenols are grouped in different families

Polyphenols represent a class of compounds structurally composed of a multitude of aromatic rings (chemical structures containing six carbons in a cyclic structure varying between single and double bonds, also commonly named benzoic structures) possessing at least one hydroxyl group (-OH), also designated phenolic compounds.⁶⁷ Thousands of compounds can fit in this category including synthetic and semi-synthetic compounds, however the vast majority are of natural origin.^{68,67} This definition is not consensual, and many authors described the monomeric units (phenols) as polyphenols. This was mainly due to their link to the polymeric structures, and the possibility to obtain the monomeric structure from a parent polyphenol, specially through metabolic reactions. For this reason, recently, the term polyphenols was recently updated to (poly)phenols in order to encompass a wider range of structurally and metabolically related phenols.^{69,70}

Natural occurring (poly)phenols are usually found in plants and vegetables and play important roles such as controlling the release of growth hormones and the prevention of fungal infections. (Poly)phenols are however most commonly found conjugated with: 1) sugars, examples include phlorizin: phloritin conjugated with glucose; rutin: quercetin conjugated with rutinose; quercitrin: quercetin conjugated with rhamnose; and many others; 2) benzoic acids like catechin-5-O-gallate consisting on catechin conjugated with gallic acid; 3) aminoacids like 4-hydroxy-cinnamoyl-L-glutamic acid or 4-hydroxy-3-methoxy-cinnamoyl-L-tyrosine; 4) Other polyphenols usually forming oligomers like proanthocyanidin class of compounds.⁷¹ The type of (poly)phenol and conjugation can be traced to specific classes of fruits or vegetables as different classes tend to produce different conjugation patterns associated with the biological function.⁷²

Classification of different groups are dependent on the number of phenolic rings and the functional group present. The diversity in the range of polyphenol groups and subgroups is shown in figure 1.4 and include phenols, phenolic acids, stilbenes, flavanoids, coumarins and lignans. Other smaller groups exist like chalcones and tannins however they were omitted as they are not as physiologically relevant.

Flavenoids represent the largest group of phenolic compounds⁷³. They are divided into flavonols, flavones, isoflavones, flavanones, anthocyanins and flavanols and are widely present in fruits and vegetables. Stilbenes and their related chalcones are specially present in wines and fermented products. Small phenolic compounds like catechol are usually present due to the metabolization of flavenoids in coffee products. Phenolic acids can be divided in two groups: hydroxybenzoic and hydroxycinnamic acids. Hydroxybenzoic acids are present in more complex compounds while hydroxycinnamic acids are normally found glycosylated⁷⁴.

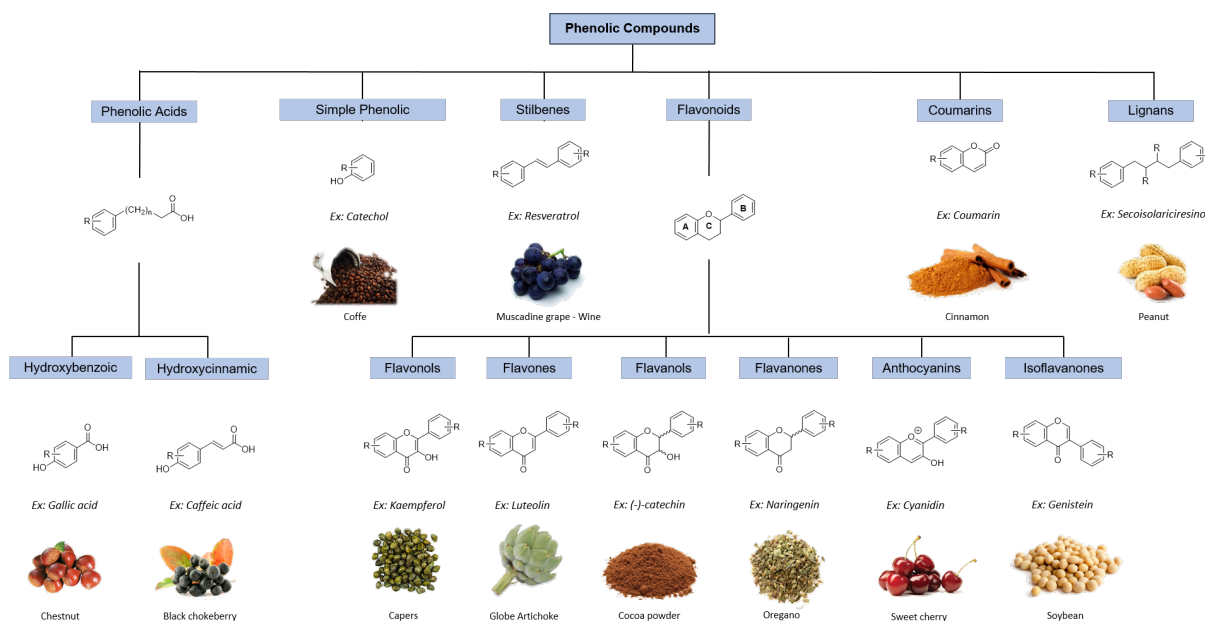


Figure 1.4: Main classes of (Poly)phenols with representative structures. Examples are given in italic, and food sources are shown below.^{75,74}

1.2.2 Natural compounds and neuroinflammation

Among all dietary natural compounds present in fruits and vegetables, (poly)phenols are considered the molecules with major role when discussing anti-inflammatory properties^{76,77}. A list of some of these (poly)phenols from different classes is present in table 1.1. Various molecules are able to modulate the release and production of TNF α and IL-1 β , and some have been proved to modulate NF- κ B pathway⁷⁸. Commonly the studies involving polyphenols and neuroinflammation are associated with a very specific pathology or disease like AD, PD, MS or with the impact of aging.

Table 1.1: List of natural compounds present in dietary food products and able to modulate inflammatory markers

Molecule(s)	Model	Effect
Epigallocatechin-O-3-gallate	Aging	Prevention of brain inflammation ⁷⁹
	AD	Reduction of NF- κ B complex present in cells ⁸⁰
Quercetin	PD	Protection against oxidative insult and IL-1 β decrease ⁸¹
	MS	Modulation of IL-1 β and TNF α ⁸²
Curcumin	Infla.	Reduction of COX-2 levels and NF- κ B inhibition ⁸³
	AD	Decrease in IL-1 β ⁸⁴
Resveratrol	Infla.	Modulation of SIRT1 and NF- κ B inhibition ⁸⁵
	PD	Decrease levels of COX-2 and TNF α ⁸⁶
Benzoic acid protocatechuic-O-3-sulfate	Infla.	Reduced TNF α levels ⁸⁷
	Infla.	Slight inhibition of NO and TNF α ⁸⁶

1.2.2.1 The interest on natural compounds

In recent years, (poly)phenols received an increased interest due to their neuroinflammation and neuroprotection properties⁸⁸. This is mainly due to the inability of medicinal and pharmaceutical research in discovering cures for complex age-related diseases such as AD and PD. In the case of PD, levodopa (L-dopa), an *in vivo* chemical compound is essential for the natural production of dopamine, is still used as a treatment for PD associated symptoms like shaking and rigidity. It is in use since George Cotzias and co-workers demonstrated L-dopa benefits and the molecule was clinically approved for use in patients of PD in 1969⁸⁹. Fifty years passed and seventh generation drugs are still using a combination of this compound with catechol-o-methyl transferase inhibitors and other neurotransmitters⁹⁰.

The development of COMT inhibitors is an example of a pharmacological approach based on natural compounds. Two of these natural compounds, catechol and pyrogallol, were known to have an inhibitory effect on COMT, as such, they were used as first generation inhibitors.^{91,92} Later these two structures, together with dopamine and other COMT inhibitors were used for the rational creation of more target specific inhibitors present today. Another important example of natural compounds with pharmacological significance include salicylic acid, and the corresponding synthetic acetylsalicylic acid which is a COX-1/COX-2 inhibitor and that gave rise to a series of nonsteroidal anti-inflammatory drugs.^{93,94}

Studies elucidating the role of natural compounds, present in dietary products, as bioactives in the prevention of age associated diseases gave rise to great possibilities, implicating the possible effect of changes in dietary habits and the impact on future health conditions. Nevertheless, a great deal of care is necessary when talking about bioactive compounds tested through *in vitro* assays and cell models. Compounds such as curcumin and resveratrol have been proved to modulate inflammation (table 1.1), however some authors use concentrations never found in circulation, with no physiological significance and not accounting for further metabolization of such compounds. Nonetheless, compounds like obovatol, a natural compound present in *Magnolia obovata* have demonstrated great potential in diminishing neuroinflammatory markers in microglia cells on mice models and at physiologically significant concentrations. and have been used as basis in the synthesis of chemical derivatives.^{95,96}

1.2.3 (Poly)phenol metabolization and the role of microbiota

(Poly)phenols and conjugates described in section 1.2.1 are present in considerable concentration in fruits and vegetables, however conjugation also means these molecules are very polar, and unable to

cross the epithelial barrier in the gastrointestinal track. A fraction of these conjugates is metabolized by mammalian β -glucosidases in the small intestine before being absorbed as aglycones.⁹⁷ Reaching the liver, (poly)phenols are seen as xenobiotics and are biotransformed by phase I and II enzymes. Phase I enzymes are responsible for the oxidation, reduction, hydrolysis and other transformations realized by cytochrome P450 enzymes. Phase II enzymes, or conjugation enzymes, are responsible for retrieving the polarity to the molecules in order to release them into the blood stream. Conjugation examples include, sulfation, glucuronidation, glutathione and aminoacid conjugation, acetylation and methylation. From those, the most commonly related with (poly)phenolic compounds are sulfation, glucuronidation and methylation from the activity of sulfotransferases (SULTs), uridine-5-diphosphate glucuronosyltransferases (UGT) and catechol-O-methyltransferases (COMT) respectively.^{98,99}

(Poly)phenols not absorbed in the upper part of the gastrointestinal track and unable to be hydrolyzed by human intestinal enzymes, together with phase I and II metabolites excreted from the liver back into the intestine through the enterohepatic cycle, reach the colon. In the colon, a highly complex microbial ecosystem, realizes a series of metabolomic operations such as cometabolism and catabolism leading to the creation of different compounds or aglycones able to be absorbed. For example quercetin rutinosides cannot be hydrolysed by human intestinal enzymes and are dependent on the activity of rhamnosidase present in Bacteroids, Enterococcus and Enterobacter to release the corresponding aglycones.^{100,98}

In some cases, the presence of circulating compounds are not only dependent on just human or microbiota metabolization but a mixture of both systems. A good example are small phenolic compounds like catechol and pyrogallol.^{98,74} These compounds can traced back to several possible origins: decarboxylation of gallic acid or catabolic degradation of flavan-3-ols or anthocyanidins. Gallic acid exists in fruits like berries and black tea or conjugated with other (poly)phenols like (-)-epicatechin ((-)-epicatechin-3-O-gallate). Reduction of gallic acid to the corresponding phenolic compounds, or hydrolysis of epicatechin conjugate can be realized through human/mitochondrial related enzymes, however catabolic degradation of flavan-3-ols and anthocyanidins are exclusive to microbiota (fig 1.5 A,B).⁷⁴

Another example is phloretin that is metabolized by different enzymes of human and microbiota origin along the gastrointestinal track, thus modulating the time and concentration of compounds present in circulation. Phloretin is transformed to the corresponding aglycone by lactase phloridzin hydrolase (LPH) or by gut microbiota and then later transformed into phloroglucinol (fig 1.5 C).^{74,101,102}

This human-microbiota system is very complex resulting in circulating compounds very different from the primary or parent compounds. Together with other factors associated with inter individual variability like differential mitochondria gene expression and microbial population due to dietary habits, this leads to a great number of questions about the use of dietary compounds in research while not considering that they might never reach human circulation.⁹⁸

1.2.4 Compound ability to cross the BBB

1.2.4.1 Gut-Brain axis

Dietary (poly)phenols undergo extensive metabolization by microbiota, the intestine epithelia, and liver, giving rise to a wide set of different metabolites from the parent compounds present in food products. Despite the ability of metabolites to produce an effect *in vitro*, the capacity to reach the target organs is the major limiting factor. For neuroprotective compounds one of the major obstacles is the Blood Brain Barrier (BBB)¹⁰³.

The BBB is a very complex structure composed of three different areas: the major constituent are the cerebrovascular endothelial cells that regulate blood and brain interstitial fluid transport; the choroid plexus that regulates blood and cerebrospinal fluid and finally, the arachnoid epithelium that regulates the passage of molecules between blood and cerebrospinal fluid.¹⁰⁴ Each area is very dynamic and able to modulate the passage of chemical molecules thus regulating the central nervous system (CNS) environment and function¹⁰⁵. The major attribute of the BBB is to keep control of the influx and efflux of chemical messengers and block the passage of toxic molecules and pathogens¹⁰⁶. It is also known that it is able to communicate directly with astrocytes and microglia thus modulating neuronal activity¹⁰⁷.

(Poly)phenols are no exception, and as such they must cross this very capable and highly regulated barrier in order to reach the brain. As the number of studies using polyphenols and their corresponding metabolites grows, an increased interest was taken on understanding if in fact these metabolites were able to reach the brain and the possible range of concentrations observed¹⁰⁸. To this day only a small subset of compounds from different (poly)phenol classes of metabolites were evaluated for their capacity to cross the BBB membrane and fewer studies focused on elucidating the mechanisms responsible for the transport across the BBB.^{74,108,75,101,109}

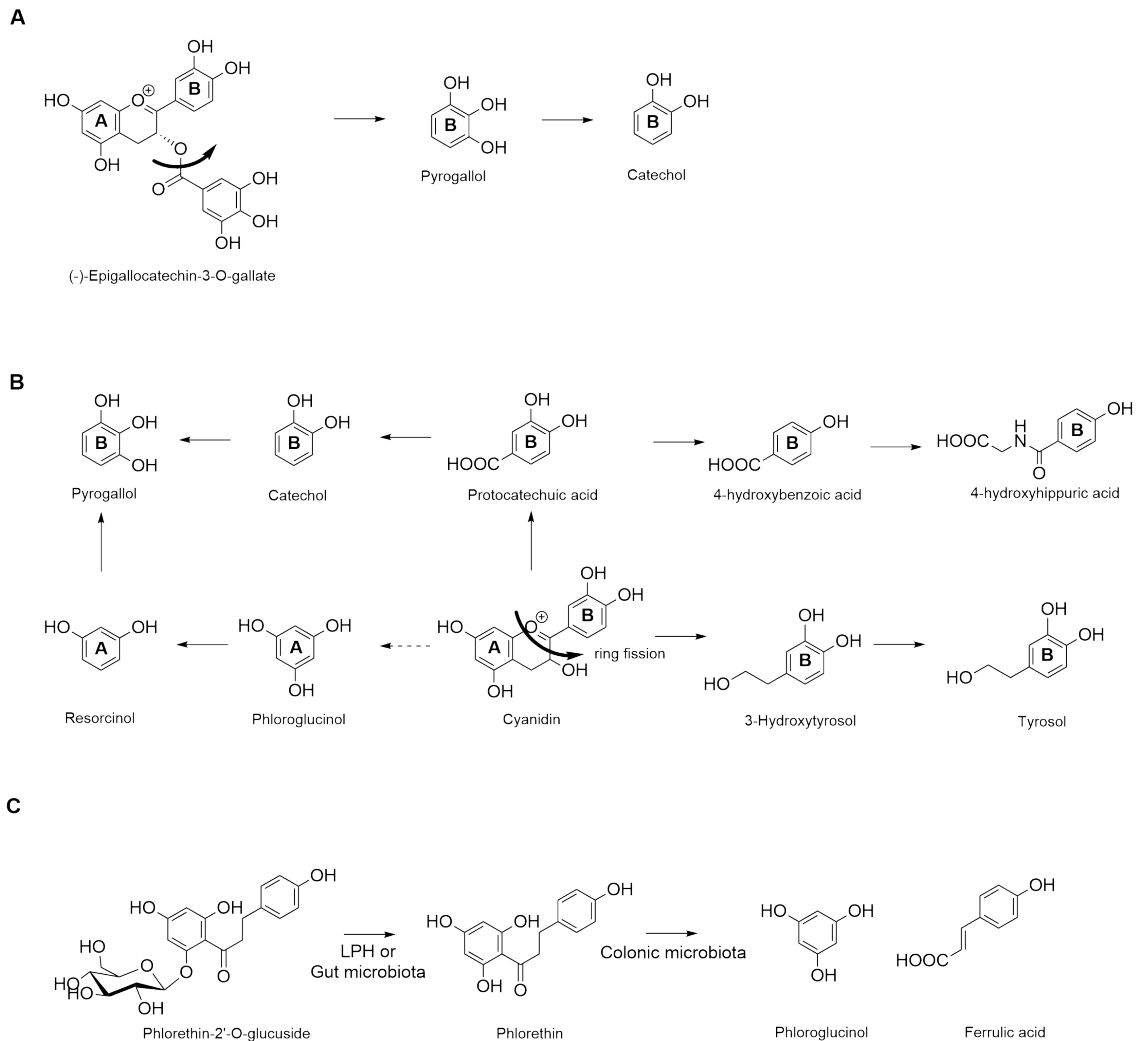


Figure 1.5: Small benzoic and phenolic compounds shown in circulation are dependent of human and microbiota metabolism. **A**, Pyrogallol and catechol are formed from the unspecific hydrolysis of the ester bound in (-)-epicatechin-3-O-gallate. **B**, Microbiota conversion of cyanidins into small phenolic compounds present in blood, urine and feces. **C**, Different metabolites are formed in different areas of the gastrointestinal track. Adapted from Del Rio et al. 2013^{74,101}

From the short list of studies focused on evaluating the mechanism of transport, most focus on elucidating whether it is based upon passive diffusion, or through active transport. However, the results are usually inconclusive or only specific for one compound¹¹⁰. Notwithstanding various (poly)phenol metabolites are known to modulate and inhibit the ATP binding cassette or ABC transporters. These are efflux pumps responsible for the transport of xenobiotics and vastly present in the BBB and epithelia, that could indicate a potential method of transport¹¹¹.

1.2.5 Mechanism of action of (poly)phenolic metabolites

The mechanism of action of (poly)phenolic metabolites and their role in modulating neuroinflammation is still poorly understood. (Poly)phenols have been described to modulate the release of cytokines and chemokines such as IL-1 β , TNF α , NO, related with NF- κ B and MAPK pathways, indicating a possible target related with these two pathways¹¹². However, different polyphenols, even those closely related seem to produce effects in different molecular targets indicating the possibility that the same compound could act in various targets simultaneously creating an pleiotropic effect¹¹³.

Other targets from different pathways but related with inflammation and regulated with these two pathways (NF- κ B and MAPK), have also been associated with (poly)phenols. Examples include cyclooxygenase-2 (COX-2) and lipoxygenase (LOX), meaning arachidonic acid pathway may also be

involved¹¹⁴. In recent studies arachidonic pathway and consequent production of prostaglandines have been demonstrated to be of great relevance by modulating microglia reactivity upon spinal cord injury¹¹⁵.

1.3 Neuroprotection

Life expectancy has been increasing in a stable manner in developed countries, and a correlation with the incidence of age-related chronic diseases, such as neurodegenerative diseases like Alzheimer's and Parkinson's disease cannot be dismissed¹¹⁶. Protein misfolding and aggregation have been emerging as a common mechanism or consequence to many neurodegenerative diseases, Parkinson's disease, Alzheimer's disease, ALS, Huntington, each with its accumulation of specific toxic aggregates of proteins: alpha synuclein, tau, TDP-43 and huntingtin respectively¹¹⁶. All these proteins are unstable and form aggregates along our lifespan, although they accumulate with age and are especially toxic for neuronal cells that are unable to do the complete clearance of these aggregates through autophagy thus needing specialized cells like microglia and astrocytes to remove and create a barrier from those toxic species.^{117,118} Moreover, evidences suggest that neurodegenerative disease association with age is dependent on a specific cell trigger, at the end of the fertile period, heading to the downregulation of chaperones, proteins responsible for the correct protein folding, preventing aggregate formations^{117,118}. The presence of toxins and other oxidative insults have also been identified as causes of neuronal death, mainly through the formation of reactive oxygen species (ROS) that eventually lead to neuronal disorders.^{119,120} Other pathogens, ROS and toxins are also involved in activating the neuro inflammatory process of astrocytes and microglia, consequently leading to toxic levels of TNF α ¹²¹. Ultimately the above mentioned diseases are multifactorial and a mixture of all factors could be combined leading to caspase mediated apoptosis of neurons, that will eventually lead to neurodegenerative diseases¹²¹.

(Poly)phenols have been a focus of study in the prevention of neurodegenerative diseases due to their anti-inflammatory potential. Furthermore, various studies relate (poly)phenols as indicated in table 1.2¹²². Various neuronal cell models exist, and primary cultures are limited in the case of neurons. When considering specifically neuroprotection, these include: PC-12, HT-22, NTERA-2 and SH-SY5Y. While all include advantages and disadvantages not discussed here, SH-SY5Y differentiated neurons are the most described and used model for the evaluation of (poly)phenols and other compounds, and this was reflected in table 1.2¹²²

Table 1.2: Neuroprotective effect of (poly)phenol metabolites on neuronal cell model of SH-SY5Y

Compound	Effect
3,4-dihydroxyphenylpropionic acid, dihydroxyphenylacetic acid, gallic acid, ellagic acid, and urolithins	Decrease of neuronal apoptosis by preventing caspase-3 activation via reduction of ROS levels and increased redox activity ¹²³
5-(3,5-dihydroxyphenyl)- γ -valerolactone	Increased number of neurites ¹²⁴
3,4-dihydroxyphenylacetic (3,4-DHPA)	Increased viability against SIN-1 control group ¹²⁵
4-Hydroxy-3-methoxybenzaldehyde (vanillin)	Atenuation of rotenone induced cell death ¹²⁶
(-)-epigallocatechin-3-gallate	Prevents from 6-OHDA toxicity ¹²⁷

2. Materials and Methods

2.1 Chemical Synthesis

All chemical reactions described were performed under argon atmosphere except when water was used as solvent. The consumption of the starting material and consequent status of completion of the reactions were followed by thin layer chromatography (TLC) on aluminum-backed silica gel (Merck 60 F₂₅₄). Flash preparative column chromatography was performed using Silica Gel Merck 60. ¹H NMR spectra were obtained at 400 MHz in D₂O, CD₃OD, CDCl₃ or DMSO-d₆ with chemical shift values in parts per million. ¹³C NMR spectra were obtained at 100.61 MHz in the same deuterated solvents. Peak assignment were supported by 2D correlation NMR studies (COSY, HMQC). In the case of isomer mixtures, only the representative carbon signals were assigned for each isomer. FT-IR spectra were obtained in a Bruker IFS 66/S through attenuated total reflection (ATR).

Most compounds used as starting materials were acquired commercially at the time of synthesis with the exception of 4-methylbenzene-1,2,3-triol and 4-(hydroxymethyl)-benzene-1,2-diol which were synthesized from available structurally related compounds (see table 2.1) The synthesis of sulfates and glucuronides using BF₃OEt₂ were conducted as previously published by our group.¹²⁸ The compounds used for comparison in our work were previously synthesized by Almeida et al. and are described in table 2.2.¹²⁸

All the properties of the synthesized compounds are shown below and condensed in table 3.3. NMR and FT-IR data is shown below. The code attributed to the compounds was chosen based upon the order they were synthesized and evaluated in microglia cells. Compound numbers containing S, represent a sulfate conjugate while G represent a glucuronide conjugate.

The following chemical modifications are divided into two sections: First and second iteration compounds. This was due to two iterations, or cycles, of synthesis and biological evaluation. The development of second iteration chemical derivatives was dependent on first iteration compounds and as such is shown after the description of first iteration chemical reactions and compounds.

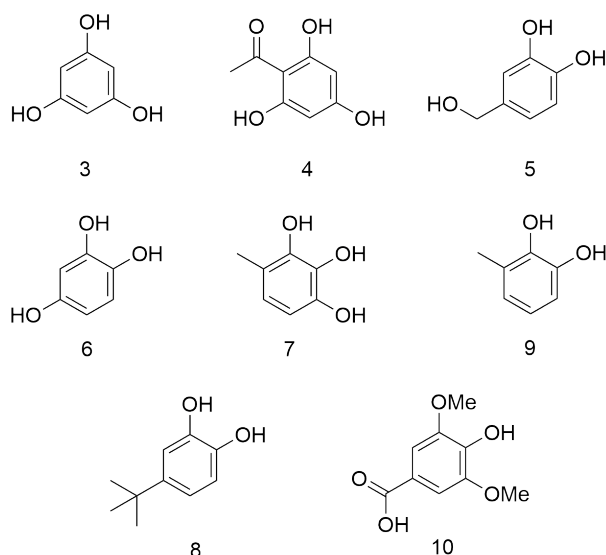


Figure 2.1: Structures of compounds used for the synthesis of conjugate derivatives.

Table 2.1: List of phenolic compounds commercially acquired for the synthesis of chemical derivatives

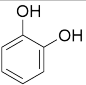
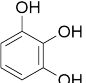
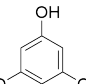
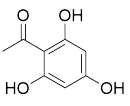
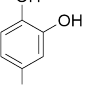
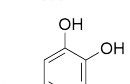
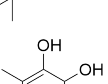
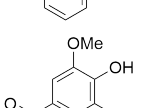
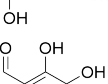
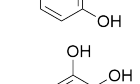
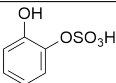
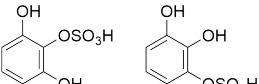
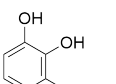
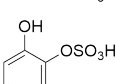
Structure	Nu.	Name	Manufacturer
	1	catechol	Sigma-Aldrich
	2	pyrogallol	Sigma-Aldrich
	3	phloroglucinol	Alfa-aesar
	4	2,4,6-trihydroxyacetophenone	Sigma-Aldrich
	6	4-hydroxycatechol	Carbosynth
	8	4-tert-butylcatechol	Sigma-Aldrich
	9	3-methylcatechol	Sigma-Aldrich
	10	syringic acid	Sigma-Aldrich
	14	2,3,4-trihydroxybenzaldehyde	Carbosynth
	16	protocatechuic acid	Sigma-Aldrich

Table 2.2: List of phenolic compounds previously synthesized by the Bioorganic Chemistry lab.¹²⁸

Structure	Nu.	Name
	1S	catechol-O-sulfate
	2S	pyrogallol-O-sulfate
	2S1	pyrogallol-O-1-sulfate
	2S2	pyrogallol-O-2-sulfate

2.1.1 Synthesis of First Iteration Compounds

Synthesis of compound 7: 4-methylpyrogallol

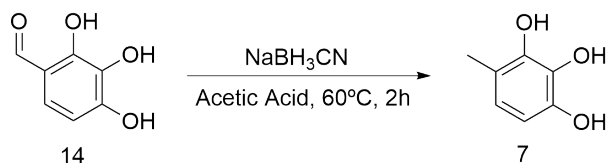


Figure 2.2: Synthesis of 4-methylpyrogallol (**7**) from 2,3,4-trihydroxybenzaldehyde (**14**)

The reaction was previously described by Honda et al. and adapted thereof.¹²⁹ The compound, 2,3,4-trihydroxybenzaldehyde (0.500g, 3.57 mmol), was dissolved in acetic acid (50 mg per mL, 2.24 mmol) followed by the addition of sodium cyanoborohydride (NaBH₃CN, 6.50 mmol) at 25°C. The temperature was increased to 60°C for two hours. Upon completion of the reaction, the product (**7**) was concentrated under vacuum and purified by column chromatography eluted with (DCM)/ (MeOH) 20:1 ratio (Fig.2.2).

4-methylpyrogallol (7): white solid, 159 mg, 35% ¹H NMR (400 MHz, D₂O), 6.56 (1H, d, J=8.3 Hz), 6.39 (1H, d, J=8.2 Hz), 2.06 (3H, s); ¹³C NMR (100 MHz, CDCl₃) δ 143.10 (C_{arom}), 142.50 (C_{arom}), 142.01 (C_{arom}), 125.20 (C_{arom}), 123.65 (C_{arom}), 113.30 (C_{arom}), 16.51 (CH₃)

Synthesis of compound 5: 4-(hydroxymethyl)catechol

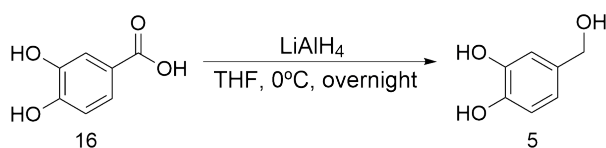


Figure 2.3: Synthesis of 4-(hydroxymethyl)catechol (**5**) from protocatechuic acid (**16**)

Protocatechuic acid (500 mg, 3.24 mmol) was dissolved in dry THF (30 mL) and the mixture cooled to 0°C. After cooling lithium aluminum hydride (LiAlH₄, 19.47mmol, 6 equiv.) was added to the solution and the reaction mixture kept under stirring overnight. After completion, aluminum complexes were destroyed through Fieser workup¹³⁰. Briefly, 1 mL of cold water (0°C) per gram of LiAlH₄ was added to the reaction mixture at 0°C, followed by 1 mL of NaOH 15 % (m/v) and 3 mL of water. The reaction mixture was then allowed to reach room temperature under stirring for 1 hour. Finally, the product was extracted with ethyl acetate dried with anhydrous sodium sulfate, filtrated and the solvent evaporated resulting in the final compound (**5**) (Fig. 2.3).

4-(hydroxymethyl)catechol (5): white solid, 209 mg, 46%, ¹H NMR (400 MHz, D₂O) 6.84 (2H, d, J=1.8 Hz), 6.83 (2H, d, J=7.7 Hz), 6.76 (1H, dd, J=2.3, 8.2 Hz), 4.42 (2H, s); ¹³C NMR (100 MHz, DMSO- d₆) δ 144.20 (C_{arom}), 143.80 (C_{arom}), 132.51 (C_{arom}), 117.36 (C_{arom}), 115.05 (C_{arom}), 114.00 (C_{arom}), 62.79 (CH₃)

Synthesis of Sulfate Derivatives

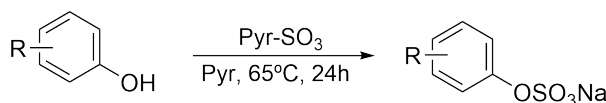


Figure 2.4: General scheme for the synthesis of sulfate derivatives.

In order to prepare sodium sulfated derivatives of the phenolic compounds, the procedure was tested with 0.1g of the phenolic compound and then the optimized reaction was scaled up to 0.5g. The chemical structures of the phenolic compounds utilized in the synthesis of sulfate derivatives are shown in

figure 2.5 . The general procedure was as follows: The compound (0.5g) was dissolved in 10 mL of anhydrous pyridine followed by the addition of sulfur trioxide pyridine complex (1 equiv.) and kept at 65°C under constant stirring for 24 hours. The reaction was quenched by the addition of water and the reaction mixture evaporated at 40°C under vacuum. The residue dissolved in water and washed with ethyl acetate in order to remove traces of the starting material (fig. 2.5). In order to produce the sodium salt, the compound was eluted with water in a Dowex 50W-X8 ion-exchange resin column, previously activated with sodium, by washing the column with a solution of sodium chloride 1M in water. The final product (compound **3S**, **4S**, **5S**, **6S**, **7S**, **8S**, **9S**, **10S**) was lyophilized and store at 2-8°C .

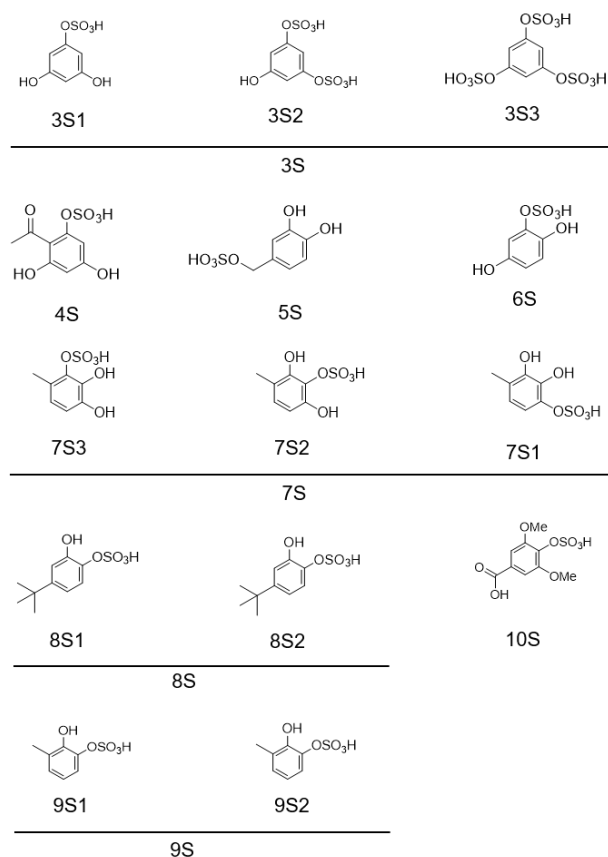


Figure 2.5: Structures of sulfate derivatives (obtained as sodium salts)

Phloroglucinol-O-sulfate (3S) - *Phloroglucinol-mono-sulfate (3S1)*, *Phloroglucinol-di-sulfate (3S2)*, *Phloroglucinol-tri-sulfate (3S3)*: yellow solid, 855 mg, 85%, a mixture of compounds was obtained 71:28:0.1. *Phloroglucinol-mono-sulfate (3S1)*: $^1\text{H NMR}$ (400 MHz, D_2O) δ 6.34 (2H, d, $J=1.6$ Hz), 6.26 (1H, d, $J=3.8$ Hz); $^{13}\text{C NMR}$ (100 MHz, D_2O) δ 157.36 (C-OH), 152.79 (C-OSO₃Na), 100.94 (C_{arom}), 100.42 (C_{arom}); *Phloroglucinol-di-sulfate*: $^1\text{H NMR}$ (400 MHz, D_2O) δ 6.77 (1H, d, $J=4.0$ Hz), 6.69 (2H, d, $J=1.3$ Hz); $^{13}\text{C NMR}$ (100 MHz, D_2O) δ ; 106.76 (2C, C_{arom}), 106.51 (C_{arom}) *Phloroglucinol-tri-sulfate*: $^1\text{H NMR}$ (400 MHz, D_2O) δ 7.15 (3H, s).

2,4,6-Trihydroxyacetophenone-O-sulfate (4S): yellow solid, 498.12 mg, 62%. $^1\text{H NMR}$ (400 MHz, DMSO-d_6) δ 13.22 (1H, s), 12.22 (1H, s), 5.83 (2H, s), 2.59 (3H, s); $^{13}\text{C NMR}$ (100 MHz, DMSO-d_6) δ 203.65 (C=O), 164.71 (C-4), 164.23 (C-2,C-6), 103.99 (C-1), 94.48 (C-3,C-5), 32.27 (CH_3).

4-(hydroxymethyl)catechol-O-sulfate (5S): white solid, 397 mg, 46%,. $^1\text{H NMR}$ (400 MHz, D_2O) δ 6.84 (1H, d, $J=1.8$ Hz), 6.83 (1H, d, $J=7.7$ Hz), 6.76 (1H, dd, $J=2.3, 8.2$ Hz), 5.19 (2H, s); $^{13}\text{C NMR}$ (100 MHz, D_2O) δ 120.44 (C_{arom}), 116.20(C_{arom}), 115.65(C_{arom}), 63.51 (CH_2)

4-Hydroxy-catechol-O-1-sulfate (6S):yellow solid, 859 mg, 95% $^1\text{H NMR}$ (400 MHz, D_2O) δ 7.11 (1H, d, $J=8.8$ Hz), 6.44 (1H, d, $J=2.9$ Hz), 6.36 (1H, dd, $J=2.9, 8.8$ Hz); $^{13}\text{C NMR}$ (100 MHz, DMSO-d_6) δ 123.83 (C_{arom}), 107.21 (C_{arom}), 104.10 (C_{arom})

4-Methyl-pyrogallol-O-sulfate (7S)- **4-Methyl-pyrogallol-O-1-sulfate (7S1)**, **4-methyl-pyrogallol-O-2-sulfate (7S2)** and **4-Methyl-pyrogallol-O-3-sulfate (7S3)**: white solid, 665 mg, 77%, a mixture of isomers was obtained with a ration of 70:25:5: ¹H NMR (400 MHz, D₂O) δ 6.87 (1H, d, J=7.6 Hz), 6.43 (1H, d, J=8.4Hz), 2.06 (3H, s); **4-methyl-pyrogallol-O-2-sulfate (7S2)**: ¹H NMR (400 MHz, D₂O) δ 6.79 (1H, d, J=8.4 Hz), 6.69 (1H, d, J=5.8 Hz), 2.12 (3H, s); **4-Methyl-pyrogallol-O-3-sulfate (7S3)**: ¹H NMR (400 MHz, D₂O) δ 6.67 (2H, d, J=5.3 Hz), 6.67 (2H, d, J=5.9 Hz), 2.15 (3H, s)

4-tert-butyl-catechol-O-sulfate (8S) - **4-tert-butyl-catechol-O-1-sulfate (8S1)**, and **4-tert-butylcatechol-O-2-sulfate (8S2)**: white solid, 323 mg, 40%, a mixture of isomers was observed 64:36. ¹H NMR (400 MHz, D₂O) δ 7.20 (2H, d, J=8.5 Hz), 7.01 (1H, d, J=2.3 Hz), 6.96 (1H, q, J=3.6 Hz), 1.20 (9H, s); **4-tert-butylcatechol-O-2-sulfate (8S2)**: ¹H NMR (400 MHz, D₂O) δ 7.35 (1H, d, J=2.4 Hz), 7.19 (2H, dd, J=2.4, 8.5 Hz), 6.89 (1H, d, J=8.5 Hz), 1.20 (9H, s); ¹³C NMR (100 MHz, D₂O) δ 151.38 (C_{arom}), 147.32(C_{arom}), 144.66(C_{arom}), 136.35(C_{arom}), 123.93 (C_{arom}), 122.37(C_{arom}), 120.01 (C_{arom}), 117.66 (C_{arom}), 116.77 (C_{arom}), 114.41 (C_{arom}), 33.89(Cq), 33.57(Cq), 30.53 (CH₃), 30.45 (CH₃).

3-Methyl-catechol-O-sulfate (9S) - **3-Methyl-catechol-O-1-sulfate (9S1)** and **3-methylcatechol-O-2-sulfate (9S2)**: white solid, 893 mg, 98%, a mixture of isomers was observed with the following proportion 50:50. ¹H NMR (400 MHz, D₂O) δ 7.13 (1H, d, J=8.3 Hz), 7.01 (2H, t, J=8.0 Hz), 6.79 (3H, d, J=7.0 Hz), 2.16 (3H, s); ¹³C NMR (100 MHz, D₂O) δ 126.94 (C_{arom}), 119.93 (C_{arom}), 114.90 (C_{arom}), 15.20 (CH₃); **3-methylcatechol-O-2-sulfate (9S2)**: ¹H NMR (400 MHz, D₂O) δ 7.03 (2H, d, J=7.9 Hz), 6.80 (3H, t, J=8.5 Hz), 6.78 (3H, d, J=8.0 Hz), 2.24 (3H, s); ¹³C NMR (100 MHz, D₂O) δ 128.15 (C_{arom}), 122.85 (C_{arom}), 120.15 (C_{arom}), 15.84 (CH₃);

Syringate-O-sulfate (10S), white solid, 314 mg, 83% ¹H NMR (400 MHz, DMSO-d₆) δ 7.29 (2H, s), 3.84 (6H, s); ¹³C NMR (100 MHz, DMSO-d₆) δ 170.03 (COONa), 152.8 (C_{arom}), 147.6 (Cq), 132.8 (qC_{arom}), 128.9 (C_{arom}), 106.9 (C_{arom}), 56.4 (CH₃)

Synthesis of Benzyl Syringate

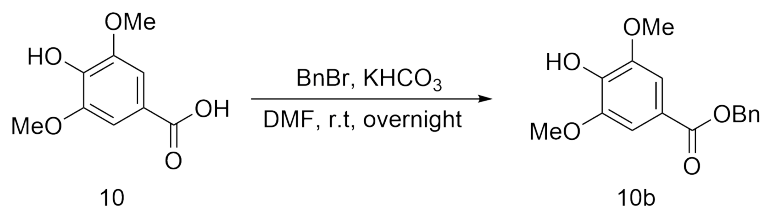


Figure 2.6: Synthesis of benzyl syringate (**10b**) from syringic acid (**10**)

In order to produce the glucuronide conjugate of syringic acid, first we needed to selectively benzylate the acid moiety of the molecule. For the preparation of benzyl syringate, syringic acid (250mg, 1.26mmol) was dissolved in DMF (15 mL) followed by the addition of benzyl bromide (216 mg, 1.26mol, 1 equiv.) and KHCO₃ (227 mg, 1.64 mmol, 1.3 equiv.). The reaction was stirred overnight. After completion the reaction was brought to a halt with water and extracted with dichloromethane. The solvent was dried with anhydrous sodium sulfate, filtered over celiteTM and the solvent evaporated affording the final product **10b** (fig. 2.6).

Benzyl syringate (10b): white solid, 288 mg, 83% ¹H NMR (400 MHz, CDCl₃) δ 7.48 - 7.32 (8H, m), 7.19 (2H, s), 3.86 (6H, d, J=21.3 Hz);

Synthesis of Glucuronide Derivatives

The synthesis of glucuronide derivatives involved five steps: first the specific deacetylation of the anomeric carbon; activation of the anomeric carbon with trichloroacetonitrile to afford the trichloroacetimidate; glucuronidation with the different phenols; deacetylation and ester hydrolysis afforded the final product for biological testing. The compounds used for glucuronidation were identical to the ones used in the synthesis of sulfate derivatives, (see figure 2.5), with the exception of syringic acid which was transformed in the benzyl syringate ester (see procedure described above).

Synthesis of Glucuronide Derivatives - Anomeric Deacetylation



Figure 2.7: Specific anomeric carbon deacetylation of the methyl glucuronate resulting in the correspondent 2,3,4-tri-O-acetyl-D-glucuronate methyl ester (**18**)

For the specific anomeric deacetylation, hydrazine acetate (270 mg, 2.66mmol, 1.1 equivalent) and 1,2,3,4-tetra-O-acetyl-D-glucuronate methyl ester (1g, 2.66 mmol, 1 equivalent) were dissolved in anhydrous DMF (30ml). The reaction was stirred at room temperature for two hours, and quenched by the addition of water. The final product was extracted with ethyl acetate and dried over MgSO_4 . The residue was purified by column chromatography eluted with hexane/ethyl acetate (1:1) to give 2,3,4-tri-O-acetyl-D-glucuronate methyl ester (Fig.2.7).

2,3,4-tri-O-acetyl-D-glucuronate methyl ester (**18**): yellow solid, 764 mg, 89 %. ^1H NMR (400 MHz, CDCl_3) δ 5.36-5.14 (m, 3H, H-2, H-3 and H-4), 4.90 (d, $J_{1,2} = 7.8$ Hz, 1H, H-1), 4.60 (d, $J_{4,5} = 8.8$ Hz, 1H, H-5), 3.77 (s, 3H, OCH_3), 2.08 (s, 3H, $\text{CH}_3\text{-OAc}$), 2.04 (s, 3H, $\text{CH}_3\text{-OAc}$), 2.03 (s, 3H, $\text{CH}_3\text{-OAc}$); ^{13}C NMR (100 MHz, CDCl_3) δ 170.2 (C=O), 170.1 (C=O), 169.7 (C=O), 168.5 (C=O, C-6), 90.17 (C-1), 70.7 (C-5), 69.5 (C-2, C-3, C-4), 53.0 (OCH_3), 20.6 ($\text{CH}_3\text{-OAc}$), 20.5 ($\text{CH}_3\text{-OAc}$), 20.5 ($\text{CH}_3\text{-OAc}$).

Synthesis of Glucuronide Derivatives - Trichloroacetimidate formation

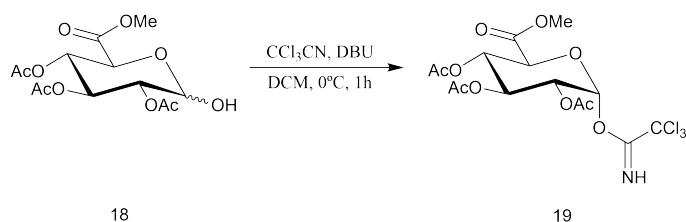


Figure 2.8: Synthesis of 2,3,4-tri-O-acetyl-1-O-trichloroacetimidoyl- α -D-glucuronate (**19**)

2,3,4-tri-O-acetyl-D-glucuronate methyl ester (764mg, 2.28 mmol, 1 equivalent) was dissolved in anhydrous dichloromethane (40 mg per mL) and the mixture cooled to 0°C followed by the addition of CCl_3CN (1.5 mL, 11.4mmol, 5 equivalents) and DBU (23 μL , 1.14mmol, 0.5 equivalent). The reaction was stirred for one hour until it reached room temperature. The solution was concentrated and purified by silica column chromatography eluted with Hex:EtOAc 1:1 (Fig.2.8).

2,3,4-tri-O-acetyl-1-O-trichloroacetimidoyl- α -D-glucuronate (**19**): yellow solid, 438 mg, 40%. ^1H NMR (400 MHz, CDCl_3) δ 5.40-5.13 (m, 3H, H-2, H-3 and H-4), 4.18 (d, $J_{1,2} = 7.8$ Hz, 1H, H-1), 3.75 (s, 3H, OCH_3), 2.12 (s, 3H, $\text{CH}_3\text{-OAc}$), 2.04 (s, 3H, $\text{CH}_3\text{-OAc}$), 2.03 (s, 3H, $\text{CH}_3\text{-OAc}$); ^{13}C NMR (100 MHz, CDCl_3) δ 170.0 (C=O), 169.4 (C=O), 169.2 (C=O), 166.3 (C=O, C-6), 90.17 (C-1), 72.1 (C-5), 71.5 (C-2, C-3, C-4), 53.0 (OCH_3), 20.6 ($\text{CH}_3\text{-OAc}$), 20.5 ($\text{CH}_3\text{-OAc}$), 20.5 ($\text{CH}_3\text{-OAc}$).

Synthesis of Glucuronide Derivatives - glucuronidation

Glucuronidation using $\text{BF}_3\cdot\text{OEt}_2$: For the glucuronidation, methyl 2,3,4-tri-O-acetyl-1-O-trichloroacetimidoyl- α -D-glucuronate (0.250 g, 0.5 mmol) and the phenol (0.7 equivalent) were dissolved in anhydrous DCM (19 mL) in the presence of 4 Å molecular sieves. The reaction was stirred at room temperature for thirty minutes and then cooled to -20°C . After five minutes of stirring at a constant temperature, $\text{BF}_3\cdot\text{OEt}_2$ (0.2 equivalent) was added dropwise. The reaction mixture was allowed to reach room temperature with constant stirring over four hours. After this time, the reaction was quenched by the addition of a saturated solution of sodium bicarbonate, extracted with dichloromethane, dried with

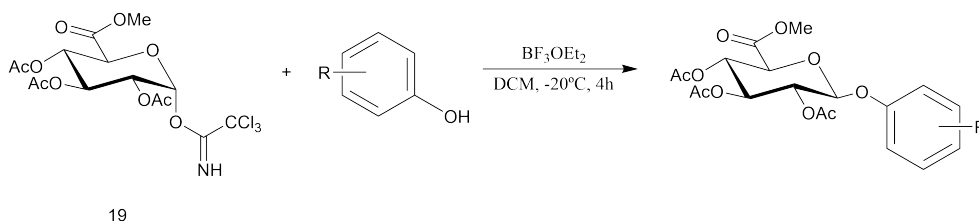


Figure 2.9: Glycosylation reaction - Synthesis of glucuronide derivatives using $\text{BF}_3 \cdot \text{OEt}_2$

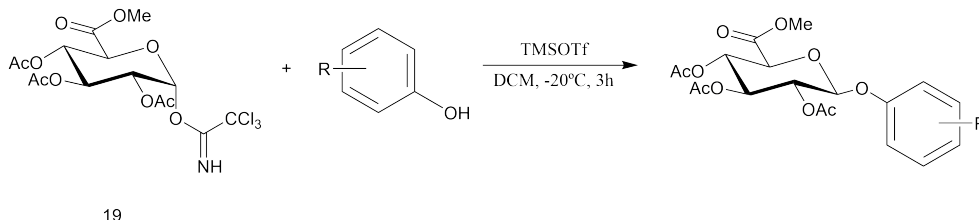


Figure 2.10: Glycosylation reaction - Synthesis of glucuronide derivatives using TMSOTf

anhydrous magnesium sulfate and concentrated. The product was purified by silica column chromatography eluted with Hex; EtAc (2:1) to give the glucuronate conjugate (fig. 2.9).

Glucuronidation using TMSOTf: Glucuronidation using TMSOTf followed the same protocol as for $\text{BF}_3 \cdot \text{OEt}_2$, however only 0.05 equivalent of TMSOTf were used and the reaction was completed at the end of 3 hours (2.10).

Synthesis of Glucuronide Derivatives - Deacetylation

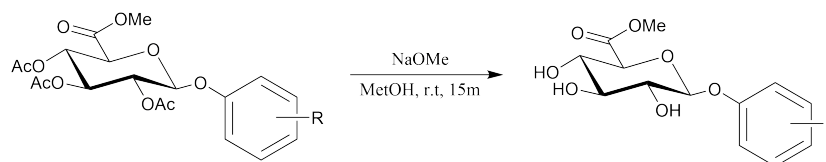


Figure 2.11: Synthesis of the deacetylated glucuronides

The glucuronide was dissolved in anhydrous methanol (1.5 mL per 100 mg) and a solution of sodium methoxide in anhydrous methanol (1M, 0.6 equivalent) added to the mixture. The solution was stirred at room temperature for 15 minutes. Then, previously activated Dowex 50W-X8, with a solution of hydrochloric acid (10%) in water, was added to the mixture until pH 7. After filtration and washing with methanol, the solvent was removed under vacuum and the crude purified by preparative chromatography eluted with ethyl acetate (fig. 2.11).

Synthesis of Glucuronide Derivatives - Ester hydrolysis

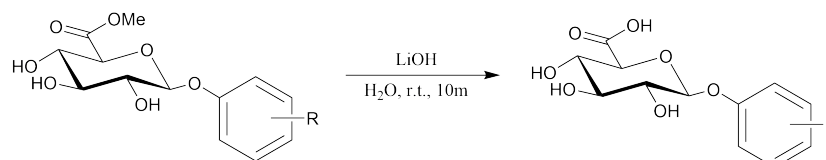


Figure 2.12: Synthesis of the glucuronide

A solution of lithium hydroxide in water (1M, 2 equivalents) was added to the glucuronide derivatives dissolved in water (1 mL per 100 mg), and the mixture stirred at room temperature for 10 minutes. The crude mixture was purified by the addition of previously activated Dowex 50W-X8 with a solution of

hydrochloridric acid (10%) in water. The final product (compound **7G**, **8G**, **9G** and **10G**) was obtained after solvent evaporation (fig. 2.13).

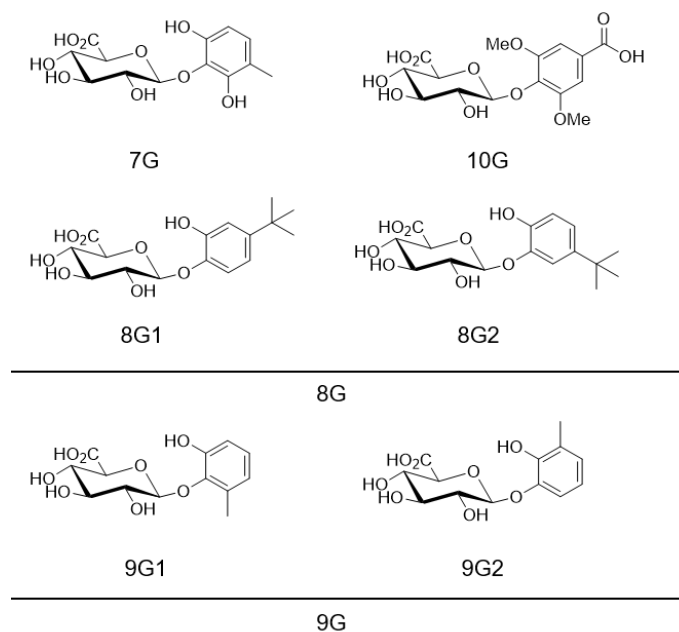


Figure 2.13: Structure of glucuronide derivatives

4-Methyl-pyrogallol-O-Glucuronide (7G): white solid, 33 mg, overall yield 19% ^1H NMR (400 MHz, CD_3OD) δ 6.75 (1H, d, $J=10.8$ Hz), 6.31 (1H, d, $J=7.7$ Hz), 4.66 (1H, d, $J=7.7$ Hz, H-1), 3.99 (1H, d, $J=10.8$ Hz, H-5), 3.62 - 3.47 (3H, m, H-2, H-3, H-4), 2.12 (3H, s, CH_3);

4-tert-butyl-catechol-O-glucuronide (8G) - **4-tert-butyl-catechol-O-1-glucuronide (8G1)**, **4-tert-butyl-catechol-O-2-glucuronide (8G2)**: white solid, 62 mg, overall yield 35%, a mixture of isomers was found 45:55. ^1H NMR (400 MHz, CD_3OD): δ 7.06 (1H, d, $J=9.2$ Hz), 6.99 (1H, dd, $J=2.6, 8.6$ Hz), 6.92 (1H, d, $J=2.2$ Hz), 3.99 (1H, d, $J=3.7$ Hz, H-1), 3.92 (1H, d, $J=6.5$ Hz, H-5), 3.70-3.49 (m, H-2, H-3, H-4), 1.28 (9H, s, $\text{C}(\text{CH}_3)_3$); 3.70-3.49 (m, H-2, H-3, H-4), 1.28 (9H, s, $\text{C}(\text{CH}_3)_3$); **4-tert-butyl-catechol-O-2-glucuronide (8G2)** δ 7.25 (1H, d, $J=2.6$ Hz), 6.83 (1H, dd, $J=2.3, 8.5$ Hz), 6.78 (1H, d, $J=8.8$ Hz), 4.02 (1H, d, $J=3.3$ Hz, H-1), 3.95 (1H, d, $J=4.9$ Hz, H-5), 3.70-3.49 (m, H-2, H-3, H-4), 1.28 (9H, s, $\text{C}(\text{CH}_3)_3$); 175.0 (C=O), 173.3 (C=O), 148.3 (C_{arom}), 148.0 (C_{arom}), 131.6 (C_{arom}), 122.8 (C_{arom}), 114.8 (C_{arom}), 113.2 (C_{arom}), 100.6 (C-1), 75.8 (C-3), 75.7 (C-5), 73.0 (C-2), 72.0 (C-4), 55.5 (OCH_3)

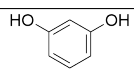
3-methylcatechol-O-Glucuronide (9G) - **3-methylcatechol-O-1-Glucuronide (9G1)**, **3-methylcatechol-O-2-Glucuronide (9G2)**: white solid, 49 mg, overall 29% a mixture of isomers was found 35:65. ^1H NMR (400 MHz, CD_3OD) δ 128.15 (C_{arom}), 122.85 (C_{arom}), 120.15 (C_{arom}), 15.84 (CH_3); **3-methylcatechol-O-1-Glucuronide (9G1)** δ 6.99 (1H, d, $J=8.4$ Hz), 6.83 (1H, d, $J=7.9$ Hz), 6.68 (1H, t, $J=7.7$ Hz), 4.77 (1H, d, $J=8.7$ Hz, H-1), 3.94 (1H, d, $J=10.0$ Hz, H-5), 3.64 (1H, d, $J=9.1$ Hz, H-4), 3.59-3.49 (2H, m, H-2, H-3) 2.21 (3H, s, CH_3); **3-methylcatechol-O-2-Glucuronide (9G2)** δ 6.90 (1H, t, $J=7.9$ Hz), 6.71 (1H, d, $J=9.0$ Hz), 6.65 (1H, d, $J=7.5$ Hz), 4.63 (1H, d, $J=7.6$ Hz, H-1), 3.81 (1H, d, $J=9.8$ Hz, H-5), 3.63 (1H, d, $J=9.2$ Hz, H-4), 3.59-3.49 (3H, m, H-2, H-3), 2.32 (3H, s, CH_3); ^{13}C NMR (400 MHz, CD_3OD) δ 175.2 (C=O), 172.3 (C=O), 171.8 (C=O), 149.9 (C_{arom}), 147.9 (C_{arom}), 144.8 (C_{arom}), 144.0 (C_{arom}), 128.2 (C_{arom}), 126.1 (C_{arom}), 124.8 (C_{arom}), 122.6 (C_{arom}), 117.9 (C_{arom}), 117.2 (C_{arom}), 116.0 (C_{arom}), 115.4 (C_{arom}), 101.0 (C-1), 100.2 (C-1), 76.2 (C-3), 75.1 (C-5), 72.6 (C-2), 71.6 (C-4).

Syringic-O-Glucuronide (10G), white solid, 30 mg, overall yield 19%. ^1H NMR (400 MHz, MeOD) δ 7.36 (2H, s), 5.11 (1H, d, $J=8.7$ Hz, H-1), 3.79 (1H, d, $J=8.7$ Hz, H-5), 3.64 (1H, t, $J=8.2$ Hz, H-4), 3.57 (1H, t, $J=7.6$ Hz, H-2), 3.47 (1H, t, $J=8.2$ Hz, H-3); ^{13}C NMR (400 MHz, CD_3OD) δ 175.4 (C=O), 144.7 (C_{arom}), 125.2 (C_{arom}), 116.9 (C_{arom}), 111.9 (C_{arom}), 100.5 (C-1), 76.2 (C-3), 75.2 (C-5), 72.7 (C-4), 71.7 (C-2), 55.9 (OCH_3).

2.1.2 Synthesis of Second Iteration Compounds

The synthesis of second iteration compounds was based on the biological evaluation of the first set of synthesized compounds. Compound **3S** (phloroglucinol sulfate or 3,5-dihydroxyphenyl sulfate) and **7** (4-methyl-pyrogallol or 4-methyl-benzene-1,2,3-triol) were the structural base selected for the synthesis of new derivatives. Compound **12** was acquired commercially. The results obtained for the synthesis are shown in table 3.3.

Table 2.3: Phenolic compounds commercially acquired for the synthesis of second iteration derivatives

Structure	Nu.	Name	Manufacturer
	11	benzene-1,3-diol	Sigma-Aldrich

Synthesis of compound 11: methoxyphloroglucinol

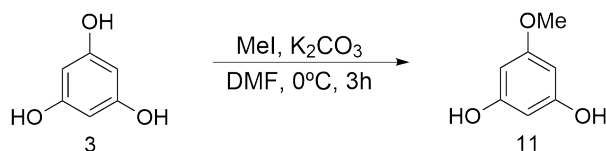


Figure 2.14: Synthesis of methoxyphloroglucinol (**11**) from phloroglucinol (**3**)

Phloroglucinol (0.500g, 3.96 mmol) was dissolved in DMF (7 mL) followed by the addition of potassium carbonate (1.095g, 7.93 mmol, 2 equiv.) and the temperature lowered to 0°C. After 5 minutes methyl iodide (0.247 mL, 3.96 mmol, 1 equiv.) was added drop wise and reaction stirred for 3 hours at 0°C. Ethyl acetate (21 mL) was added and the reaction mixture washed with water followed by washing with brine (sodium sulfate), filtration and concentration of the solvent under vacuum. The product (**11**) was purified by column chromatography eluted with Hex:EtAc 1:1 (fig.2.14).

Methoxy-phloroglucinol (11S) yellow solid, 356 mg, 64%: $^1\text{H NMR}$ (400 MHz, D_2O) δ 6.45 (1H, s), 6.40 (1H, s), 6.33 (1H, s), 3.73 (3H, s); $^{13}\text{C NMR}$ (100 MHz, D_2O) δ 101.7 (C_{arom}), 99.6 (C_{arom}), 99.4 (C_{arom}), 55.7 (C_3).

Synthesis of compound 13: 4-(hydroxymethyl)pyrogallol

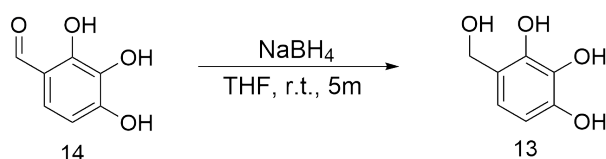


Figure 2.15: Synthesis 4-(hydroxymethyl)pyrogallol (**13**) from 2,3,4-trihydrobenzaldehyde (**14**)

2,3,4-Trihydrobenzaldehyde (0.300g, 1.97 mmol), was dissolved in a solvent system composed of THF and H_2O (6 mL and 0.2 mL respectively), followed by the addition of NaBH_4 (0.064g, 1.97 mmol, 1 equiv.). 4 mL of methanol were added followed by 2 mL of water and a saturated solution of ammonium chloride until the reaction mixture reached pH 7. The reaction mixture was vigorously stirred for 10 minutes, diluted with methanol, washed with water, dried with sodium sulfate, filtered and the solvent evaporated giving the final product (**13**) (Fig.2.15).

4-hydroxymethylpyrogallol (13): white solid, 456 mg, 90% $^1\text{H NMR}$ (400 MHz, D_2O) δ 6.50 (1H, d, $J=9.3$ Hz), 6.27 (1H, d, $J=10.4$ Hz), 4.46 (1H, s); $^{13}\text{C NMR}$ (100 MHz, D_2O) δ 160.0 (qC_{arom}), 157.7 (Cq_{arom}), 155.1 (Cq_{arom}), 118.1 (C_{arom}), 107.2 (C_{arom}), 55.6 (CH_2)

Synthesis of compound 15: 2,3,4-trihydroxybenzoic acid



Figure 2.16: Synthesis of 2,3,4-trihydroxybenzoic acid (**15**) from 2,3,4-trihydroxybenzaldehyde (**14**)

2,3,4-Trihydroxybenzaldehyde (0.250g, 1.64 mmol) was dissolved in DMF (8 mL) followed by the addition of Oxone (Potassium peroxymonosulfate, 0.499g, 1.64 mmol, 1 equiv.) and the reaction stirred for 3 hours at room temperature. The mixture was filtered over celite and the solvent evaporated under vacuum giving the final product (**15**) (Fig.2.16).

2,3,4-trihydroxybenzoic acid (**15**): brown solid, 496 mg, 90% ¹H NMR (400 MHz, D₂O) 6.56 (1H, d, J=9.4 Hz), 6.40 (1H, d, J=8.4 Hz). ¹³C NMR (100 MHz, DMSO-d₆) δ 172.33 (C=OOH), 151.55 (C_{arom}), 132.04 (C_{arom}), 121.20 (C_{arom}), 108.51 (C_{arom}), 103.44 (C_{arom})

Synthesis of the second iteration sulfate derivatives

In order to produce sulfate derivatives of second iteration compounds the procedure followed was the same as described above for the first iteration compounds. The list of compounds used as starting materials is shown in figure 2.17. Results from the synthesized products, **3S**, **11S** and **12S** is shown in table 3.3.

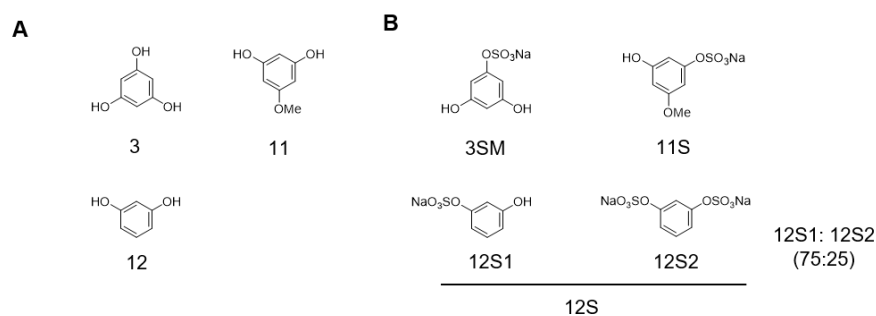


Figure 2.17: Structure of compounds used the synthesis of second iteration sulfate conjugates

Phloroglucinol-mono-sulfate (**3SM**): white solid, 750 mg 83%. ¹H NMR (400 MHz, D₂O) δ 6.33 (2H, d, J=2.16Hz) 6.23 (1H, dd, J= 2.16); ¹³C NMR (100 MHz, D₂O) δ 157.36 (C-OH), 152.79 (C-OSO₃Na), 100.94 (C_{arom}), 100.42 (C_{arom});

Methoxy-phloroglucinol-O-sulfate (**11S**) white solid, 717 mg, 87%: ¹H NMR (400 MHz, D₂O) δ 6.45 (1H, s), 6.40 (1H, s), 6.33 (1H, s), 3.73 (3H, s); ¹³C NMR (100 MHz, D₂O) δ 101.7 (C_{arom}), 99.6 (C_{arom}), 99.4 (C_{arom}), 55.7 (C₃)

Resorcinol-O-sulfate (**12S**) - *resorcinol mono-sulfate* (**12S1**) and *resorcinol di-sulfate* (**12S2**): white solid, 1.058g, 98%, a mixture of isomers was obtained 75:25. *resorcinol mono-sulfate* (**12S1**) ¹H NMR (400 MHz, D₂O) δ 7.41 (1H, t, J=8.3 Hz), 7.21 (2H, s), 7.19 (2H, d, J=7.6 Hz). *resorcinol di-sulfate* (**12S2**): 7.25 (1H, t, J=7.9 Hz), 6.82 (3H, d, J=8.6 Hz), 6.78 (3H, s), 6.76 (3H, d, J=9.7Hz); Mixture of isomers: ¹³C NMR (100 MHz, D₂O) δ 156.52 (C_{qarom}), 152.05 (C_{qarom}), 151.60 (C_{qarom}), 130.55 (C_{arom}), 130.41 (C_{arom}), 119.18 (C_{arom}), 115.12 (C_{arom}), 113.30 (C_{arom}), 113.26 (C_{arom}), 108.75 (C_{arom}) .

2.2 Biological Evaluation

2.2.1 Cell culture

N9 microglia cell line

N9 murine microglial cell line (CVCL-0452) were kindly provided by Dr. Teresa Faria Pais. Cells were cultured in EMEM (Eagle Minimum Essential Media, Sigma-Aldrich) supplemented with 10% FBS (Fetal bovine serum, Gibco), 200mM L-glutamine (Sigma-Aldrich) and maintained at 37°C, 5% CO₂. Cells were subcultured every two to three days at a confluence of 60%. Detachment was obtained using vigorous agitation, no chemical detachment agent was used.

SH-SY5Y neuroblastoma cell line

SH-SY5Y (ATCC® CRL-2266™) were cultured in DMEM:F12 supplemented with 10% FBS and 1% Penicillin-Streptomycin (Thermo-Scientific) and maintained at 37°C, 5% CO₂. Cells were subcultured every three to four days at confluency (80-90%). For subculture cells were detached using Trypsin-EDTA 0.05% for 1 to 2 minutes in order to increase neuronal population over epithelial. For seedings, cells were detached using Accutase (Thermo-Scientific), for 5 minutes, in order to minimize cell clumping.

For differentiation cells were seeded in 96 well plates (4x10⁵ cells/well) or 24 well plates (4x10⁴ cells/well). After 24 hours media was discarded cells and fresh media containing 10 μM of all-trans retinoic acid (Sigma-Aldrich) were added. Media was replaced every 48 hours for 7 days. For every media change cells were washed with PBS.¹³¹

HBMEC cell line

Human Brain microvascular endothelial cell (HBMEC) line cell line were cultured in RPMI 1640 (Roswell Park Memorial Institute medium, (Sigma-Aldrich) supplemented with 10% FBS, 10% NuSerum IV (BD Biosciences, Erembodegem, Belgium), 1% Non-essential amino acids (Sigma-Aldrich), 1% minimal essential medium (Sigma-Aldrich), 1mM sodium pyruvate (Sigma-Aldrich), 2mM L-glutamine (Sigma-Aldrich) and 1% Penicillin-Streptomycin (Thermo-Scientific). Cells were kept at 37°C, 5% CO₂ and subcultured every three to four days at confluence with trypsin-EDTA 0.05%.

In order to evaluate compound transport, cell were seeded on polyester transwell inserts (0.4 μm, Corning Costar Corp., USA), coated with rat-tail collagen-I (BD Biosciences) at a density of 5x10⁴ cells/insert and treated after 8 days in culture, after monolayer formation.

2.2.2 Anti-inflammatory potential of synthesized compounds

Cellular model of neuroinflammation

N9 murine microglial cells were seeded (2.5x10⁵ cells.mL⁻¹) in twenty-four well plates from Thermo-Fisher (1mL per well) and then pre-incubated at a confluence of 50% with 5μM of each synthesized compound. After a period of six hours the medium was discarded and cells were washed once with fresh medium prior to addition of fresh medium with lipopolysaccharide from Escherichia coli 055:B5 (LPS, Sigma–Aldrich) at a final concentration of 300 ng/mL.

Cytokine analysis

Cell supernatants were collected twenty-four hours after the stimulus with LPS and immediately stored at -80°C. The cytokine (Murine TNF-α) release was assayed by sandwich ELISA according to the manufacturer's instructions (PeproTech; Princeton Business Park, Rocky Hill NJ, United States). All the reagents and plates used were provided in the kit. Absorbance (Abs) was read in a Synergy HT microplate reader (Biotek, Winooski, USA) at 25°C for 35 min, with 5 min intervals. Readings were taken at Abs_{405nm} and corrected with Abs_{650nm}. Reliable readings were selected according to manufacturer's instructions (Abs_{405nm} between 0.2 for the lowest value of the standard curve and 1.2 for the highest). A mathematical 4 parameter logistic equation describing the standard curve (in logarithmic units) was created using GraphPad Prism 6 (GraphPad Software, California, USA). The amount of cytokine present was calculated as relative to control (LPS stimulated cells with compounds).

Compound toxicity in microglia

Cell viability was estimated through the metabolic capacity of viable cells to reduce the dye resazurin to resorufin (CellTiter-Blue®, Promega Corporation, Madison, Wisconsin, United States). The procedure was as follows: after media collection for cytokine analysis, fresh media containing resazurin (20 μL per 100 μL of media) was added and the cells incubated at 37°C with 5% CO_2 , for the duration of one hour (during the procedure all light exposure sources were reduced as much as possible). After the incubation period, fluorescence (excitation 560nm and emission 590nm) was measured in a Synergy HT microplate reader (Biotek, Winooski, USA). The average fluorescence background of cell culture media containing resazurin but no cells was subtracted. Results are shown, in percentage, as metabolic capability relative to control.

2.2.3 Membrane permeation

In silico predictions of pharmacokinetic properties of the compounds

Maestro software (Schrödinger Release 2018-1: Maestro, Schrödinger, LLC, New York, NY, 2018.) was used to create the three-dimensional structures of the tested compounds. The global minimal energy geometry was calculated using LigPrep application (Schrödinger Release 2018-1: LigPrep, Schrödinger, LLC, New York, NY, 2018.) and used as an input for QikProp application (Schrödinger Release 2018-1: QikProp, Schrödinger, LLC, New York, NY, 2018.) in order to calculate theoretical descriptors of relevance for compound permeability through the Blood Brain Barrier. The following theoretical parameters were evaluated for the different compounds: apparent Caco-2 and MDCK cell permeability; predicted CNS activity; predicted brain/blood partition coefficient; predicted binding to human serum albumin; predicted octanol/water coefficient; Van der Waals surface area of polar nitrogen and oxygen atoms (PSA) together with other parameters not shown in this work.

HBMEC monolayer integrity

In order to confirm that the compounds were able to pass across the cell monolayer and not due to its disruption or incorrect assemble two assays were conducted: BBB integrity and paracellular permeability.

Blood brain barrier integrity was evaluated by measuring trans-endothelial electrical resistance (TEER) as previously reported by our group⁷⁵. TEER readings were performed using an EVOM (World Precision Instruments, Inc. USA) resistance meter. Briefly two electrodes are used, one in the top portion of the membrane and the other on the bottom, and electrical resistance is measured in ohms after 1 minute of stabilization. Readings were performed at days 3, 5 and 8 before the addition of the compounds and at the end of incubation time. TEER was calculated as percentage of variation from average control readings, after deducting the values of empty insert.

To assess paracellular permeability of the monolayer after exposure to the compounds, a permeation assay was conducted with sodium fluorescein (Sigma-Aldrich) as described before⁷⁵. For this, cell culture inserts were transferred to new plates containing Ringer–Hepes solution (118 mM NaCl, 4.8 mM KCl, 2.5 mM CaCl_2 , 1.2 mM MgSO_4 , 5.5 mM D-glucose, 20 mM Hepes, pH 7.4) and the sodium fluorescein solution (10 mg/mL sodium fluorescein, 1% BSA in Ringer–Hepes buffer) was added to the upper chamber. The process is then repeated three times at 20, 40 and 60 minutes. At the end of each time point the plates are collected and fluorescein levels are determined in a Synergy HT microplate reader (excitation 400nm and emission 525nm). The endothelial permeability coefficient P_e was calculated as percentage and corrected to control.¹³²

Compound permeation assay

Compound transport was evaluated as the ability of compounds to cross the monolayer present in the semi-permeable membranes of the transwell inserts. In this system the wells are divided in two chambers, the upper and lower chambers, each representing the two physiological compartments, blood and brain, correspondingly. The confluence monolayer HBMEC cells were incubated with 5 μM of each compound in HBSS with calcium and magnesium (Hank's Balanced Salt Solution, Gibco) and supplemented with 0.1% FBS. HBMEC cells were incubated with the compounds for two hours.

In the end of the experiment, cell medium from the upper and lower compartments were collected and frozen at -80°C until analysis in a LC-Orbitrap MS for the percentage of compounds in both compartments.

2.2.4 Neuroprotective effects in SH-SY5Y

Compound toxicity and neuroprotective effect

At the seventh day of differentiation, media was discarded, cells washed with PBS and fresh media containing $5\mu\text{M}$ of each compound was added. Cell metabolic capacity was assessed using resazurin (CellTiter-Blue[®], Promega Corporation, Madison, Wisconsin, United States) and luciferin (Celltiter-Glo[®], Promega Corporation, Madison, Wisconsin, United States). In order to evaluate the neuroprotective effects of the compounds cells were incubated with the compound for 6 hours, followed by an oxidative insult using tert-butylperoxyde (t-BHP) at a concentration of $20\mu\text{M}$ for 16 hours. For toxicity, the compounds were incubated for 24 hours followed by the addition of the corresponding reagents.

For CellTiter-Blue[®], fluorescence (excitation 560nm and emission 590nm) was measured in a Synergy HT microplate reader for 3 hours. The results are expressed as relative to control.

In the case of Celltiter-Glo[®], the reagent was added to cells and incubated for 10 minutes. After this time the contents were transferred to a costar solid white 96 well plate (Corning[®], New York, U.S.) and luminescence was read in a Synergy HT microplate reader. The results are given as relative to control.

Flow cytometry analysis

To further evaluate the effects of the compounds to prevent cell death, the percentage of live, apoptotic and dead cells was calculated using annexin V/Propidium iodide (PI) double staining through flow cytometry. Briefly, cells were detached using accutase and diluted in $100\mu\text{L}$ of annexin binding buffer containing $3\mu\text{L}$ annexin V-FITC and $10\mu\text{L/mL}$ PI per condition into a FACS tube, and incubated for fifteen minutes in the dark at 37°C before reading the samples in a Sysmex CyFlow Cube 1 (Sysmex, Goerlitz, Germany). Compensation was adjusted using unstained cells. The data was analyzed in FlowJo software (FlowJo LLC, Oregon U.S). In summary, scatter plots were referenced to annexin V (FL-1) vs propidium iodide (FL-3). Quadrants were created using control cells as reference. The percentage of events was calculated automatically by FlowJo upon applying the quadrants to all samples. Cells were considered dead in quadrant two, apoptotic in quadrant three and viable in quadrant four. Population graphs were performed in GraphPad Prism 6.

2.3 Statistical analysis

The results reported in this work are the average of triplicates of at least three biological independent experiments and are represented as $\pm\text{SD}$ unless stated otherwise. Statistical analysis was performed using GraphPad Prism 6 software (GraphPad Software, California, USA). One-Way ANOVA with Turkey's post multiple comparison test was executed in order to verify differences between multiple conditions.

3. Results

3.1 Synthesis of chemical derivatives- First Iteration derivatives

3.1.1 Synthesis of catechol and pyrogallol (metabolic) derivatives

A library of compounds was built based upon the chemical structure of catechol and pyrogallol sulfate conjugates, in order to improve their ability to reduce the release of inflammatory cytokines, more precisely $\text{TNF}\alpha$. Since previous studies have focused on these sulfate conjugates that are present in blood circulation, all compounds to be evaluated also had a sulfate conjugate. Nevertheless, another common type of conjugation found in circulation, glucuronidation, was also employed.

The compounds used in the synthesis of metabolic derivatives were acquired commercially with the exception of 4-(hydroxymethyl)-catechol (**5**) synthesized from compound protocatechuic acid (**16**) and 4-methylpyrogallol (**7**) from 2,3,4-trihydroxybenzaldehyde (**15**) which were synthesized *in house*.

In brief, 8 compounds were used for the synthesis of their sulfate and glucuronide conjugates. Due to the existence of isomers, 14 sulfates were synthesized as well as 6 glucuronides. In total 20 compounds, that to our knowledge were never synthesized before have been prepared. The compounds used for comparison, pyrogallol and catechol sulfates, were previously synthesized in the Bioorganic Chemistry Lab.

The chemical structures of the synthesized compounds are represented in figure 3.5. The number of isomers obtained, the ratio, overall yield and morphological features are listed in table A.4.

The 20 compounds obtained were used in 12 test conditions, due to the inability to isolate the isomers produced by this synthetic route.

In the synthesis of sulfate derivatives, the number of isomers obtained corresponded to the number of hydroxyl groups present in the benzene ring, with the exception of compounds **4S**, **5S** and **10S** where only one isomer was found (table A.4). For practical reasons (in order to not further increase the number of testing conditions), the isolation of the isomers was not pursued at this point.

Glucuronidation was successful for compounds **7-10**, however the chemical synthetic route was not successful for the remaining compounds: the hydrolysis product was obtained instead. Various alternatives were tested: 1) Varying the time of the reaction from 2 hours to 4 and 5 hours; 2) Increasing the number of equivalents of the promoter $\text{BF}_3\cdot\text{OEt}_2$; 3) Substitution of the reaction activator, switching $\text{BF}_3\cdot\text{OEt}_2$ with TMSOTf ; 4) Protecting various hydroxyl groups through acetylation (using only half the number of equivalents of the acetylation reagent relative to the number of hydroxyl of the compound). Nevertheless none of these modifications were successful.

All compounds were characterized by proton and carbon NMR and Fourier Transformed Infrared spectroscopy. Spectral data containing weak signals and possibly missing the assignment of atoms were omitted. For the correct assignment of the compounds, as well as the identification of the presence of isomers, two dimensional NMR experiments (COSY and HMQC) were used. The ratios between isomers were calculated by comparing the integral area of a hydrogen peak in ^1H of one isomer with the hydrogen in the same chemical position of the other isomer. At least three peaks were used in order to average the ratio between isomers.

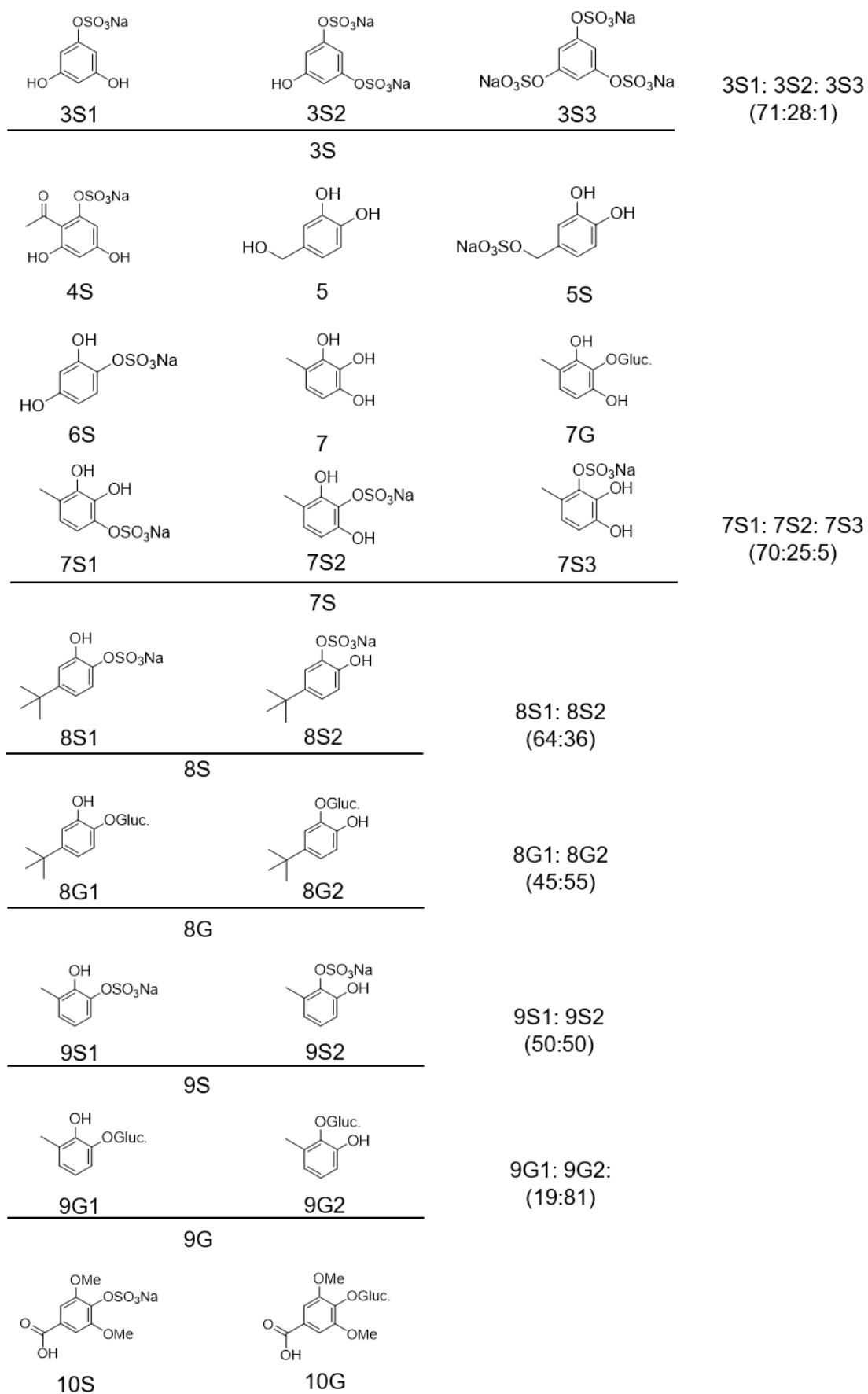


Figure 3.1: Chemical structures of the synthesized compounds. The ratios present in case of a mixture of isomers is shown in the figure. Further information is included in tables 3.1 and 3.2

Table 3.1: List of chemical synthesized compounds (compounds are numbered in the order by which they were evaluated)

Nr.	Sub Nr.	Name	IUPAC	Iso.	Iso. ratio	Yield (%)	Morphology
3S		Phloroglucinol-O-sulfate	-	3	71:28:01	85	Yellow Solid
	3S1	Phloroglucinol-mono-sulfate	Sodium 3,5-dihydroxyphenyl sulfate	1(3)	71	60(85)	-
	3S2	Phloroglucinol-di-sulfate	Sodium 5-hydroxy-1,3-phenylene bi (sulfate)	2(3)	28	24(85)	-
	3S3	Phloroglucinol-tri-sulfate	Sodium benzene-1,3,5-triyl tri(sulfate)	3(3)	01	1(85)	-
4S		2,4,6-trihydroxyacetophenone-O-sulfate	Sodium 4-acetyl-3,5-dihydroxyphenyl sulfate	-	-	62	yellow solid
5		4-(hydroxymethyl)-catechol	3,4-dihydroxybenzoic acid	-	-	46	White solid
5S		4-(hydroxymethyl)-catechol-O-sulfate	Sodium 3,4-dihydroxybenzyl sulfate	-	-	95	White solid
6S		4-hydroxy-catechol-O-sulfate	Sodium 3,4-dihydroxyphenyl sulfate	-	-	95	Yellow solid
7		4-methyl-pyrogallol	4-methylbenzene-1,2,3-triol	-	-	35	white solid
7S		4-methyl-pyrogallol-O-sulfate	-	3	70:25:5	77	White solid
	7S3	4-methyl-pyrogallol-O-1-sulfate	Sodium 2,3-dihydroxy-4-methylphenyl sulfate	1(3)	70	58(77)	-
	7S2	4-methyl-pyrogallol-O-2-sulfate	Sodium 2,6-dihydroxy-3-methylphenyl sulfate	2(3)	25	14(77)	-
	7S1	4-methyl-pyrogallol-O-3-sulfate	Sodium 2,3-dihydroxy-6-methylphenyl sulfate	3(3)	5	1(77)	-
7G		4-methyl-pyrogallol-O-glucuronide	(2S,3S,4S,5R,6S)-6-(2,6-dihydroxy-3-methylphenoxy)-3,4,5-trihydroxytetrahydro-2H-pyran-2-carboxylic acid	-	-	19	White solid
8S		4-tertbutylcatechol-O-sulfate	Sodium 4-tert-butyl-2-hydroxyphenyl sulfate	2	64:36	40	white solid
	8S1	4-tertbutylcatechol-O-1-sulfate	Sodium 4-tert-butyl-2-hydroxyphenyl sulfate	1(2)	64	26(40)	-
	8S2	4-tertbutylcatechol-O-2-sulfate	Sodium 5-tert-butyl-2-hydroxyphenyl sulfate	2(2)	36	14(40)	-
8G		4-tert-butylcatechol-O-glucuronide	(2S,3S,4S,5R,6S)-6-(5-(tert-butyl)-2-hydroxyphenoxy)-3,4,5-trihydroxytetrahydro-2H-pyran-2-carboxylic acid	2	45:55	35	white solid
	8G1	4-tert-butylcatechol-O-1-glucuronide	(2S,3S,4S,5R,6S)-6-(4-(tert-butyl)-2-hydroxyphenoxy)-3,4,5-trihydroxytetrahydro-2H-pyran-2-carboxylic acid	1(2)	45	16(35)	-
	8G2	4-tertbutylcatechol-O-2-glucuronide	(2S,3S,4S,5R,6S)-6-(4-(tert-butyl)-2-hydroxyphenoxy)-3,4,5-trihydroxytetrahydro-2H-pyran-2-carboxylic acid	2(2)	55	19(35)	-

Table 3.2: List of chemical synthesized compounds (compounds are numbered in the order by which they were evaluated) - Continued

Nr.	Sub Nr.	Name	IUPAC	Iso.	Iso. ratio	Yield (%)	Morphology
9S		3-methyl-Catechol-O-sulfate		2	50:50	98	white solid
	9S1	3-methyl-Catechol-O-1-sulfate	Sodium 2-hydroxy-3-methylphenyl sulfate	1(2)	50	49(98)	-
	9S2	3-methyl-Catechol-O-2-sulfate	Sodium 2-hydroxy-6-methylphenyl sulfate	2(2)	50	49(98)	-
9G		3-methyl-catechol-O-glucuronide		2	19:81	29	white solid
	9G1	3-methyl-catechol-O-1-glucuronide	(2S,3S,4S,5R,6S)-3,4,5-trihydroxy-6-(2-hydroxy-6-methylphenoxy)tetrahydro-2H-pyran-2-carboxylic acid	1(2)	19	6(29)	-
	9G2	3-methyl-Catechol-O-2-glucuronide	2S,3S,4S,5R,6S)-3,4,5-trihydroxy-6-(2-hydroxy-3-methylphenoxy)tetrahydro-2H-pyran-2-carboxylic acid	2(2)	81	23(29)	-
10S		Syringic acid-O-sulfate		-	-	83	White solid
10G		Syringic acid-O-glucuronide	1-(4-hydroxy-3,5-dimethoxyphenyl)-2-phenylethan-1-one (2S,3S,4S,5R,6S)-6-(4-carboxy-2,6-dimethoxyphenoxy)-3,4,5-trihydroxytetrahydro-2H-pyran-2-carboxylic acid	-	-	19	White solid

3.2 Biological evaluation of the synthesized compounds

3.2.1 Pyrogallol-2-sulfate, the isomer present in higher concentration in blood stream, showed increased protection over pyrogallol-1-sulfate

In a previous study conducted by our group, we demonstrated that the two sulfate isomers of pyrogallol: pyrogallol-1-sulfate (**2S1**) and pyrogallol-2-sulfate (**2S2**), were present in the blood circulation at a max concentration of $11.43 \mu\text{M} \pm 0.67 \mu\text{M}$ and 0.65 ± 0.33 respectively⁹². Recently, we stated that these molecules can be further metabolized and converted to their unmetabolized forms, at least partially, by the action of enzymes such as arylsulfatase A capable of removing the sulfate group, and that are present in the brain^{75,133}. In order to further understand if the previously observed effect: the reduction of the release of $\text{TNF}\alpha$ by microglia cells, was due to the unmetabolized form, or just to one of the isomers, we decided to test each isomer individually. Our results indicated that the effects of sulfated compounds were higher than the unmetabolized form of the compound (fig. 3.2) Moreover, comparing the mixture of pyrogallol-O-sulfate isomers with the isolated isomers demonstrated that the isolated isomer pyrogallol-O-2-sulfate (**2S2**) effects seemed to be higher. For this reason and due to the higher concentration of this isomers in circulation, **2S2** was used instead of the mixture containing both isomers. Compounds **1**, **1S**, **2** and **2S2** were used in further assays for comparison with the synthesized compounds.

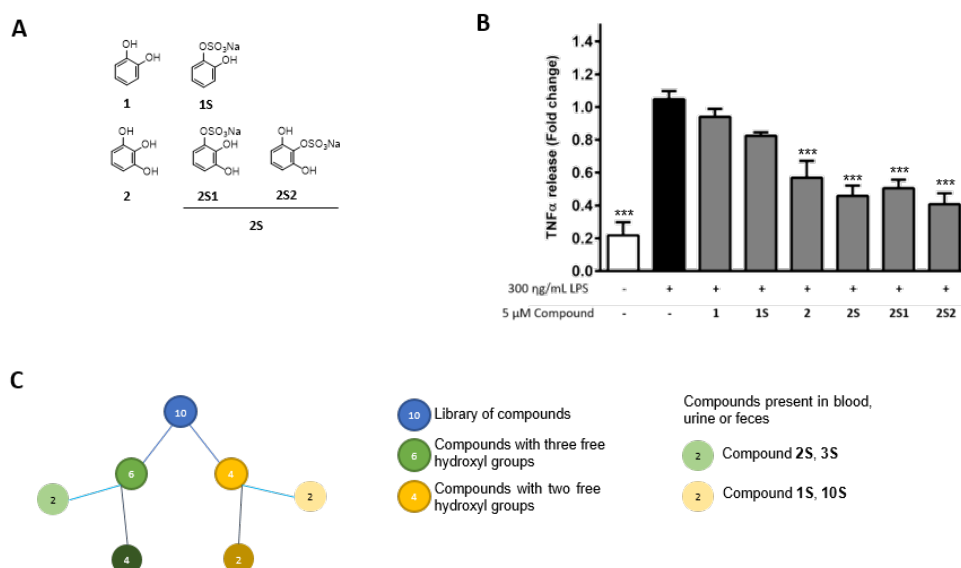


Figure 3.2: Evaluation of the effects of (un)sulfated compounds in the release of $\text{TNF}\alpha$ by microglia cells. **A** Chemical structures of the compounds found in circulation (compound 1S, 2S1 and 2S2) and their corresponding (un)sulfated structures (compounds 1 and 2). **B** Comparison between the effect of (un)sulfated compounds and each of the isomers as well as the mixture of pyrogallol-sulfate isomers. **C** Schematic overview of the division between the two groups and consequent subgroups of compounds. Statistical differences are denoted as *** $p < 0.001$, ** $p < 0.01$ and * $p < 0.05$ relatively to LPS insult and as ### $p < 0.001$, ## $p < 0.01$ and # $p < 0.05$ relatively to untreated cells. Data are presented as means \pm SD, $n = 3$.

3.2.2 Two derivatives showed promising results in the modulation of TNF α release

For practical reasons, the set of compounds evaluated was divided in two groups: (i) compounds, like pyrogallol, that have three free hydroxyl groups in the ring structure and (ii) catechol-like compounds that have two free hydroxyl groups. For future prospects these compounds were further differentiated in two subgroups due to a potential nutritional versus an exclusive supplementation/pharmacological approach. The two subgroups consisted in: (i) chemical compounds found in blood, urine, feces after a particular food ingestion; (ii) remaining set of molecules that would not fit this group (figure 3.3-C).

For the same reason mentioned above in section 3.2.1, we also decided to test the unconjugated compounds, meaning that 8 unconjugated compounds were also evaluated, increasing the total number of compounds evaluated to twenty eight (although, as stated before, for practical reasons, synthesized isomers were evaluated as a mixture of isomers).

The compounds were tested by ELISA in order to evaluate the release of TNF α (figure 3.3-A-C) and results based on the chemical structure can be observed in figure 3.3-B-D). All compounds tested showed a tendency to modulate the inflammatory cytokine. With the exception of 4-hydroxy-catechol (**6**) and the sulfate conjugate (**6S**), all compounds showed potential in reducing neuroinflammation.

From the list of naturally occurring/ relevant compounds, compounds **3** and **3S** showed the most promising results, while compound **10** revealed a very poor ability to reduce the release of TNF α . Two compounds, compound **3S** and **7**, were able to further reduce the release of TNF α comparatively to pyrogallol and nearly 60-70% relative to the stimulated cells (fig. 3.2).

Following the results obtained, further chemical derivatives of compound **3S** and **7** were designed as can be observed in fig. 3.2- **B** and **C** respectively.

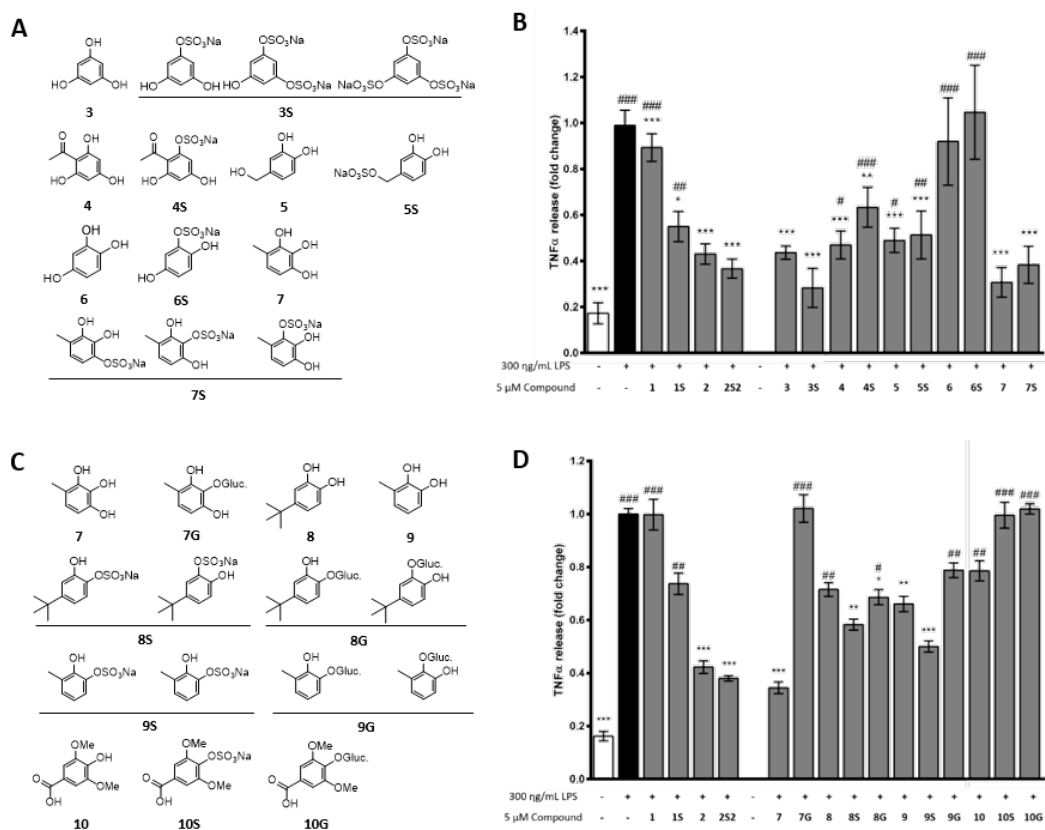


Figure 3.3: Evaluation of the effects of (un)sulfated compounds in the release of TNF α by microglia cells. **A, C** Chemical structures of the two subgroups of compounds, evaluated in **B** and **D** respectively. **B, D** Evaluation of the ability of the compounds to reduce the release of TNF α from microglial cells stimulated with LPS. Statistical differences are denoted as *** p <0.001, ** p <0.01 and * p <0.05 relatively to LPS insult and as # # # p <0.001, # # p <0.01 and # p <0.05 relatively to untreated cells. Data are presented as means \pm SD, n =3.

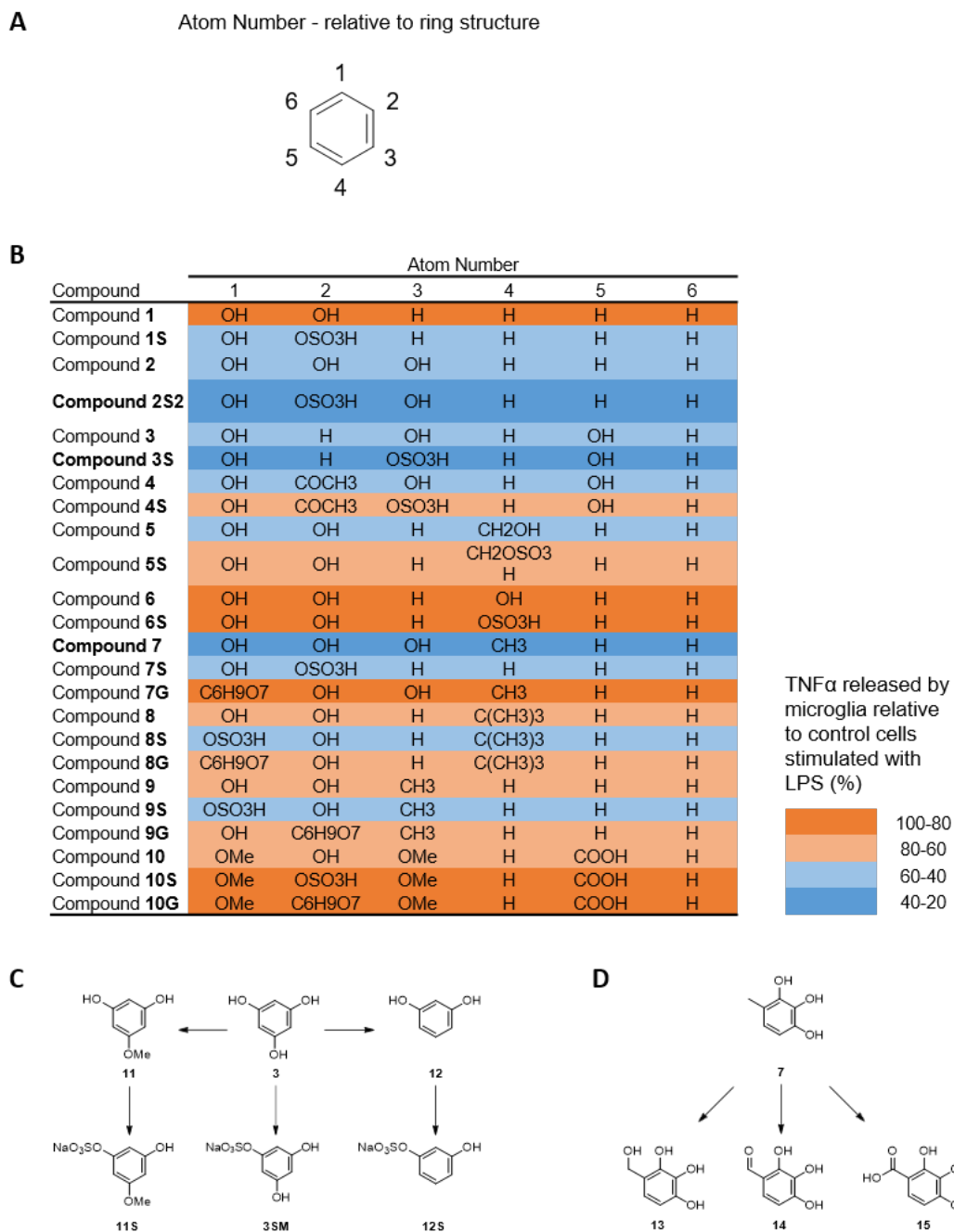


Figure 3.4: **A**, Atoms numbers relative to the cyclic benzenic aromatic ring. **B** The relative position of the different chemical groups on the benzene ring and the corresponding release of TNF α was designed in order to analyze the structure-activity relationship. **C**, **D** Based on the structural features and the effects observed, chemical derivatives of compounds 3 and 7, were selected and synthesized.

3.3 Synthesis of chemical derivatives- Second Iteration derivatives

3.3.1 Synthesis of 4-methylpyrogallol and phloroglucinol sulfate derivatives

A set of derivatives based on compound **3S** and **7** were proposed (fig. 3.3 C, D), successfully synthesized (table 3.3) and characterized. In total, six compounds (**3SM**, **11**, **11S**, **12S**, **13** and **15**) were synthesized, plus the isolation of phloroglucinol-mono-sulfate (**3SM**). Through NMR we identified small traces of phloroglucinol-di-sulfate (<5%) in **3SM**. Resorcinol-di-sulfate was detected when synthesizing resorcinol-O-sulfate (table 3.3).

3.4 Biological evaluation- Second Iteration derivatives

3.4.1 Resorcinol-sulfate a second iteration derivative elucidates a possible main core structure

Evaluation of second iteration compounds (fig. 3.5) was made as described for first iteration derivatives, without changing the protocol. The significant effects of 4-methylpyrogallol (**7**) were reduced in the results, while phloroglucinol remained a strong reducer of $\text{TNF}\alpha$ release. Nevertheless the three compounds **2S2**, **3SM** and **7** showed a substantial effect in mitigating neuroinflammation. Regarding phloroglucinol-O-sulfate (**3S**) derivatives, compound **12S** (resorcinol-O-sulfate) also showed activity comparable with **2S2** and **3SM**, while having an interesting core shared between these three molecules. Compound **14** also showed a significant improvement over compound **7**, although the activity of compound **7** in this assay was inferior to what was observed previously (fig. 3.7- B).

Structure activity relationship showed the structure similarities between the compounds with the best activity (figure. 3.7- C). A core structure seem to be associated with the compounds activity. Resorcinol (**12**) structure is conserved in pyrogallol (**2**) and phloroglucinol (**3**), (Fig. 3.7- D). The presence of a sulfate group is critical for activity and demonstrated a 10 to 20% increase in activity in any of these three compounds.

Although the sulfate position in **2S2** is not identical to the other two compounds **12S** and **3SM**, a three dimensional analysis (not shown) revealed that the position of the sulfate primary hydroxyl is almost identical in all three structures.

The toxic effects of these compounds were evaluated using celltiter blue, and no statistical significant effect was noticed while comparing with control cells (annex C).

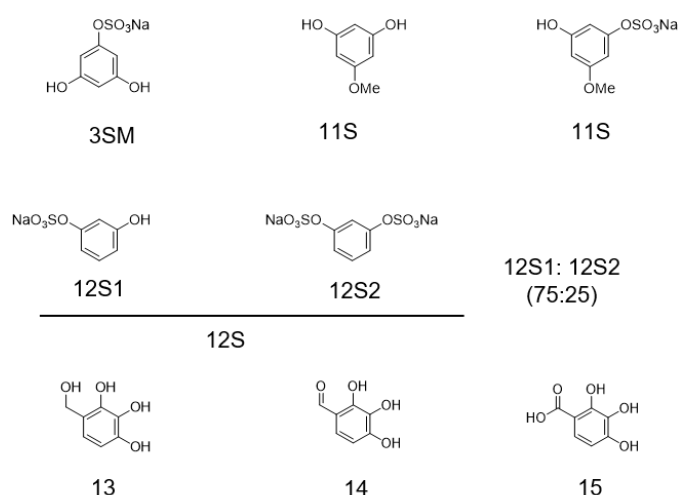


Figure 3.5: Chemical structures of second iteration derivatives. All further information is included in table 3.3

Table 3.3: Synthesized and tested compounds- Second iteration

Nr.	Sub Nr.	Name	IUPAC	Iso.	Iso. ratio	Yield (%)	Morphology
3	3SM	Phloroglucinol-mono-sulfate	Sodium 3,5-dihydroxyphenyl sulfate	-	-	83	White Solid
11	-	Methoxy-phloroglucinol	Methoxy-benzene-2,4-diol	-	-	64	Yellow solid
11S	-	Methoxyphloroglucinol-sulfate	3-hydroxy-5-methoxyphenyl sulfate	-	-	87	White solid
12S	-	Resorcinol-O-sulfate	3-hydroxyphenyl hydrogen sulfate	2	75:25	98	White solid
	12S1	Resorcinol-mono-sulfate	3-hydroxyphenyl hydrogen sulfate	1(2)	75	74(98)	-
	12S2	Resorcinol-di-sulfate	3-hydroxyphenyl hydrogen sulfate	2(2)	25	25(98)	-
13	-	4-(hydroxymethyl)pyrogallol	1-(4-hydroxy-3,5-dimethoxyphenyl)-2-phenylethan-1-one	-	-	89	White solid
15	-	4-carboxyl-pyrogallol	2,3,4-trihydroxybenzoic acid	-	-	90	Brown solid

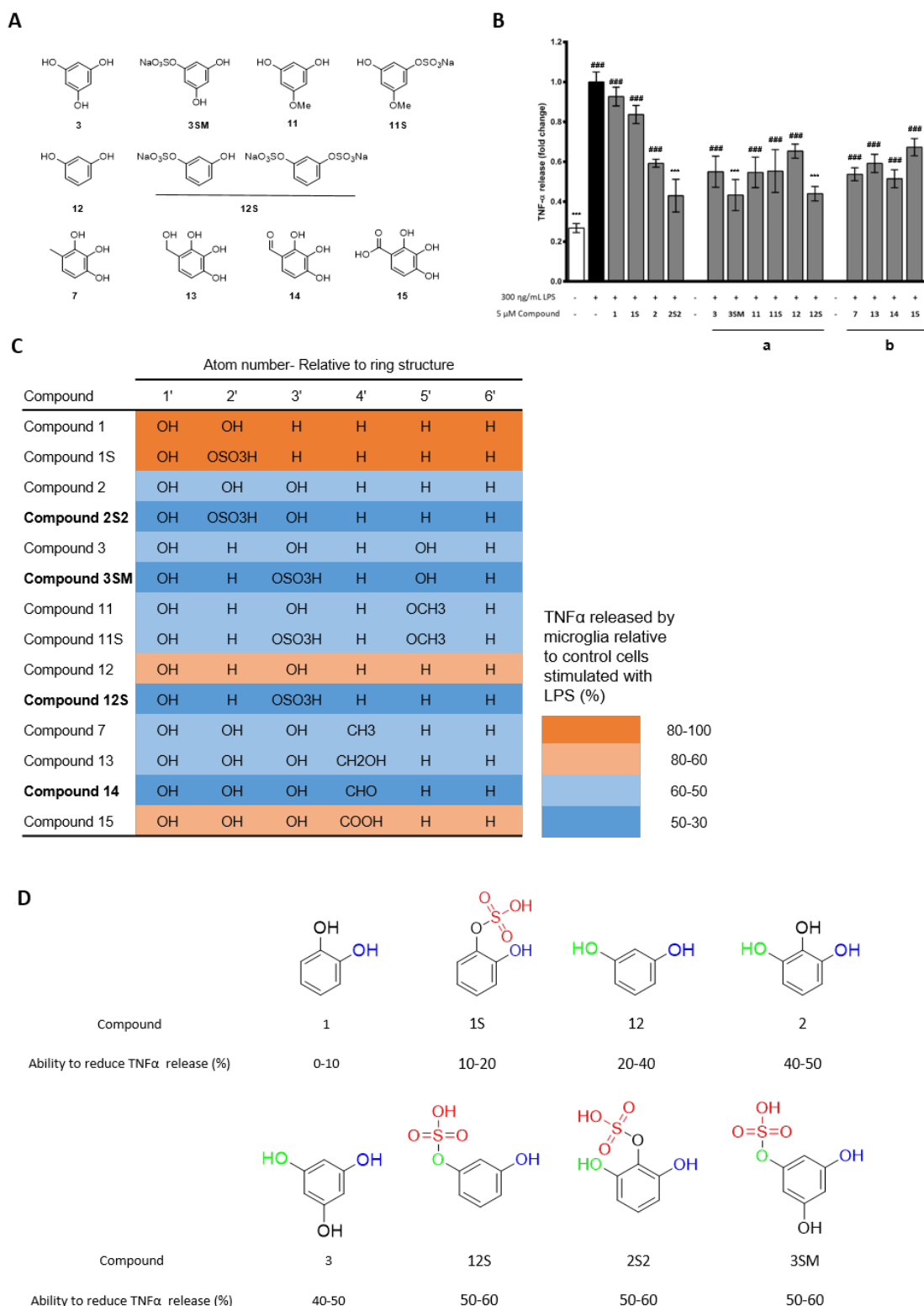


Figure 3.6: **A** Chemical derivatives based on compounds **3** and **7** were synthesized. **B** Biological evaluation of second iteration derivatives showed that three compounds **2S2**, **3SM** and **12S** have a significant activity in reducing TNF α released by microglia. Compounds marked in **B** with **a** represent compound derivatives of compound **3**, and **b** derivatives of compound **7**. **C** Structure activity relationship of the compounds was represented in a heatmap, showing the structurally significant core for the activity of these molecules. **D** Chemical groups associated with increased activity are highlighted with color. The information was extracted from **C**. Green chemical groups represent a group necessary for an increase in 10% in protection, blue represent an cumulative increase of 20%, and red represent a further increase of 10 to 20%. Statistical differences are noted as ***<0.001 relative to LPS stimulated cells and # # # <0.001 relatively to control cells.

3.4.2 Incubation of cells with different concentrations indicates the results are dose dependent

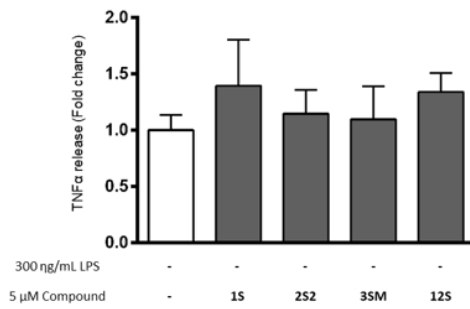
From the list of second iteration compounds evaluated in figure 3.5-B, we have chosen four compounds in order to evaluate two essential questions: the isolated effect of the compounds at the end of six hours of incubation; and a possible dose-response assay. For this we have chosen phloroglucinol-mono-sulfate (**3SM**) and resorcinol-O-sulfate (**12S**), the two synthesized compounds with higher potency in reducing $\text{TNF}\alpha$, since their results, as well as core structure are almost identical, and curiously, they are referenced as possible dietary compounds.⁷⁴ We have also chosen pyrogallol-O-2-sulfate (**2S2**) for its effects and catechol-O-sulfate (**1S**) because it was previously found in circulation.

In order to evaluate if the compounds would have any effect on the concentration of $\text{TNF}\alpha$ at the end of the incubation time media was collected from the 6 hours time-point, evaluated and results are shown in figure 3.6 A. Results showed no statistical significance between the compounds and the control, however, a tendency of compounds to increase the levels of $\text{TNF}\alpha$ was observed.

To answer a second question about if the effects of the compounds would be maintained at lower concentrations and if the release of $\text{TNF}\alpha$ would follow a saturation curve, where an increase in the concentration of compounds would lead to an increasingly smaller effect, five concentrations, ranging from 5 micromolar to 100 nanomolar were evaluated.

The data demonstrates that the release of $\text{TNF}\alpha$ seems to be dose-dependent. Curiously, for compound **2S2** and **3SM** the effect at 5 and 2.5 μM seems to be almost identical, meaning these compounds might be very close to reach a saturation point at physiologically relevant concentrations. Also, significant effects can also be observed at 100 nanomolar concentrations, with the exception of **1S** where no differences between 100 and 500 nanomolar and control cells can be observed.

A



B

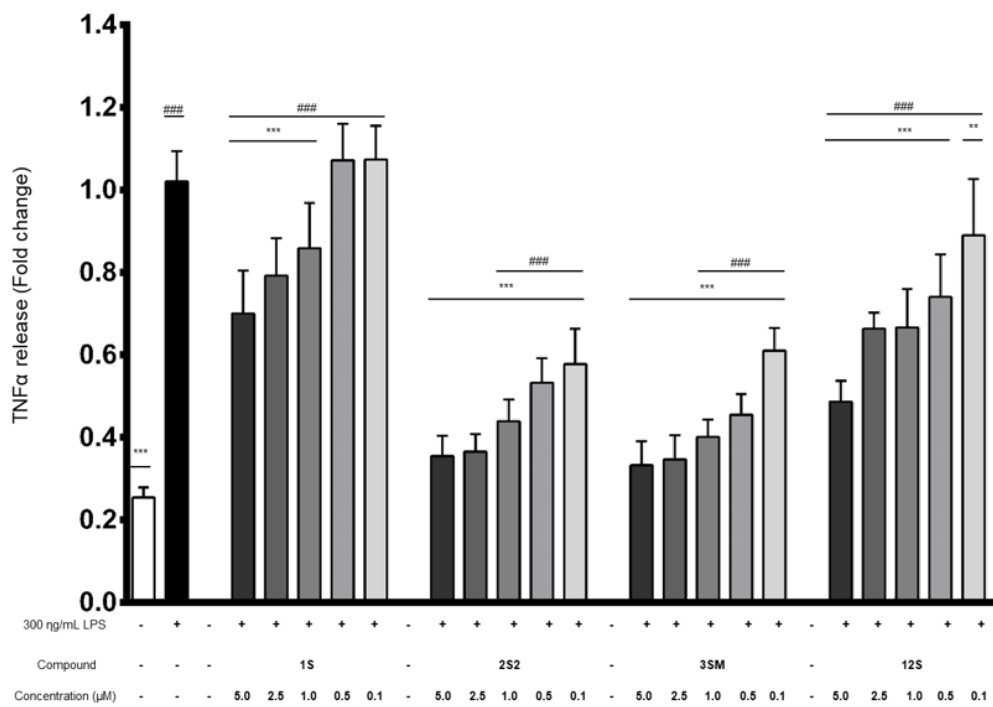


Figure 3.7: **A** The levels of TNF α were evaluated after 6 hours of incubation, without LPS. No statistical significance was detected. **B** The levels of TNF α were evaluated while using different concentrations of the compounds. Compounds were incubated for 6 hours followed by incubation with LPS for 24 hours. Statistical differences are noted as ***<0.001 relative to LPS stimulated cells and # # # <0.001 relative to control cells.

3.5 Blood Brain Barrier permeability

3.5.1 *In silico* membrane permeability model shows the ability of compounds to cross various membrane including the BBB

The ability of the compounds to reach circulation and pass the BBB is of the utmost importance to our objective of modulating brain cell function, however most of the compounds synthesized are not from natural origin, no known parent compounds is associated, and they were never quantified in circulation (with some exceptions, like phloroglucinol)¹³⁴. Therefore it was important to evaluate compound permeability to passively cross the membranes including the BBB. To achieve such predictions we have used an *in silico* model of brain permeation.

The inability of the compounds to reach the brain was attributed if the compounds were to fail in five or more parameters out of the 50 calculated for 95% of all known drugs that reach the brain. The results showed that all compounds were able to passively pass the membranes and the BBB, with the exception of two compounds, catechol and resorcinol (data is shown in table 3.4 , however not all factors evaluated by our model are displayed). The data indicate the inability of catechol to passively cross the membranes, although this can be explained by the fact the model is only accounting for passive diffusion, and not active transport.

3.5.2 HBMEC permeation results

Transendothelial electric resistance (TEER) measurements were taken in order to evaluate the integrity of the HBMEC monolayer membrane. Results showed that the TEER readings were consistent in the last three days before the assay, and with the literature.¹³⁵ A drop in TEER was observed for all compounds, as expected from the literature and with no statistical significance relative to control.¹³⁵

Tight junction integrity was also evaluated using sodium fluorescein. In this assay, none of the compounds showed indications of having impacted HBMEC cell tight junctions.

Table 3.4: *In silico* calculations of membrane permeation for the tested compounds

Molecule	PBBB	Dipole	dHB	accepHB	QPIogPo/w	QPIogBB	CNS	QPPCaco	QPPMDCK	QPIogKhsa	QPIogs	PSA
1	No	2.18	2.00	1.50	0.80	-0.32	-1.00	1067.74	-0.32	-0.69	0.72	44.24
1S	Yes	0.81	2.00	5.25	0.10	-1.16	-2.00	43.37	-1.16	-0.98	-0.91	91.59
2	Yes	3.66	3.00	2.25	0.09	-0.74	-1.00	384.77	-0.74	-0.81	-0.33	65.71
2S1	Yes	0.77	3.00	6.00	-0.49	-1.61	-2.00	15.66	-1.61	-1.02	-0.86	113.00
2S2	Yes	1.69	3.00	6.00	-0.38	-1.50	-2.00	20.24	-1.50	-1.02	-0.82	110.39
3	Yes	2.50	3.00	2.25	-0.02	-0.85	-1.00	288.89	129.26	-0.82	-0.34	66.76
3MS/3S1	Yes	4.99	3.00	6.00	-0.63	-1.85	-2.00	9.20	4.09	-1.02	-0.93	115.89
3S2	Yes	8.48	3.00	9.75	-1.28	-2.92	-2.00	0.31	0.14	-1.45	-1.00	163.83
3S3	Yes	2.56	0.00	2.25	1.90	-0.29	0.00	9906.44	5899.29	-0.36	-2.21	24.58
5	Yes	3.71	3.00	3.20	-0.07	-0.91	-1.00	320.87	114.80	-0.77	-0.66	67.44
5G1	Yes	2.96	3.00	5.5	-0.13	-2.00	-2.00	9.78	4.36	-0.95	-1.29	116.10
6	Yes	1.55	3.00	2.25	0.04	-0.81	-1.00	323.61	146.13	-0.81	-0.35	66.81
6S1	Yes	2.25	3.00	6.00	-0.52	-1.68	-2.00	13.25	6.03	-1.02	-0.87	114.09
7	Yes	2.72	3.00	2.25	0.33	-0.70	-1.00	471.84	219.67	-0.70	-0.76	63.90
7S1	Yes	4.10	3.00	6.00	-0.17	-1.58	-2.00	19.51	9.19	-0.95	-1.20	110.78
7S2	Yes	1.90	3.00	6.00	-0.09	-1.47	-2.00	24.76	11.85	-0.95	-1.16	108.51
7S3	Yes	1.04	3.00	6.00	-0.15	-1.50	-2.00	21.65	10.25	-0.95	-1.10	108.97
7G1	Yes	1.98	5.00	10.05	-0.72	-2.51	-2.00	4.51	1.84	-1.01	-1.82	166.30
7G2	Yes	4.50	5.00	10.05	-0.56	-2.21	-2.00	7.16	3.02	-0.98	-1.66	165.82
7G3	Yes	5.05	5.00	10.05	-0.67	-2.28	-2.00	5.35	2.21	-0.98	-1.60	165.55
8	Yes	2.57	2.00	1.50	1.79	-0.42	0.00	1071.92	533.27	-0.19	-1.89	44.22
8S1	Yes	0.65	2.00	5.25	1.18	-1.31	-2.00	43.80	21.95	-0.60	-2.14	91.55
8S2	Yes	0.41	2.00	5.25	1.22	-1.26	-2.00	46.77	23.63	-0.60	-2.08	91.52
8G1	Yes	4.50	4.00	9.30	0.58	-2.24	-2.00	10.45	4.56	-0.72	2.64	146.04
8G2	Yes	4.91	4.00	9.30	0.77	-2.04	-2.00	14.13	6.33	-0.68	-2.53	145.85

Table 3.5: *In silico* calculations of membrane permeation for the tested compounds (Continued)

Molecule	PBBB	Dipole	dHB	acceptHB	QPIlogPo/w	QPIlogBB	CNS	QPPCaco	QPPMDCK	QPIlogKhsa	QPIlogS	PSA
9	Yes	2.19	2.00	1.50	0.85	-0.27	0.00	1307.63	661.08	-0.56	0.13	42.46
9S1	Yes	2.87	2.00	5.25	0.42	-1.12	-2.00	54.00	27.61	-0.88	-1.25	89.39
9S2	Yes	0.70	2.00	5.25	0.43	-1.03	-2.00	60.71	31.19	-0.89	-1.12	87.54
9G1	Yes	2.30	4.00	9.30	-0.04	-2.06	-2.00	13.07	5.81	-0.93	-2.08	144.79
9G2	Yes	3.15	4.00	9.30	-0.10	-1.82	-2.00	14.50	6.49	-0.92	-1.65	89.39
11	Yes	3.24	2.00	2.25	0.95	-0.46	0.00	911.71	447.67	-0.61	-0.67	53.43
11S	Yes	4.64	2.00	6.00	0.11	-1.38	-2.00	-	15.82	-0.97	-1.12	101.53
12	No	2.17	2.00	1.50	0.80	-0.38	-1.00	-	445.84	-0.69	0.69	45.15
12S	Yes	2.22	1.00	1.50	1.23	0.03	1.00	-	14.93	-0.46	-0.88	30.77
13	Yes	2.75	4.00	3.95	-0.67	-1.23	-2.00	155.86	66.34	-0.87	-0.50	87.32
15	Yes	5.83	3.00	3.25	-0.05	-1.51	-2.00	14.40	6.43	-0.90	-0.73	111.40

In silico calculations of permeation for the tested compounds. The following Qikprop descriptors were obtain for each compound: Dipole, dHB, acceptHB, QPIlogPo/w, CNS, QPPCaco, QPPMDCK, QPIlogKhsa, QPIlogS, PSA.

PBBB - Possibility to cross the BBB (Yes/No. a molecule is unable to cross the BBB by failing 5 or more out of the 36 parameters evaluated)

Dipole - Computed dipole moment of the molecule. (must be between 1.0 – 12.5)

Donor HB - number of hydrogen bonds donors (recommended range of 0 to 6);

Acceptor HB - number of hydrogen bond acceptors (recommended between 2-20 based on 95% of known drugs);

QPIlogPo/w- predicted octanol/water partition coefficient (recommended between -2-6.5 based on 95% of known drugs);

QPIlogBB - predicted brain/blood partition coefficient for orally delivered drugs (recommended between -3-1.2 based on 95% of known drugs) ;

CNS - predicted central nervous system activity (between -2 (inactive) and 2 (active) scale);

QPPCaco - predicted apparent Caco-2 cell line permeability for non-active transport (<25 poor, >500 great);

QPPMDCK - predicted apparent of Madin-Darby Canine Kidney Epithelial cell line for non-active transport (<25 poor, >500 great);

QPIlogKhsa - predicted binding to human serum albumin (recommended between -1.5-1.5 based on 95% of known drugs);

QPIlogS - predicted aqueous solubility in a saturated solution (recommended between -6.5-0.5 based on 95% of known drugs) ;

PSA - Van der Waals surface area of pola nitrogen and oxygen atoms and carbonyl atoms (recommended between 7-200 based on 95% of known drugs).

3.6 Compounds with ability to protect neurons from oxidative insult

The ability of compounds to reduce the effects of oxidative stress caused by t-BHP, and thus increase cell viability in neuronal cells was evaluated for a selected group of compounds. This selection was based on the ability to reduce the release of the $TNF\alpha$ in LPS-stimulated microglia cells indicating a potential for neuroprotection through the mitigation of brain inflammatory outcomes. These molecules were also chosen due to their structural similarity with catecholamines, meaning there is also the potential to affect neurons by interacting with catechol-o-methyl transferases.

In total, eighteen compounds were evaluated (annex D). From these, three compounds and their respective sulfate derivatives were able to significantly increase cell viability (Fig. 3.7 - **B,D**). These compounds showed minor signs of toxicity (Fig.3.7 - **C**) although they seem to modulate the overall amount of ATP present in cells (fig.3.7 **A**).

In order to further understand if the effects shown were due to a decrease of non-viable (dead) cells or increase in the apoptotic population we used AnnexinV/PI double staining. Results suggest that the effects on cell viability observed before are not only dependent on the number of viable but also apoptotic (annexin-V positive) cells (fig.3.7 **E, F**). Overall all compounds tested seem to increase the number of viable plus apoptotic cells in relation with control cells exposed to the oxidative insult. Moreover three of the six compounds, **1S,9** and **9S** were able to significantly increase the number of viable cells and compound **9** significantly reduced the number of dead cells (fig.3.7 **F**).

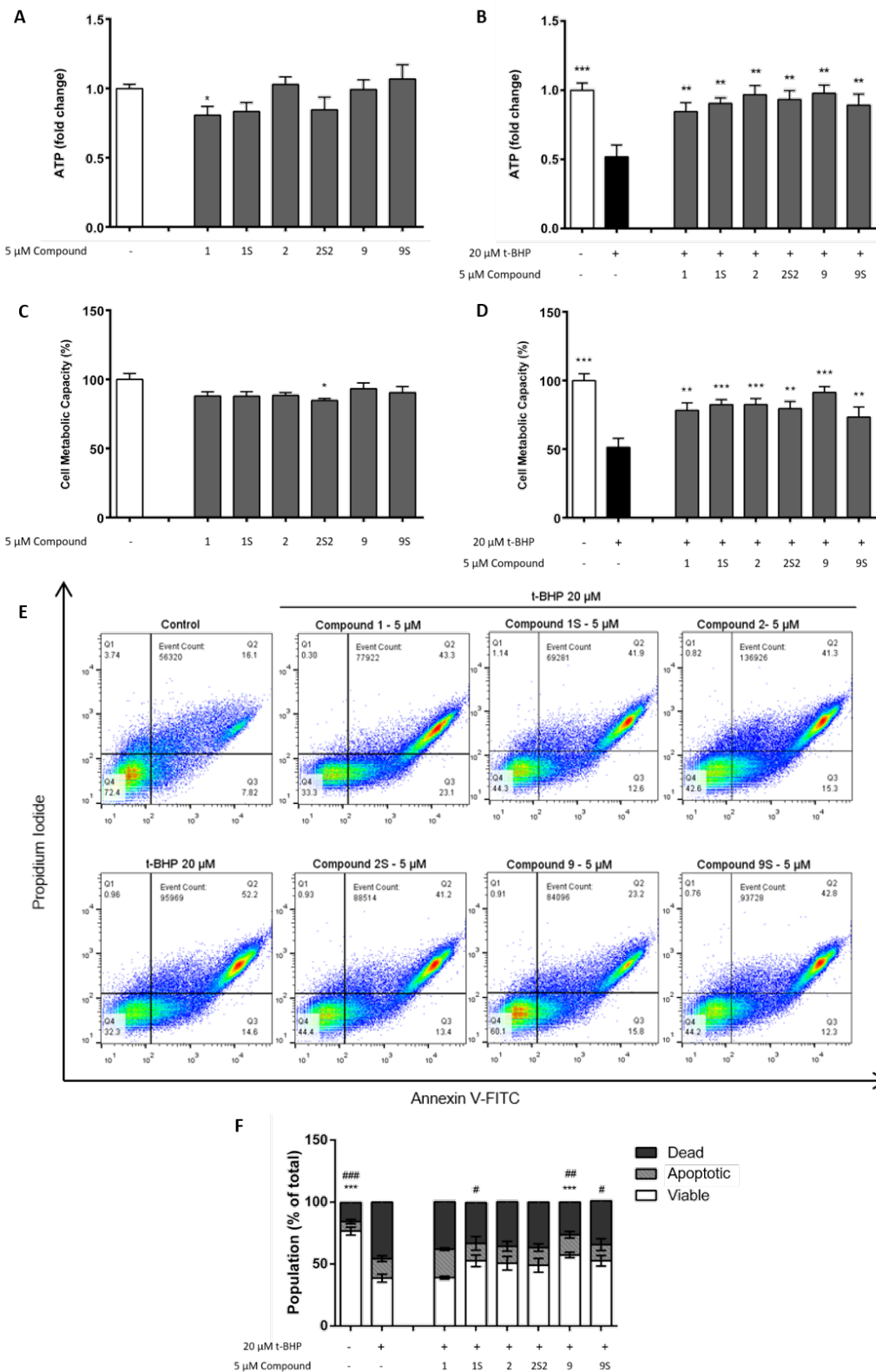


Figure 3.8: A selection of compounds were evaluated in SH-SY5Y upon oxidative insult with t-BHP. Three compounds and the corresponding sulfates showed a high capacity to prevent cell death. Cytotoxic effects were assessed by measuring ATP content **A** and cell metabolic capacity **C**. Statistical differences are noted as * $p < 0.05$ relatively to control. Neuroprotective effects were also measured by these two methods **B,D**. Statistical differences are noted as *** $p < 0.001$, ** $p < 0.01$ and * $p < 0.05$ relatively to t-BHP insult. To further increase the understanding on neuron viability, apoptosis was measured using annexin V, while dead cell were measured using propidium iodide through flow cytometry. Statistical differences are denoted as *** $p < 0.001$ relatively to the percentage of dead cells present in t-BHP insulted cells and as ### $p < 0.001$ relatively the percentage of viable cells present in t-BHP insulted cells.

4. Discussion

(Poly)phenols present in fruit and vegetables are targets of multiple studies involving their capability to modulate the release of inflammatory factors. Nevertheless, many studies focus on parent compounds, instead of their metabolites found in human circulation, leading to the use of high concentrations and often without verifying their ability to cross the BBB. In our work, we focused on synthesizing chemical derivatives of compounds known to be present in circulation and showing effects at a physiologically relevant concentration, with the objective of having compounds of physiological relevance.

Due to the high number of synthesized compounds leading to a larger library of compounds than expected, compromises on the number of microglia inflammatory markers had to be done. Having this information in mind we chose the main inflammatory marker expressed in microglia cells, and the one that had shown the major impact with previously evaluated (poly)phenol metabolites: Tumor necrosis factor alpha.⁷⁵

4.1 First Iteration Compounds

4.1.1 Synthesis of First Iteration Compounds

The first step in building the library of compounds consisted in the synthesis of sulfate derivatives. This required the synthesis of 4-methylpyrogallol from 2,3,4-trihydroxybenzaldehyde and 4-(hydroxymethyl)catechol from protocatechuic acid.

The compounds 4-(hydroxymethyl)catechol, syringic acid and 2,4,6-trihydroxyacetophenone were not in the initial work plan but we decided to also include these sulfate derivatives in order to diversify the structures to be evaluated, although maintaining the focus on di- and tri-hydroxylated phenolic compounds and possibly excluding some functional groups like the ketone in 2,4,6-trihydroxyacetophenone and also because they had not been tested by the Molecular Nutrition and Health group before.

In the synthesis of sulfate derivatives, all compounds were successfully synthesized with good yields. In the case of compounds **4S**, **5S** and **6S** only one isomer was present, probably to the different reactivity of the hydroxyl groups (figure 4.1). For compounds **4** and **6** this may be due to the formation of the enol and consequent presence of tautomers in equilibrium (figure 4.2) directing the sulfation to the most reactive hydroxyl group present. In compound **4**, the most reactive hydroxyl group is adjacent to the ketone, that acts as a withdrawing group, while in compound **6** the hydroxyl groups in the ortho and para positions direct the reactivity towards the obtained sulfate conjugate.

Compound **5S** only presented one sulfate product due the higher reactivity of primary hydroxyl groups over the less reactive phenolic hydroxyl groups.

Two isomers of compound **6** were eventually detected yet the sample degraded overnight probably due to heat instability and the ability of the compound to react like a quinone and easily oxidizing. Different concentrations of the sulfation reagent (Sulfur trioxide pyridine complex, half the equivalents and double the equivalents) or a change in the reaction time (by half, 24 hours, and double, 48 hours) did not alter the outcome obtained. The limited amount of information available about the sulfation of these phenolic compounds was also a considering factor in synthesizing the other isomers of this compound.

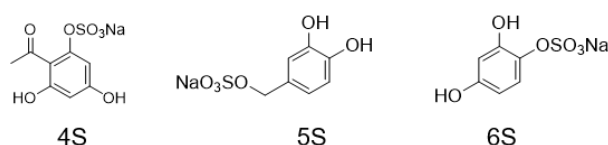


Figure 4.1: Compound **4S**, **5S** and **6S** only showed one sulfated conjugate

The synthesis of glucuronide conjugates was also one of the objectives of our work. From the compounds proposed for the synthesis of glucuronides, compounds **3**, **6**, **7**, **8** and **9**, we also added com-

compound **10** (other compounds were not included due to time constraints). From these, only compounds **8-10** were successfully synthesized by using $\text{BF}_3\cdot\text{OEt}_2$ as the promotor in the glycosilation reaction and compound **7** with TMSOTf as the promotor.

In the synthesis of glucuronides, the critical step is the formation of a glycoside bond between the anomeric carbon of the pyranose and the hydroxyl group of the phenol. Various conditions can modulate the success of the reaction: the type of protection used in the hydroxyl groups of the pyranose; the leaving group present in the anomeric carbon; the reaction activator; and finally the one of most important, the alcohol acceptor, the only changing factor, in our case. The main difference between compounds **3** and **6** and the other phenols is the benzenic substitution pattern with the presence of hydroxyl groups in the meta position relative to other hydroxyl groups leading to the existence of an enol system and the coexistence of tautomers in equilibrium (Fig. 4.2)

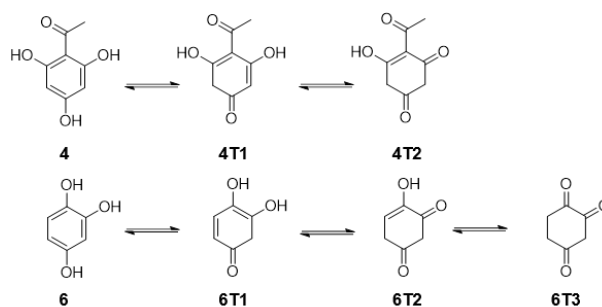


Figure 4.2: Compounds **4** and **6** have multiple tautomers that are in equilibrium in solution, thus reducing the reactivity of the phenol. **4**: 2,4,6-trihydroxyacetophenone; **6**: 4-hydroxy-catechol.

The synthesis of glucuronates can be also impaired by the lower reactivity of the sugar due to the presence of an electron withdrawing carboxylic acid group at C-5.¹³⁶ In order to overcome this adversity and to synthesize the remaining glucuronides, another catalyst, TMSOTf, was tested. Nevertheless, this approach only worked with compound **7**. Acetylation was also an option, in order to alter phenolic reactivity. However, despite the fact that we were able to synthesize acetyl derivatives of compound **6**, the glucuronidation was of such low yield that we decided not to pursue the synthesis of this compound. Acetylation of phloroglucinol resulted in the synthesis of tri-acetyl-phloroglucinol, even in the presence of only half equivalent of acetic anhydride. A mixture of initial compound and tri-acetylated product was observed, thus hindering the ability to produce the corresponding glucuronide. Due to time constraints we decided not to pursue other alternatives and test the remaining synthesized compounds, and if glucuronidation would represent better results in the biological evaluation on the corresponding aglycone, then we would revisit the synthetic pathway for the synthesis of the remaining unglucuronide compounds. This, however, did not happen as the glucuronides synthesized revealed a lower ability to reduce the release of $\text{TNF}\alpha$ comparatively to the corresponding aglycone and sulfated compounds. We have used acetate (ester) protecting groups in the glycosyl donor, the beta anomer of the glucuronides was exclusively obtained, as expected, due to the neighbouring participation effect of an ester at the C2 position of the sugar donor.

Other synthetic options were considered, including the use of other leaving groups reported in the literature in cases where trichloroacetimidate was not successful, and the use of other strong Lewis acids besides $\text{BF}_3\cdot\text{OEt}_2$ and TMSOTf such as TBDMSOTf, AgOTf or $\text{I}_2/\text{Et}_3\text{SiH}$ ^{137,138,139}. Other protection groups were also considered for example benzylation and silylation¹⁴⁰.

4.1.2 Choosing pyrogallol-2-sulfate as the compound of reference

The approach used in our study was already implemented by the Molecular Nutrition and Health lab and corresponds to a nutritional model where cells are incubated for six hours with the metabolites - the time at which C_{max} was obtained and at a concentration of $5 \mu\text{M}$, which is about half the one found in circulation, thus trying to replicate physiological conditions⁷⁵.

Previously, the Molecular Nutrition and Health lab, together with the Bioorganic Chemistry lab, have demonstrated that pyrogallol-O-sulfate was a metabolite present in human circulation and capable of reducing the inflammatory levels of tumor necrosis factor alpha.⁷⁵ However, two isomers of pyrogallol-O-sulfate were actually found: pyrogallol-O-1-sulfate and pyrogallol-O-2-sulfate. Previously, they were evaluated as a 1:1 mixture, even though their *in vivo* ratio was of 19:1%.⁹² In order to understand if the

effects shown by the compounds were due to only one of the isomers or a synergistic effect, the isomers were isolated (previously to this project) and now evaluated.

Our results showed that both isomers were producing an effect, although a slightly higher effect for pyrogallol-O-2-sulfate (**2S2**), the isomer present in the highest concentration in circulation can be observed. We then decided to use only pyrogallol-2-sulfate due its higher prevalence in human circulation, found in previous studies.⁹²

Recently, our group addressed the fact that sulfated compounds can be converted to their corresponding unsulfated compounds through the activity of arylsulfatases, that we know to be present in the brain, and able to pass the BBB.^{133,75} For this reason we decided to evaluate also the unconjugated compounds. Notwithstanding, further studies will be necessary in the future to understand the full scope of this information, since only the sulfated compounds were found in circulation, although they were not looked for in the brain or in any particular tissue.

4.1.3 Two compounds from the initial library of compounds revealed an increase protection over pyrogallol-O-2-sulfate

For the comparison between the library of synthesized compounds and the compound with major impact on $TNF\alpha$ (pyrogallol-O-2-sulfate) - we decided to keep the remaining set of compounds **1,1S** and **2** as internal controls in order to account for the variability of the method and operator and to be able to directly compare the results from the synthesized compounds with pyrogallol-O-2-sulfate.

Most compounds present in the library of compounds are of synthetic origin and for this reason, limited information about the possible circulating concentration is available. For this reason and in order to compare the synthesized compounds with our target molecule, pyrogallol-O-2-sulfate (**2S2**), previously evaluated in Figueira et al., we decided to keep the same conditions: the time of incubation and concentration, constant for all compounds to be evaluated.⁷⁵

With future perspectives in mind and focusing on possible ways to apply our research in the field, it was important to understand if any of these compounds were part of the Human metabolome or could typically appear in human circulation. From our literature search we able to find two compounds: syringic acid which is found in blood, urine and feces and phloroglucinol which is found in blood and feces^{134,141,142}. The remaining compounds could not be found in human circulation with the exception of very particular cases, such as of compound **5** (4-hydroxycatechol) which was found in circulation in chemical factory workers exposed to catechol and derivatives¹⁴³.

Our results from the first iteration of compounds identified compounds that were able to reduce the release of $TNF\alpha$ at levels comparable to **2S2**: compounds **3S** and **7**. The activity of compound **3S** was clearly increased over compound **3** by the presence of the sulfate group. The same was observed in the case of compounds **1,2,8** and **9**, indicating that the presence of the sulfate is of great importance to the activity, although dependent on its position in the molecular structure: compounds **6S**, **8S** and **9S** showed no clear increase in activity over their unsulfated parent compounds.

In the case of compound **7** the presence of the sulfate actually diminishes the activity. This can however be due to the presence of three isomers with possibly different activities. For compound **4** the presence of the sulfate group outside the ring (compound **4S**) decreased the activity of the compound indicating that sulfate should be present in the hydroxyls of the benzene ring. Compounds **6** and **6S** presented a great variability and also seemed to increase the release of the inflammatory cytokine $TNF\alpha$. The reason that lead to an increase in the inflammatory marker in microglia is unknown, however information taken from the literature indicates that compound **6** induces DNA damage leading to apoptosis, which could possibly lead to increased levels of inflammatory stimuli in the environment, and consequent increase in $TNF\alpha$.¹⁴⁴

The synthesized glucuronides seemed to have no impact on the release of $TNF\alpha$ or a significant lesser effect than the corresponding sulfated compound. At this point, we decided to proceed with the synthesis of derivatives of both compounds that gave the best results (compound **3S** and **7**).

4.2 Second Iteration Compounds

4.2.1 Synthesis of Second Iteration Compounds

Two derivatives of compound **3** (phloroglucinol), were proposed, as well as their corresponding sulfates. Compound **11** was synthesized from compound **3** through O-methylation. A first approach

using acetone under reflux lead to the formation of the desired product together with the di- and tri-O-methoxyphloroglucinol and also the formation of methylphloroglucinol probably due to the enol balance formed in the basic conditions of the reaction (data not shown). To counteract the formation of methylphloroglucinol we opted to use DMF at 0°C. Under these conditions the di- and tri-O-methoxyphloroglucinol were obtained to a much lower extent (aprox. 25 % yield) and as such we were able to synthesize the mono O-methoxylated compound at a much higher yield (64 % yield).

The glucuronidation of compound **3** was not successful as mentioned previously. Nevertheless upon obtaining the results we decided not to pursue the synthesis of the glucuronide due to the overall poor activity of the various glucuronides in comparison with the sulfate conjugates.

Regarding the synthesis of compound **7** derivatives, isolation of the various isomers of compound **7** was also considered but the use of various solvent mixtures proved ineffective at least when using flash silica column chromatography. However, this can in the future be accomplished with other options like the use of a highly efficient HPLC method, although previous tests conducted by the bioorganic chemistry group in isolating the two pyrogallol-sulfate isomers through HPLC turn out to be a challenging task. The main structural difference between compound **7** and pyrogallol is the presence of a 4-methyl group, and as such we decided to introduce modifications on this methyl group in order to improve activity (see figure 4.3-A). We decided to synthesize derivatives of compound **7** based on compound **14** since aldehydes are a very versatile class of compounds that can be easily reduced and oxidized leading to the formation of compound **13** and **15**.

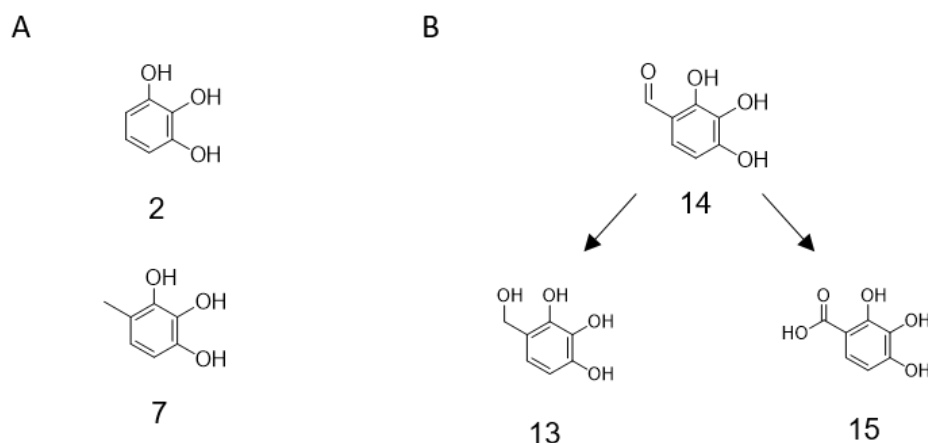


Figure 4.3: **A** The chemical Structures of pyrogallol (**2**) and 4-methylpyrogallol differ only on a methyl group (**7**). **B** 2,3,4-Trihydrobenzaldehyde (**14**) can serve as basis for the synthesis of compound **13** and **15**

Other class of compound **7** derivatives inspired on the chemical structures of known neurotransmitters were also considered but purification was not successful. These compounds would include the main pyrogallol core with an amine group (**21**). In case the purification of these compounds could be achieved, that would mean a new class of compounds could be evaluated in the future. An example of one of the compounds synthesized is shown in figure 4.4

4.2.2 Biological evaluation of second iteration compounds

Overall, there is no significant differences between compounds **2S2** and **3S** in terms of their ability to reduce the levels of the inflammatory cytokine $\text{TNF}\alpha$. Moreover, a loss of effect of compound **7** was observed. The loss in effect on compound **7** could be due to the fact compound **7** had to be re-synthesized, and contaminants not shown by NMR, like inorganic salts, could be present or maybe it might be a question of operator error.

Our results also showed the ability of one of the second iteration compounds, compound **12S**, to reduce the levels of the released cytokine, at levels comparable to compound **2S2** and **3S**. Structures comparison of these three compounds suggested that the common motif between these compounds which is in fact the structure of compound **12S** is the minimal core needed for the major impact on the compounds activity in diminishing the release of $\text{TNF}\alpha$ (see figure 3.5 D).

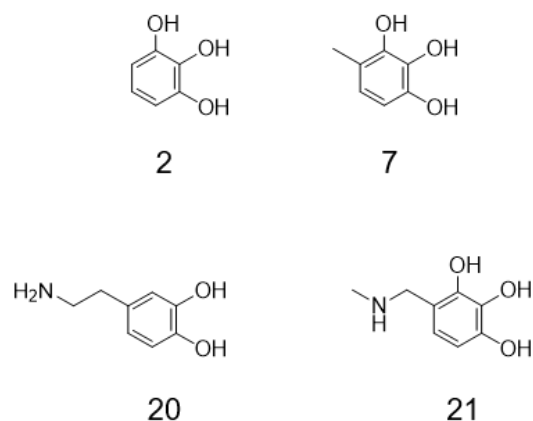


Figure 4.4: Other classes of compounds, like compound **21**, could be synthesized based upon the structure of pyrogallol (**2**) and 4-methylpyrogallol (**7**) and of known neurotransmitters like dopamine (**20**)

While observing the very similar effects on the levels of α of both compounds **3SM** and **2S2**, one might consider the hypothesis that the effects observed might be close to saturation or equilibrium point where the mechanisms present in microglia would not allow a further decrease in $\text{TNF}\alpha$. As mentioned before, basal $\text{TNF}\alpha$ levels are essential for proliferation and keeping cells viable.¹⁴⁵ Moreover, chronic low levels of $\text{TNF}\alpha$ in the brain are also associated with neurodegeneration.¹⁴⁶

In order to evaluate if in fact the cell mechanisms associated with reducing the release of this inflammatory cytokine are close to a saturation point, one could change the compound concentration to even lower concentrations and observe if the amount of release $\text{TNF}\alpha$ is maintained at lower compound concentrations. Time is also a important factor that impacts on the levels of cytokine present in the media. One study reported that compound **3** was able to reduce the release of $\text{TNF}\alpha$ by 30% in just one hour in human macrophage cells¹⁴⁷.

4.2.3 The activity of the compounds appear to be dose-dependent

In order to evaluate if the effect of the compounds would reach saturation, an increase in concentration would not significantly increase the activity, we selected two compounds (**3SM** and **12S**) with the highest capacity to reduce the released levels of $\text{TNF}\alpha$ by microglia cells upon exposure to LPS. Five different concentrations were tested ranging from 5 micromolar to 100 nanomolar. Interestingly the effects observed at 2.5 micromolar were similar to those at 5 micromolar. This indicates the possibility that the compounds, at these concentrations, are reaching the full ability of cells to reduce the release of this cytokine upon insult with LPS. The data also shows that the effects seem to be dose dependent and for compounds **2S2**, **3SM** and **12S**, the ability to reduce $\text{TNF}\alpha$ is significant even at nanomolar concentrations. This is very interestingly, specially for compound **2S2** that was found at 10 μM concentrations in blood.⁹²

The amount of $\text{TNF}\alpha$ present at the end of a six hours, incubation showed no significant difference between the control and cells exposed to compounds. Notwithstanding, some differences between the compounds seem to be present and should be analyzed in the future.

Together, these results demonstrate the potential effects of these compounds at physiologically relevant concentrations and open the doors for re-evaluating the compounds at lower concentrations.

4.2.4 Compound mechanism of action could be related with GPR35

4.2.4.1 G-protein coupled receptor 35

G-protein-coupled receptors (GPCRs) constitute one of the largest families of genes identified, yet around 120 of these genes encode for non-olfactory GPCRs whose function remains a mystery,^{148,149}. G-coupled receptor 35 or GPR35 is a membrane receptor widely expressed across cells of the immune systems, like CD14^+ monocytes, T cells, neutrophils, and dendritic cells, as well as, epithelial cells from the gastrointestinal area¹⁴⁸. Its endogenous ligand, kynurenic acid, is one of the metabolites of tryptophan, fig 1.2-A, present and isolated from mammals, and known to have an impact in various brain functions, e specially inflammation^{148,150}. GPR35 activation with kynurenic acid involves the activation

of the $G\alpha_{12/13}$ subunit and subsequent activation of RodA, $G\alpha_{q/11}$ and followed by activation of phosphoinositol phosphate pathway (PI_3) and $G\alpha_{i/o}$, and modulation of MAPK, $NF-\kappa B$ and NFAT pathways, fig.4.5-B¹⁵¹.

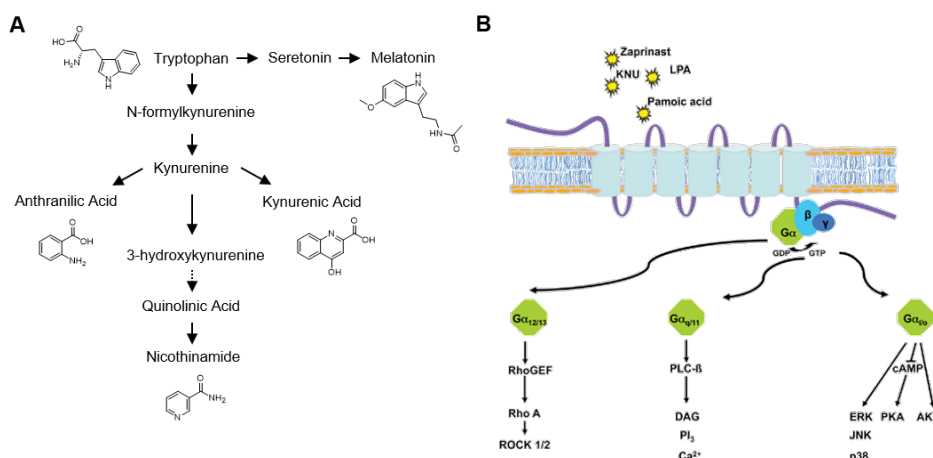


Figure 4.5: Kynurenic acid is a metabolite of tryptophan that can to activate GPR35. **A**, tryptophan metabolic pathway. **B**, GPR35 subunits and cascade of events¹⁵¹.

The complete mechanism of action of this receptor is still unknown, however studies indicated that activation of the receptor with kynurenic acid was able to reduce the release of $TNF\alpha$ in a dose dependent way¹⁴⁸.

Recently, we have found that pyrogallol and catechol are also GPR35 agonists, together with a selection of other natural compounds, such as quercetin, ellagic acid, myricetin, luteolin and others¹⁴⁸. A list of GPR35 agonists is shown in table 4.1, including, pyrogallol and other natural compounds, as well as Zaprinast the main reference compound for gpr35 activation.

Table 4.1: Selection of agonistic compounds of GPR35. EC_{50} were obtained through dynamic mass redistribution assay^{152,148}

Compound	EC_{50} (μM)	Reference
Zaprinast	0.16	(152)
Pyrogallol	1.30	(148)
Catechol	319.00	(148)
Syringic acid	147.00	(148)
Gallic acid	1.16	(148)

Wang et al. have demonstrated that pyrogallol is able to activate GPR35 at a concentration of 7 μM , and unrelated results have demonstrated that the receptor is responsible for modulating the effects of $TNF\alpha$, however the link between the receptor and the release of the cytokine was never uncovered. Previously, our group demonstrated the ability of pyrogallol-O-sulfate in modulating the levels of $I\kappa B\alpha$, the levels of phosphorylated p65 and the internalization of $NF-\kappa B$, indicating the compounds were affecting the $NF-\kappa B$ pathway. Nevertheless, the hypothesis of the compounds to act upstream of the pathway or in the cell membrane was considered.

By conjugating the information available for GPR35 various subunits and the several pathways present in KEGG and Wikipathways we were able to suggest the possible connection between the compounds and various inflammatory pathways (Fig.4.6) including the $NF-\kappa B$ pathway where we were able to hypothesize AKT as the link between GPR35 and the $NF-\kappa B$ pathway, although evidence suggests that RhoA is also able to modulate the release of inflammatory cytokines related with $NF-\kappa B$.¹⁵³ Other work also suggests that the GPR35 subunit $G\alpha_{i/o}$ modulates MAPK pathway: ERK, JNK and P38, thus interfering in the expression of inflammatory cytokines and modulating various mechanisms of inflammation¹⁵⁴.

Although no direct information exists about phloroglucinol (**3**) relation with GPR35, compound **3** has been shown to impact inflammatory bowel disease and syndrome, that seems to be related with a SNP

(rs4676410) in GPR35, associated with ulcerative colitis^{155,156}. Compound **7**, by opposition to compound **3**, was actually referenced in the patent US 20130316985: "*GPR35 Ligands And Uses Thereof*" (Corning Inc.) for treatment of diseases physiologically related to GPR35. In this patent compound **15** is also mentioned.

Having all this information as a hypothesis for the possible mechanism of action of these compounds, an effort to evaluate this receptor should be considered. This means evaluating GPR35 gene expression upon cell incubation with the compounds, and comparing, through ELISA, the levels of inflammatory cytokines upon incubation with the compounds, in the presence of various GPR35 inhibitors available in the market. If GPR35 really is important in the modulation of inflammatory cytokines by the compounds then a more focused study could be made, by recreating the active center of the receptor and developing more potent and specific compounds.

Title: GPR35 Pathway
Organism: Mus musculus

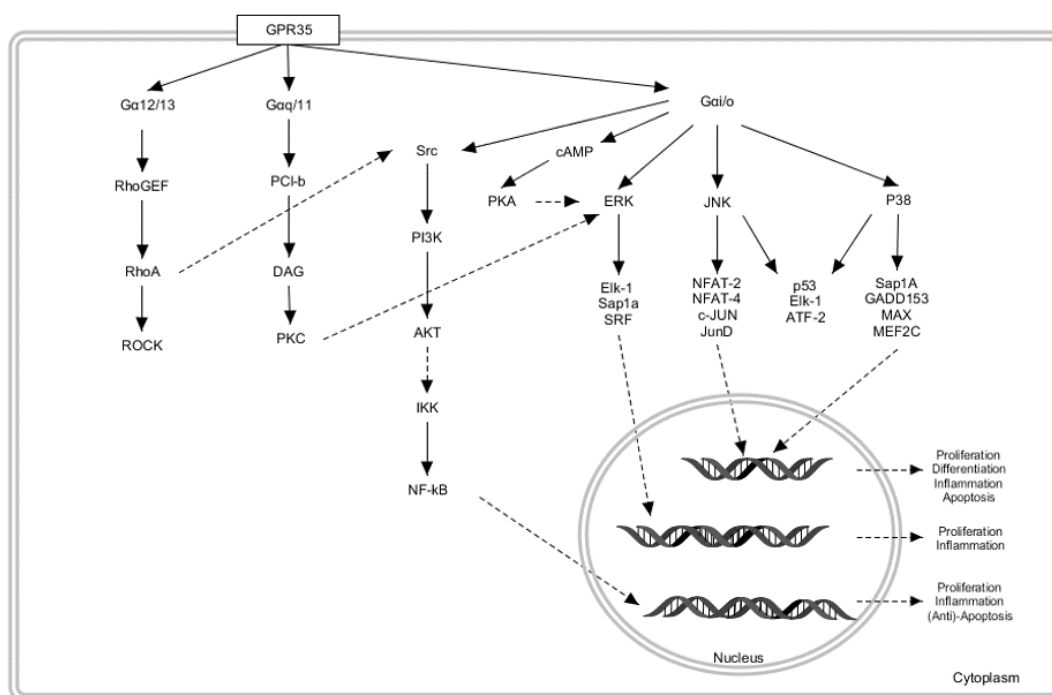


Figure 4.6: Hypotetic *mus musculus* GPR35 inflammatory pathway based on the analysis of KEGG pathways: mmu04010-MAPK; mmu04062- chemokine; mmu04151-PI3K-Akt; mmu04064-NF-kB. Pathway was built using Pathvisio 3.3 (2018)¹⁵⁷

4.2.5 Compound transport across the BBB

4.2.5.1 *In Silico* assay

The ability of compounds to cross the BBB was evaluated by an *in silico* model of permeation by passive diffusion. This method involves the calculation of a series of molecular descriptors based upon physico-chemical properties such as the dipole moment, number of acceptor and donor hydrogen bonds and also number of rotating bonds, volume, molecular mass, Van der Waals surface of polar atoms, besides others. Based on this information, the software is able to predict, based upon a large database, interesting information such as CaCO₂ and MDCK permeation, BBB penetration, binding percentage to albumin and other information not shown like central nervous system activity. In total, the method uses 50 different parameters and defines a range for each specific parameter based upon more than 95% of all drugs known to passively reach the brain. In this model, compounds are considered unable to passively cross the BBB by staying out of the defined range in more than five different parameters.

This model has seen a increased use in recent years thanks to its high throughput capability and predictive power^{158,159,160}. In the past, we have used this model to assess the ability of compounds present in circulation to cross the BBB⁷⁵. We were also able to cross that information with our *in vitro* BBB model composed of HBMEC to see that the information was in agreement between both methods.⁷⁵

In our results, only two of the compounds were unable to cross the BBB: catechol and resorcinol. These compounds are the orto and meta isomers of benzenediol. This information could however be of minor relevance since catechol and resorcinol in their unmetabolized forms are almost never found in circulation^{92,161}. Catechol seems to mainly transformed in the sulfated metabolite by SULT enzymes, while resorcinol in the glucuronide conjugate^{162,161}

While we consider the passive transport of these molecules, active transport should also be considered. Catechol is the main structural core of catecholamines or neurotransmitters such as dopamine and epinephrine. These molecules of low lifetime are unable to cross the BBB by passive diffusion and as such cross the BBB through neurotransmitter transporters (NTTs) mainly SLC6 NTTs¹⁶³. Due to their structural relationship, further studies could be considered for the interaction between small phenolic metabolites and these transporters.

4.2.5.2 HBMEC evaluation of permeation

The evaluation of compound permeation through the BBB was evaluated in a transwell monolayer model of HBMEC. This model was used in collaboration with Dr. Inês Figueira, as previously described in Figueira et al⁷⁵. The rundown of samples by Orbitrap is made in collaboration with Dr. Alexandre Foito, The James Hutton Institute, Scotland UK. The analysis of the media was not complete at the time of delivery of this document, for equipment reasons. Nevertheless, results regarding the stability of the HBMEC monolayer revealed no tight junction disrupting (evaluated through sodium fluorescein assay), or impact on TEER.

4.2.6 Compounds ability to protect SH-SY5Y

The ability of the compounds to protect differentiated SH-SY5Y neuroblastoma cells against an oxidative insult was evaluated. In total eighteen compounds were evaluated. The selection of these compounds were based on their ability to modulate the release of $TNF\alpha$. Compounds **1** and **1S** (catechol and the corresponding sulfate conjugate) were also evaluated since they are known to act on COMT and are present at interesting physiological concentrations.

Our results showed three compounds and their corresponding sulfates have the ability to improve cell metabolic capacity by at least thirty percent. From the compounds with higher ability to reduce $TNF\alpha$ only compound **2** showed significant activity. On the other hand, compounds **1** and **9** showed little effect in microglia cells, however demonstrated a very significant impact in SH-SY5Y. This suggests that the molecular target and cell mechanisms should be different from those possible in microglia cells. This means that different molecular mechanisms of different cells types can be displaced, however these compounds can demonstrate a pleiotropic effect and act on a diverse number of targets.

The mechanisms associated with these compounds are still unknown, however various hypothesis could be made: (i) The electron scavenging ability of these molecules thus reducing the levels of ROS (ii) Activation of Nrf2 and consequent expression of drug metabolizing enzymes such as GST and NQO1^{164,165} Although much is still to be discovered regarding the relation with Nrf2.

One interesting factor is that the unmetabolized forms of these molecules are catechol-O-methyl transferase (COMT) substrates⁹⁷. In fact, catechol and pyrogallol were used as first generation COMT inhibitors for patients with Parkinson's disease^{97,166}. This means the effect observed could be by the compounds may be modulated by COMT metabolism.

Another final but very important factor to consider is the phenotype displayed by SH-SY5Y differentiated cells, that will have a major role on the activity displayed by the compounds. In the literature RA-differentiated SH-SY5Y are described to present a dopaminergic and acetylcholinergic phenotype at the end of 7 days and usually present high levels of dopamine active transporter (DAT) and tyrosine hydroxylase (TH) activity^{167,168,169}. This means the neuroprotective mechanism observed by the compounds may also be due directly to dopamine biosynthesis and degradation.

5. Conclusions

In this project we have synthesized a series of novel sulfate and glucuronide phenolic derivatives that might be useful for future applications by reducing inflammatory markers in the brain and mitigating neuron oxidative stress.

By comparing the structure of the two compounds, phloroglucinol-mono-sulfate (**3SM**) and resorcinol-O-sulfate (**12S**) (figure 5.1- **A**), that have shown the highest bioactive effect, we can suggest a core structure, that may be associated with their biological role.

In other studies, these two compounds, at least in their unconjugated forms, have been found in urine, blood and feces.¹⁶¹ Together with compound catechol-O-sulfate (**1S**) and pyrogallol-o-sulfate (**2S**), previously found by Molecular nutrition and Health group in circulation after the uptake of a mixture of fruits and berries, this information opens the possibility to modulate neuroinflammation by the application of a balanced dietary plan containing these compounds or their corresponding parent compounds. We have to state however, that a considerable amount of information is still missing about the way these molecules reach their target, if they reach the brain, and their impact of the diverse types of cells present in the rich but delicate environment of the CNS. Questions like the mechanism of action of these molecules are of great relevance to understand if preconditioning is a factor to consider. There is much to be done in the future concerning the possible targets like GPR35 and other orphan membrane receptors still to be unveiled. Confirming the expression of the receptor in microglia, its internalization, and determining the EC₅₀ might be on the *to do list*, for the future.

We have also demonstrated the ability of three compounds to prevent the cytotoxic effects of an oxidative insult in neurons. These three compounds, **1**, **2** and **9** (see figure 5.1- **B**), and sulfate conjugates, are structurally related, meaning the protection observed might also be related with a structural motif, probably related with COMT. Further assays of COMT activity might elucidate this hypothesis, and might lead to the synthesis of the new class of compounds based upon pyrogallol and neurotransmitters (fig. 4.4). In the future, the characterization of the neuronal population might also reveal crucial for our understanding of the neuronal mechanisms observed. Interestingly, two of the compounds (**1S** and **2S**) were detected in circulation and should be considered in further studies concerning dietary compounds and neurodegeneration.⁹² From all compounds, pyrogallol-O-2-sulfate was the only molecule showing pleiotropy and able to protect microglia cells from inflammatory insult but also from oxidative stress in neurons.

In silico permeability predictions, in order to evaluate the compounds ability to reach the BBB by passive diffusion have also been done. Results showed that all conjugates synthesized should be able to passively cross the BBB membrane and reach the brain. Moreover, compound **3S** and **12S** have been tested in a HBMEC model of BBB permeation, and the future analysis of the data will soon give new information about the fate of these small phenolic compounds. By the analysis of this BBB model we hope to unveil if the compounds are being further metabolized by the HBMEC, as described before.¹⁰⁸ Furthermore, due to the structural relationship with neurotransmitters, active transport through NTT should also be considered.

Understanding the pathways involved (NF- κ B, MAPK, NFAT, and others) and the sequence of events that leads to the expression of cytokines, and the real impact of these cytokines in other cells, is essential for unveiling the mechanisms of action of this compounds in modulating cytokine production, something that we hope to archive in the future. Also, to understand the mechanisms displaced by microglia, working with isolated cells is a must in order to specifically analyze the impact of a stimuli, however, in the brain cells are modulated to a series of factors in the environment. In the future the use of co-culturing systems with microglia and neurons or other cells of the CNS and evaluating cell migration, viability and chemokines should be considered, specially using different types of stimuli.

Our results are based on what we consider physiological concentrations present in humans. We have used a cell model of inflammation, oxidative insult and membrane permeation as a way of recapitulating physiological conditions trying to understand the mechanisms, and we have also demonstrated the effects of these compounds at nanomolar concentrations. Nevertheless, we are aware of some limitations our study and to counteract these and to better understand and to translate even more to the real life

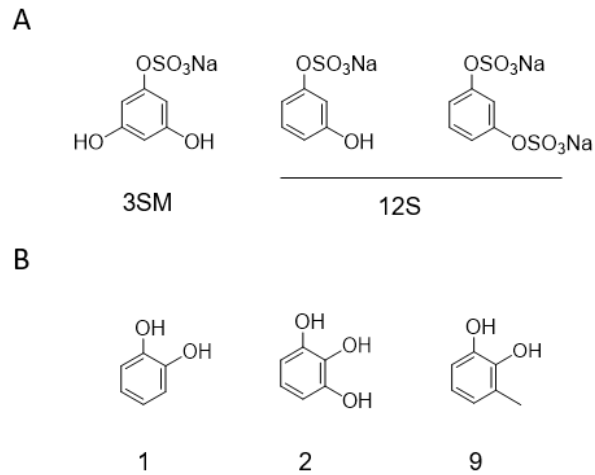


Figure 5.1: Structure of the compounds that showed the highest activity in: **A** the reduction of the inflammatory cytokine $\text{TNF}\alpha$, in microglia cells, upon exposure to LPS; **B** in the reduction of cytotoxic effects, in neurons, upon oxidative insult. **3SM**- phloroglucinol-mono-sulfate; **12S**- resorcinol-O-sulfate; **1** - catechol; **2** pyrogallol; **9**- 3-methylcatechol.

conditions, human cell lines, primary cell lines and animal models are always a useful tool and should be considered. Together, our results showed the ability of small phenolic compounds to reach the brain and modulate inflammation and cell viability, in a way that is preventive, thus opening doors for dietary habits that could prevent brain aging and neurodegenerative diseases like AD and PD.

References

- (1) Ginhoux, F., Lim, S., Hoeffel, G., Low, D., and Huber, T. (2013). Origin and differentiation of microglia. *Frontiers in Cellular Neuroscience* 7, 45.
- (2) Sarlus, H., and Heneka, M. T. (2017). Microglia in Alzheimers disease. *The Journal of clinical investigation* 127, 3240–3249.
- (3) Hansen, D. V., Hanson, J. E., and Sheng, M. (2017). Microglia in Alzheimers disease. *The Journal of Cell Biology*, DOI: 10.1083/jcb.201709069.
- (4) Pelvig, D., Pakkenberg, H., Stark, A., and Pakkenberg, B. (2008). Neocortical glial cell numbers in human brains. *Neurobiology of aging* 29, 1754–1762.
- (5) Lawson, L., Perry, V., Dri, P., and Gordon, S. (1990). Heterogeneity in the distribution and morphology of microglia in the normal adult mouse brain. *Neuroscience* 39, 151–170.
- (6) Mittelbronn, M., Dietz, K., Schluesener, H., and Meyermann, R. (2001). Local distribution of microglia in the normal adult human central nervous system differs by up to one order of magnitude. *Acta neuropathologica* 101, 249–255.
- (7) Colonna, M., and Butovsky, O. (2017). Microglia Function in the Central Nervous System During Health and Neurodegeneration. *Annual Review of Immunology* 35, 441–468.
- (8) Cherry, J. D., Olschowka, J. A., and O'Banion, M. (2014). Neuroinflammation and M2 microglia: the good, the bad, and the inflamed. *Journal of Neuroinflammation* 11, 98.
- (9) Andreou, K. E., Soto, M. S., Allen, D., Economopoulos, V., de Bernardi, A., Larkin, J. R., and Sibson, N. R. (2017). Anti-inflammatory Microglia/Macrophages As a Potential Therapeutic Target in Brain Metastasis. *Frontiers in Oncology* 7, DOI: 10.3389/fonc.2017.00251.
- (10) Holtman, I. R., Skola, D., and Glass, C. K. (2017). Transcriptional control of microglia phenotypes in health and disease. *Journal of Clinical Investigation* 127, 3220–3229.
- (11) Colonna, Y. W. M. (2015). TREM2 Lipid Sensing Sustains the Microglial Response in an Alzheimers Disease Model. *Cell* 160, 1061–1071.
- (12) Barczyk, K. P., and Mika, J. (2016). Targeting the Microglial Signaling Pathways: New Insights in the Modulation of Neuropathic Pain. *Current Medicinal Chemistry* 23, 2908–2928.
- (13) Walker, D. G., and Lue, L.-F. (2013). Understanding the neurobiology of CD200 and the CD200 receptor: a therapeutic target for controlling inflammation in human brains. *Future Neurology* 8, 321–332.
- (14) Perry, V. H., and Teeling, J. (2013). Microglia and macrophages of the central nervous system: the contribution of microglia priming and systemic inflammation to chronic neurodegeneration. *Seminars in Immunopathology* 35, 601–612.
- (15) Zhang, Q., Lenardo, M. J., and Baltimore, D. (2017). 30 Years of NF- κ B: A Blossoming of Relevance to Human Pathobiology. *Cell* 168, 37–57.
- (16) Lawrence, T. (2009). The Nuclear Factor NF- κ B Pathway in Inflammation. *Cold Spring Harbor Perspectives in Biology* 1, a001651–a001651.
- (17) Shih, R.-H., Wang, C.-Y., and Yang, C.-M. (2015). NF-kappaB Signaling Pathways in Neurological Inflammation: A Mini Review. *Frontiers in Molecular Neuroscience* 8, DOI: 10.3389/fnmol.2015.00077.
- (18) Shelest, E., Kel, A. E., Göessling, E., and Wingender, E. (2003). Prediction of potential C/EBP/NF-kappaB composite elements using matrix-based search methods. *In silico biology* 3, 71–79.
- (19) Sun, S.-C. (2017). The non-canonical NF- κ B pathway in immunity and inflammation. *Nature Reviews Immunology* 17, 545–558.

- (20) Kim, E. K., and Choi, E.-J. (2010). Pathological roles of MAPK signaling pathways in human diseases. *Biochimica et Biophysica Acta (BBA) - Molecular Basis of Disease* 1802, 396–405.
- (21) Schaeffer, H. J., and Weber, M. J. (1999). Mitogen-Activated Protein Kinases: Specific Messages from Ubiquitous Messengers. *Molecular and Cellular Biology* 19, 2435–2444.
- (22) Murshid, A., Gong, J., Prince, T., Borges, T. J., and Calderwood, S. K. (2015). Scavenger Receptor SREC-I Mediated Entry of TLR4 into Lipid Microdomains and Triggered Inflammatory Cytokine Release in RAW 264.7 Cells upon LPS Activation. *PLOS ONE* 10, ed. by Kim, C. H., e0122529.
- (23) Cristina, and Rao, A. (2001). Bridging the NFAT and NF- κ B Families. *Immunity* 15, 47–58.
- (24) Wilkins, B. J. (2004). Calcineurin NFAT Coupling Participates in Pathological, but not Physiological, Cardiac Hypertrophy. *Circulation Research* 94, 110–118.
- (25) Rao, A., Luo, C., and Hogan, P. G. (1997). TRANSCRIPTION FACTORS OF THE NFAT FAMILY: Regulation and Function. *Annual Review of Immunology* 15, 707–747.
- (26) Nagamoto-Combs, K., and Combs, C. K. (2010). Microglial Phenotype Is Regulated by Activity of the Transcription Factor, NFAT (Nuclear Factor of Activated T Cells). *Journal of Neuroscience* 30, 9641–9646.
- (27) Turner, M. D., Nedjai, B., Hurst, T., and Pennington, D. J. (2014). Cytokines and chemokines: At the crossroads of cell signalling and inflammatory disease. *Biochimica et Biophysica Acta (BBA) - Molecular Cell Research* 1843, 2563–2582.
- (28) Pascual, O., Achour, S. B., Rostaing, P., Triller, A., and Bessis, A. (2011). Microglia activation triggers astrocyte-mediated modulation of excitatory neurotransmission. *Proceedings of the National Academy of Sciences* 109, E197–E205.
- (29) Dunn, A. J. (2006). Effects of cytokines and infections on brain neurochemistry. *Clinical Neuroscience Research* 6, 52–68.
- (30) Wojdasiewicz, P., and Szukiewicz, D. (2014). The Role of Inflammatory and Anti-Inflammatory Cytokines in the Pathogenesis of Osteoarthritis. *Mediators of Inflammation* 2014, 1–19.
- (31) Parameswaran, N., and Patial, S. (2010). Tumor Necrosis Factor- α Signaling in Macrophages. *Critical Reviews in Eukaryotic Gene Expression* 20, 87–103.
- (32) Chen, C.-C., Sun, Y.-T., Chen, J.-J., and Chiu, K.-T. (2000). TNF-Induced Cyclooxygenase-2 Expression in Human Lung Epithelial Cells: Involvement of the Phospholipase C-2, Protein Kinase C-, Tyrosine Kinase, NF- κ B-Inducing Kinase, and I-B Kinase 1/2 Pathway. *The Journal of Immunology* 165, 2719–2728.
- (33) MAINI, R. N., ELLIOTT, M. J., BRENNAN, F. M., and FELDMANN, M. (1995). Beneficial effects of tumour necrosis factor- α (TNF- α) blockade in rheumatoid arthritis (RA). *Clinical & Experimental Immunology* 101, 207–212.
- (34) Vassalli, P. (1992). The Pathophysiology of Tumor Necrosis Factors. *Annual Review of Immunology* 10, 411–452.
- (35) Swaroop, J., Naidu, J., and Rajarajeswari, D. (2012). Association of TNF- α with insulin resistance in type 2 diabetes mellitus. *The Indian Journal of Medical Research* 135, 127.
- (36) Esposito, E., and Cuzzocrea, S. (2009). TNF-Alpha as a Therapeutic Target in Inflammatory Diseases, Ischemia- Reperfusion Injury and Trauma. *Current Medicinal Chemistry* 16, 3152–3167.
- (37) Neurath, M. F. (2014). Cytokines in inflammatory bowel disease. *Nature Reviews Immunology* 14, 329–342.
- (38) Probert, L. (2015). TNF and its receptors in the CNS: The essential, the desirable and the deleterious effects. *Neuroscience* 302, 2–22.
- (39) Bernardino, L., Agasse, F., Silva, B., Ferreira, R., Grade, S., and Malva, J. O. (2008). Tumor Necrosis Factor- α Modulates Survival, Proliferation, and Neuronal Differentiation in Neonatal Subventricular Zone Cell Cultures. *Stem Cells* 26, 2361–2371.
- (40) Paganelli, R., Iorio, A. D., Patricelli, L., Ripani, F., Sparvieri, E., Faricelli, R., Iarlori, C., Porreca, E., Gioacchino, M. D., and Abate, G. (2002). Proinflammatory cytokines in sera of elderly patients with dementia: levels in vascular injury are higher than those of mild-moderate Alzheimers disease patients. *Experimental Gerontology* 37, 257–263.

- (41) Mogi, M., Harada, M., Riederer, P., Narabayashi, H., Fujita, K., and Nagatsu, T. (1994). Tumor necrosis factor- α (TNF- α) increases both in the brain and in the cerebrospinal fluid from parkinsonian patients. *Neuroscience Letters* 165, 208–210.
- (42) Chang, R., Yee, K.-L., and Sumbria, R. K. (2017). Tumor necrosis factor α Inhibition for Alzheimers Disease. *Journal of Central Nervous System Disease* 9, 117957351770927.
- (43) Gutierrez, E. G., Banks, W. A., and Kastin, A. J. (1993). Murine tumor necrosis factor alpha is transported from blood to brain in the mouse. *Journal of Neuroimmunology* 47, 169–176.
- (44) Banks, W. A., Kastin, A. J., and Broadwell, R. D. (1995). Passage of Cytokines across the Blood-Brain Barrier. *Neuroimmunomodulation* 2, 241–248.
- (45) Gahring, L. C., Carlson, N. G., Kulmer, R. A., and Rogers, S. W. (1996). Neuronal Expression of Tumor Necrosis Factor Alpha in the OVOUII fme Brain. *Neuroimmunomodulation* 3, 289–303.
- (46) Welser-Alves, J. V., and Milner, R. (2013). Microglia are the major source of TNF- α and TGF- β 1 in postnatal glial cultures: regulation by cytokines, lipopolysaccharide, and vitronectin. *Neurochemistry International* 63, 47–53.
- (47) Wen, Y.-R., Tan, P.-H., Cheng, J.-K., Liu, Y.-C., and Ji, R.-R. (2011). Microglia: A Promising Target for Treating Neuropathic and Postoperative Pain, and Morphine Tolerance. *Journal of the Formosan Medical Association* 110, 487–494.
- (48) Streit, W. J., Mrak, R. E., and Griffin, W. S. T. (2004). Microglia and neuroinflammation: a pathological perspective. *Journal of Neuroinflammation* 1, 14.
- (49) Kawabori, M., and Yenari, M. A. (2014). The role of the microglia in acute CNS injury. *Metabolic Brain Disease* 30, 381–392.
- (50) Neniskyte, U., Vilalta, A., and Brown, G. C. (2014). Tumour necrosis factor alpha-induced neuronal loss is mediated by microglial phagocytosis. *FEBS Letters* 588, 2952–2956.
- (51) Vila, M., and Przedborski, S. (2003). Targeting programmed cell death in neurodegenerative diseases. *Nature Reviews Neuroscience* 4, 365–375.
- (52) Godbout, J. P., Chen, J., Abraham, J., Richwine, A. F., Berg, B. M., Kelley, K. W., and Johnson, R. W. (2005). Exaggerated neuroinflammation and sickness behavior in aged mice following activation of the peripheral innate immune system. *The FASEB Journal* 19, 1329–1331.
- (53) Henry, C. J., Huang, Y., Wynne, A. M., and Godbout, J. P. (2009). Peripheral lipopolysaccharide (LPS) challenge promotes microglial hyperactivity in aged mice that is associated with exaggerated induction of both pro-inflammatory IL-1 β and anti-inflammatory IL-10 cytokines. *Brain, Behavior, and Immunity* 23, 309–317.
- (54) Ting, J. P.-Y., and Trowsdale, J. (2002). Genetic Control of MHC Class II Expression. *Cell* 109, S21–S33.
- (55) Sierra, A., Gottfried-Blackmore, A. C., McEwen, B. S., and Bulloch, K. (2007). Microglia derived from aging mice exhibit an altered inflammatory profile. *Glia* 55, 412–424.
- (56) Saurwein-Teissl, M., Blasko, I., Zisterer, K., Neuman, B., Lang, B., and Grubeck-Loebenstien, B. (2000). AN IMBALANCE BETWEEN PRO- AND ANTI-INFLAMMATORY CYTOKINES, A CHARACTERISTIC FEATURE OF OLD AGE. *Cytokine* 12, 1160–1162.
- (57) Caldeira, C., Oliveira, A. F., Cunha, C., Vaz, A. R., Falcão, A. S., Fernandes, A., and Brites, D. (2014). Microglia change from a reactive to an age-like phenotype with the time in culture. *Frontiers in Cellular Neuroscience* 8, DOI: 10.3389/fncel.2014.00152.
- (58) Davies, D. S., Ma, J., Jegathees, T., and Goldsbury, C. (2016). Microglia show altered morphology and reduced arborization in human brain during aging and Alzheimers disease. *Brain Pathology* 27, 795–808.
- (59) Streit, W. J., Braak, H., Xue, Q.-S., and Bechmann, I. (2009). Dystrophic (senescent) rather than activated microglial cells are associated with tau pathology and likely precede neurodegeneration in Alzheimers disease. *Acta Neuropathologica* 118, 475–485.
- (60) Serrano-Pozo, A., Frosch, M. P., Masliah, E., and Hyman, B. T. (2011). Neuropathological Alterations in Alzheimer Disease. *Cold Spring Harbor Perspectives in Medicine* 1, a006189–a006189.
- (61) Floden, A. M., and Combs, C. K. (2011). Microglia Demonstrate Age-Dependent Interaction with Amyloid-upbeta Fibrils. *Journal of Alzheimers Disease* 25, 279–293.

- (62) Janssen, L., Dubbelaar, M. L., Holtman, I. R., de Boer-Bergsma, J., Eggen, B. J., Boddeke, H. W., Deyn, P. P. D., and Dam, D. V. (2017). Aging, microglia and cytoskeletal regulation are key factors in the pathological evolution of the APP23 mouse model for Alzheimers disease. *Biochimica et Biophysica Acta (BBA) - Molecular Basis of Disease* 1863, 395–405.
- (63) Machado, V., Zoller, T., Attaai, A., and Spittau, B. (2016). Microglia-Mediated Neuroinflammation and Neurotrophic Factor-Induced Protection in the MPTP Mouse Model of Parkinsons Disease-Lessons from Transgenic Mice. *International Journal of Molecular Sciences* 17, 151.
- (64) Kanaan, N. M., Kordower, J. H., and Collier, T. J. (2008). Age and region-specific responses of microglia, but not astrocytes, suggest a role in selective vulnerability of dopamine neurons after 1-methyl-4-phenyl-1,2,3,6-tetrahydropyridine exposure in monkeys. *Glia* 56, 1199–1214.
- (65) Roodveldt, C., Labrador-Garrido, A., Gonzalez-Rey, E., Lachaud, C. C., Guilliams, T., Fernandez-Montesinos, R., Benitez-Rondan, A., Robledo, G., Hmadcha, A., Delgado, M., Dobson, C. M., and Pozo, D. (2013). Preconditioning of Microglia by α -Synuclein Strongly Affects the Response Induced by Toll-like Receptor (TLR) Stimulation. *PLoS ONE* 8, ed. by Gay, N., e79160.
- (66) Bliederaeuser, C. et al. (2015). Age-dependent defects of alpha-synuclein oligomer uptake in microglia and monocytes. *Acta Neuropathologica* 131, 379–391.
- (67) Tsao, R. (2010). Chemistry and Biochemistry of Dietary Polyphenols. *Nutrients* 2, 1231–1246.
- (68) Quideau, S., Deffieux, D., Douat-Casassus, C., and Pouységu, L. (2011). Plant Polyphenols: Chemical Properties, Biological Activities, and Synthesis. *Angewandte Chemie International Edition* 50, 586–621.
- (69) Rodriguez-Mateos, A., Heiss, C., Borges, G., and Crozier, A. (2013). Berry (Poly)phenols and Cardiovascular Health. *Journal of Agricultural and Food Chemistry* 62, 3842–3851.
- (70) Feliciano, R. P., Boeres, A., Massacessi, L., Istas, G., Ventura, M. R., dos Santos, C. N., Heiss, C., and Rodriguez-Mateos, A. (2016). Identification and quantification of novel cranberry-derived plasma and urinary (poly)phenols. *Archives of Biochemistry and Biophysics* 599, 31–41.
- (71) Stark, T., Lang, R., Keller, D., Hensel, A., and Hofmann, T. (2008). Absorption of N-phenylpropenoyl-L-amino acids in healthy humans by oral administration of cocoa (Theobroma cacao). *Molecular Nutrition & Food Research* 52, 1201–1214.
- (72) Cirillo, G., Curcio, M., Vittorio, O., Iemma, F., Restuccia, D., Spizzirri, U. G., Puoci, F., and Picci, N. (2014). Polyphenol Conjugates and Human Health: A Perspective Review. *Critical Reviews in Food Science and Nutrition* 56, 326–337.
- (73) Wang, T.-y., Li, Q., and Bi, K.-s. (2018). Bioactive flavonoids in medicinal plants: Structure, activity and biological fate. *Asian Journal of Pharmaceutical Sciences* 13, 12–23.
- (74) Rio, D. D., Rodriguez-Mateos, A., Spencer, J. P., Tognolini, M., Borges, G., and Crozier, A. (2013). Dietary (Poly)phenolics in Human Health: Structures, Bioavailability, and Evidence of Protective Effects Against Chronic Diseases. *Antioxidants & Redox Signaling* 18, 1818–1892.
- (75) Figueira, I. et al. (2017). Polyphenols journey through blood-brain barrier towards neuronal protection. *Scientific Reports* 7, DOI: 10.1038/s41598-017-11512-6.
- (76) González-Gallego, J., García-Mediavilla, M. V., Sánchez-Campos, S., and Tuñón, M. J. (2010). Fruit polyphenols, immunity and inflammation. *British Journal of Nutrition* 104, S15–S27.
- (77) Joseph, S. V., Edirisinghe, I., and Burton-Freeman, B. M. (2015). Fruit Polyphenols: A Review of Anti-inflammatory Effects in Humans. *Critical Reviews in Food Science and Nutrition* 56, 419–444.
- (78) Karunaweera, N., Raju, R., and Gyengesi, E. (2015). Plant polyphenols as inhibitors of NF- κ B induced cytokine production - a potential anti-inflammatory treatment for Alzheimers disease? *Frontiers in Molecular Neuroscience* 8, DOI: 10.3389/fnmo.2015.00024.
- (79) Aktas, O., Prozorovski, T., Smorodchenko, A., Savaskan, N. E., Lauster, R., Kloetzel, P.-M., Infante-Duarte, C., Brocke, S., and Zipp, F. (2004). Green Tea Epigallocatechin-3-Gallate Mediates T Cellular NF- κ B Inhibition and Exerts Neuroprotection in Autoimmune Encephalomyelitis. *The Journal of Immunology* 173, 5794–5800.
- (80) Lee, J. W., Lee, Y. K., Ban, J. O., Ha, T. Y., Yun, Y. P., Han, S. B., Oh, K. W., and Hong, J. T. (2009). Green Tea (-)-Epigallocatechin-3-Gallate Inhibits β -Amyloid-Induced Cognitive Dysfunction through Modification of Secretase Activity via Inhibition of ERK and NF- κ B Pathways in Mice. *The Journal of Nutrition* 139, 1987–1993.

- (81) Dajas, F. (2012). Life or death: Neuroprotective and anticancer effects of quercetin. *Journal of Ethnopharmacology* 143, 383–396.
- (82) Sternberg, Z., Chadha, K., Lieberman, A., Hojnacki, D., Drake, A., Zamboni, P., Rocco, P., Grazioli, E., Weinstock-Guttman, B., and Munschauer, F. (2008). Quercetin and interferon- β modulate immune response(s) in peripheral blood mononuclear cells isolated from multiple sclerosis patients. *Journal of Neuroimmunology* 205, 142–147.
- (83) *The Molecular Targets and Therapeutic Uses of Curcumin in Health and Disease*; Aggarwal, B. B., Surh, Y.-J., and Shishodia, S., Eds.; Springer US: 2007.
- (84) Garcia-Alloza, M., Borrelli, L. A., Rozkalne, A., Hyman, B. T., and Bacskai, B. J. (2007). Curcumin labels amyloid pathology in vivo, disrupts existing plaques, and partially restores distorted neurites in an Alzheimer mouse model. *Journal of Neurochemistry* 102, 1095–1104.
- (85) Jang, J. (2003). Protective effect of resveratrol on β -amyloid-induced oxidative PC12 cell death. *Free Radical Biology and Medicine* 34, 1100–1110.
- (86) Jin, F., Wu, Q., Lu, Y.-F., Gong, Q.-H., and Shi, J.-S. (2008). Neuroprotective effect of resveratrol on 6-OHDA-induced Parkinsons disease in rats. *European Journal of Pharmacology* 600, 78–82.
- (87) di Gesso, J. L., Kerr, J. S., Zhang, Q., Raheem, S., Yalamanchili, S. K., OHagan, D., Kay, C. D., and OConnell, M. A. (2015). Flavonoid metabolites reduce tumor necrosis factor- α secretion to a greater extent than their precursor compounds in human THP-1 monocytes. *Molecular Nutrition & Food Research* 59, 1143–1154.
- (88) Spagnuolo, C., Napolitano, M., Tedesco, I., Moccia, S., Milito, A., and Russo, G. L. (2016). Neuroprotective Role of Natural Polyphenols. *Current Topics in Medicinal Chemistry* 16, 1943–1950.
- (89) DO Dr. Stewart A. Factor, M. D. D. W. W., *Parkinsons Disease*; Springer Publishing: 2007; 1024 pp.
- (90) Titova, N., Jenner, P., and Chaudhuri, K. R. (2017). The Future of Parkinsons Treatment - Personalised and Precision Medicine. *European Neurological Review* 12, 15.
- (91) Bonifacio, M. J., Palma, P. N., Almeida, L., and Soares-da-Silva, P. (2007). Catechol-O-methyltransferase and Its Inhibitors in Parkinsons Disease. *CNS Drug Reviews* 13, 352–379.
- (92) Pimpão, R. C., Ventura, M. R., Ferreira, R. B., Williamson, G., and Santos, C. N. (2015). Phenolic sulfates as new and highly abundant metabolites in human plasma after ingestion of a mixed berry fruit puree. *British Journal of Nutrition* 113, 454–463.
- (93) Drake, C. R., Estevez-Salmeron, L., Gascard, P., Shen, Y., Tlsty, T. D., and Jones, E. F. (2015). Towards aspirin-inspired self-immolating molecules which target the cyclooxygenases. *Organic & Biomolecular Chemistry* 13, 11078–11086.
- (94) Vane, J., and Botting, R. (2003). The mechanism of action of aspirin. *Thrombosis Research* 110, 255–258.
- (95) Ock, J., Han, H. S., Hong, S. H., Lee, S. Y., Han, Y.-M., Kwon, B.-M., and Suk, K. (2010). Obvatol attenuates microglia-mediated neuroinflammation by modulating redox regulation. *British Journal of Pharmacology* 159, 1646–1662.
- (96) Suk, K., and Ock, J. (2011). Chemical genetics of neuroinflammation: natural and synthetic compounds as microglial inhibitors. *Inflammopharmacology* 20, 151–158.
- (97) Walle, T. (2004). Absorption and metabolism of flavonoids. *Free Radical Biology and Medicine* 36, 829–837.
- (98) Espín, J. C., González-Sarrías, A., and Tomás-Barberán, F. A. (2017). The gut microbiota: A key factor in the therapeutic effects of (poly)phenols. *Biochemical Pharmacology* 139, 82–93.
- (99) Braune, A., and Blaut, M. (2016). Bacterial species involved in the conversion of dietary flavonoids in the human gut. *Gut Microbes* 7, 216–234.
- (100) González-Sarrias, A. (2017). Non-extractable polyphenols produce gut microbiota metabolites that persist in circulation and show anti-inflammatory and free radical-scavenging effects. *Trends in Food Science & Technology* 69, 281–288.
- (101) Gonzalez-Barrio, R., Edwards, C. A., and Crozier, A. (2011). Colonic Catabolism of Ellagitannins, Ellagic Acid, and Raspberry Anthocyanins: In Vivo and In Vitro Studies. *Drug Metabolism and Disposition* 39, 1680–1688.

- (102) Crozier, A., and Spencer, J., *FLAVONOIDS & RELATED COMPOUNDS*; CRC PR INC: 2016; 471 pp.
- (103) Schaffer, S., and Halliwell, B. (2011). Do polyphenols enter the brain and does it matter? Some theoretical and practical considerations. *Genes & Nutrition* 7, 99–109.
- (104) Dando, S. J., Mackay-Sim, A., Norton, R., Currie, B. J., John, J. A. S., Ekberg, J. A. K., Batzloff, M., Ulett, G. C., and Beacham, I. R. (2014). Pathogens Penetrating the Central Nervous System: Infection Pathways and the Cellular and Molecular Mechanisms of Invasion. *Clinical Microbiology Reviews* 27, 691–726.
- (105) Keane, J., and Campbell, M. (2015). The dynamic blood-brain barrier. *FEBS Journal* 282, 4067–4079.
- (106) Wu, K.-W., Mo, J.-L., Kou, Z.-W., Liu, Q., Lv, L.-L., Lei, Y., and Sun, F.-Y. (2017). Neurovascular Interaction Promotes the Morphological and Functional Maturation of Cortical Neurons. *Frontiers in Cellular Neuroscience* 11, DOI: 10.3389/fncel.2017.00290.
- (107) da Fonseca, A. C. C., Matias, D., Garcia, C., Amaral, R., Geraldo, L. H., Freitas, C., and Lima, F. R. S. (2014). The impact of microglial activation on blood-brain barrier in brain diseases. *Frontiers in Cellular Neuroscience* 8, DOI: 10.3389/fncel.2014.00362.
- (108) Figueira, I., Menezes, R., Macedo, D., Costa, I., and dos Santos, C. N. (2017). Polyphenols Beyond Barriers: A Glimpse into the Brain. *Current Neuropharmacology* 15, 562–594.
- (109) Kim, S. M., Chung, M. J., Ha, T. J., Choi, H. N., Jang, S. J., Kim, S. O., Chun, M. H., Do, S. I., Choo, Y. K., and Park, Y. I. (2012). Neuroprotective effects of black soybean anthocyanins via inactivation of ASK1–JNK/p38 pathways and mobilization of cellular sialic acids. *Life Sciences* 90, 874–882.
- (110) Youdim, K. A., Qaiser, M., Begley, D. J., Rice-Evans, C. A., and Abbott, N. (2004). Flavonoid permeability across an in situ model of the blood–brain barrier. *Free Radical Biology and Medicine* 36, 592–604.
- (111) Hussain, S., Sulaiman, A., Alhaddad, H., and Alhadidi, Q. (2016). Natural polyphenols: Influence on membrane transporters. *Journal of Intercultural Ethnopharmacology* 5, 97.
- (112) Joven, J., Micol, V., Segura-Carretero, A., and Alonso-Villaverde, C. (2014). Polyphenols and the Modulation of Gene Expression Pathways: Can We Eat Our Way Out of the Danger of Chronic Disease. *Critical Reviews in Food Science and Nutrition* 54, 985–1001.
- (113) Afzal, M., Safer, A. M., and Menon, M. (2015). Green tea polyphenols and their potential role in health and disease. *Inflammopharmacology* 23, 151–161.
- (114) Hadad, N., and Levy, R. (2017). Combination of EPA with Carotenoids and Polyphenol Synergistically Attenuated the Transformation of Microglia to M1 Phenotype Via Inhibition of NF-κB. *NeuroMolecular Medicine* 19, 436–451.
- (115) Xu, D., Omura, T., Masaki, N., and Matsuyama, Y. (2016). Increased arachidonic acid-containing phosphatidylcholine is associated with reactive microglia and astrocytes in the spinal cord after peripheral nerve injury. *Scientific Reports* 6, DOI: 10.1038/srep26427.
- (116) Yacoubian, T. In *Drug Discovery Approaches for the Treatment of Neurodegenerative Disorders*; Elsevier: 2017, pp 1–16.
- (117) Morimoto, R. I. (2008). Proteotoxic stress and inducible chaperone networks in neurodegenerative disease and aging. *Genes & Development* 22, 1427–1438.
- (118) Prahlad, V., and Morimoto, R. I. (2009). Integrating the stress response: lessons for neurodegenerative diseases from *C. elegans*. *Trends in Cell Biology* 19, 52–61.
- (119) McNally, J. S., Davis, M. E., Giddens, D. P., Saha, A., Hwang, J., Dikalov, S., Jo, H., and Harrison, D. G. (2003). Role of xanthine oxidoreductase and NAD(P)H oxidase in endothelial superoxide production in response to oscillatory shear stress. *American Journal of Physiology-Heart and Circulatory Physiology* 285, H2290–H2297.
- (120) Spina, M. B., and Cohen, G. (1989). Dopamine turnover and glutathione oxidation: implications for Parkinson disease. *Proceedings of the National Academy of Sciences* 86, 1398–1400.
- (121) Guadagno, J., Xu, X., Karajgikar, M., Brown, A., and Cregan, S. P. (2013). Microglia-derived TNF α induces apoptosis in neural precursor cells via transcriptional activation of the Bcl-2 family member Puma. *Cell Death & Disease* 4, e538–e538.

- (122) Gordon, J., Amini, S., and White, M. K. In *Neuronal Cell Culture*; Humana Press: 2013, pp 1–8.
- (123) Unno, K., Pervin, M., Nakagawa, A., Iguchi, K., Hara, A., Takagaki, A., Nanjo, F., Minami, A., and Nakamura, Y. (2017). Blood-Brain Barrier Permeability of Green Tea Catechin Metabolites and their Neuritogenic Activity in Human Neuroblastoma SH-SY5Y Cells. *Molecular Nutrition & Food Research* 61, 1700294.
- (124) González-Sarrías, A., Núñez-Sánchez, M. Á., Tomás-Barberán, F. A., and Espín, J. C. (2016). Neuroprotective Effects of Bioavailable Polyphenol-Derived Metabolites against Oxidative Stress-Induced Cytotoxicity in Human Neuroblastoma SH-SY5Y Cells. *Journal of Agricultural and Food Chemistry* 65, 752–758.
- (125) Esteban-Fernández, A., Rendeiro, C., Spencer, J. P. E., del Coso, D. G., de Llano, M. D. G., Bartolomé, B., and Moreno-Arribas, M. V. (2017). Neuroprotective Effects of Selected Microbial-Derived Phenolic Metabolites and Aroma Compounds from Wine in Human SH-SY5Y Neuroblastoma Cells and Their Putative Mechanisms of Action. *Frontiers in Nutrition* 4, DOI: 10.3389/fnut.2017.00003.
- (126) Dhanalakshmi, C., Manivasagam, T., Nataraj, J., Thenmozhi, A. J., and Essa, M. M. (2015). Neurosupportive Role of Vanillin, a Natural Phenolic Compound, on Rotenone Induced Neurotoxicity in SH-SY5Y Neuroblastoma Cells. *Evidence-Based Complementary and Alternative Medicine* 2015, 1–11.
- (127) Wang, L., Xu, S., Xu, X., and Chan, P. (2009). (-)-Epigallocatechin-3-Gallate Protects SH-SY5Y Cells Against 6-OHDA-Induced Cell Death through STAT3 Activation. *Journal of Alzheimer's Disease* 17, 295–304.
- (128) Almeida, A. F., Santos, C. N., and Ventura, M. R. (2017). Synthesis of New Sulfated and Glucuronated Metabolites of Dietary Phenolic Compounds Identified in Human Biological Samples. *Journal of Agricultural and Food Chemistry* 65, 6460–6466.
- (129) Honda, S., Fukuyama, Y., Nishiwaki, H., Masuda, A., and Masuda, T. (2017). Conversion to purpurogallin, a key step in the mechanism of the potent xanthine oxidase inhibitory activity of pyrogallol. *Free Radical Biology and Medicine* 106, 228–235.
- (130) Fieser, M., *Fieser and Fiesers Reagents for Organic Synthesis, Volume 1*; JOHN WILEY & SONS INC: 1967, p 584; 1472 pp.
- (131) Cheung, Y.-T., Lau, W. K.-W., Yu, M.-S., Lai, C. S.-W., Yeung, S.-C., So, K.-F., and Chang, R. C.-C. (2009). Effects of all-trans-retinoic acid on human SH-SY5Y neuroblastoma as in vitro model in neurotoxicity research. *NeuroToxicology* 30, 127–135.
- (132) Palmela, I., Sasaki, H., Cardoso, F. L., Moutinho, M., Kim, K. S., Brites, D., and Brito, M. A. (2012). Time-dependent dual effects of high levels of unconjugated bilirubin on the human blood-brain barrier lining. *Frontiers in Cellular Neuroscience* 6, DOI: 10.3389/fncel.2012.00022.
- (133) Matzner, U., Harzer, K., Learish, R., Barranger, J., and Gieselmann, V. (2000). Long-term expression and transfer of arylsulfatase A into brain of arylsulfatase A-deficient mice transplanted with bone marrow expressing the arylsulfatase A cDNA from a retroviral vector. *Gene Therapy* 7, 1250–1257.
- (134) Kim, H., Roh, H., Lee, H. J., Chung, S. Y., Choi, S. O., Lee, K. R., and Han, S. B. (2003). Determination of phloroglucinol in human plasma by high-performance liquid chromatography - mass spectrometry. *Journal of Chromatography B* 792, 307–312.
- (135) Daniels, B. P., Cruz-Orengo, L., Pasioka, T. J., Couraud, P.-O., Romero, I. A., Weksler, B., Cooper, J. A., Doering, T. L., and Klein, R. S. (2013). Immortalized human cerebral microvascular endothelial cells maintain the properties of primary cells in an in vitro model of immune migration across the blood brain barrier. *Journal of Neuroscience Methods* 212, 173–179.
- (136) Hayball, P. J. (1995). Formation and reactivity of acyl glucuronides: The influence of chirality. *Chirality* 7, 1–9.
- (137) Das, R., and Mukhopadhyay, B. (2016). Chemical O-Glycosylations: An Overview. *Chemistry-Open* 5, 401–433.
- (138) Lucas, R., Alcantara, D., and Morales, J. C. (2009). A concise synthesis of glucuronide metabolites of urolithin-B, resveratrol, and hydroxytyrosol. *Carbohydrate Research* 344, 1340–1346.

- (139) Yu, B., and Sun, J. (2010). Glycosylation with glycosyl N-phenyltrifluoroacetimidates (PTFAI) and a perspective of the future development of new glycosylation methods. *Chemical Communications* 46, 4668.
- (140) Suzuki, K., Ohtsuka, I., Kanemitsu, T., Ako, T., and Kanie, O. (2005). Single-Step Multisyntheses of Glycosyl Acceptors: Benzylolation of 1-Hydroxyl Groups of Phenylthio Glycosides of Xylose, Mannose, Glucose, Galactose, 2-Azido-2-deoxy-glucose, and 2-Azido-2-deoxy-galactose. *Journal of Carbohydrate Chemistry* 24, 219–236.
- (141) Bolarinwa, A., and Linseisen, J. (2005). Validated application of a new high-performance liquid chromatographic method for the determination of selected flavonoids and phenolic acids in human plasma using electrochemical detection. *Journal of Chromatography B* 823, 143–151.
- (142) D. K. Salunkhe, J. K. C., *Dietary Tannins: Consequences and Remedies*; CRC Press: 1989.
- (143) Rothman, N., Bechtold, W. E., Yin, S. N., Dosemeci, M., Li, G. L., Wang, Y. Z., Griffith, W. C., Smith, M. T., and Hayes, R. B. (1998). Urinary excretion of phenol, catechol, hydroquinone, and muconic acid by workers occupationally exposed to benzene. *Occupational and environmental medicine* 55, 705–711.
- (144) Kawanishi, S., Inoue, S., and Kawanishi, M. (1989). Human DNA damage induced by 1,2,4-benzenetriol, a benzene metabolite. *Cancer research* 49, 164–168.
- (145) Kraft, A. D., McPherson, C. A., and Harry, G. J. (2009). Heterogeneity of microglia and TNF signaling as determinants for neuronal death or survival. *NeuroToxicology* 30, 785–793.
- (146) Ezcurra, A. L. D. L., Chertoff, M., Ferrari, C., Graciarena, M., and Pitossi, F. (2010). Chronic expression of low levels of tumor necrosis factor- α in the substantia nigra elicits progressive neurodegeneration, delayed motor symptoms and microglia/macrophage activation. *Neurobiology of Disease* 37, 630–640.
- (147) Kim, M.-M., and Kim, S.-K. (2010). Effect of phloroglucinol on oxidative stress and inflammation. *Food and Chemical Toxicology* 48, 2925–2933.
- (148) Wang, J., Simonavicius, N., Wu, X., Swaminath, G., Reagan, J., Tian, H., and Ling, L. (2006). Kynurenic Acid as a Ligand for Orphan G Protein-coupled Receptor GPR35. *Journal of Biological Chemistry* 281, 22021–22028.
- (149) Fredriksson, R. (2005). The Repertoire of G-Protein-Coupled Receptors in Fully Sequenced Genomes. *Molecular Pharmacology* 67, 1414–1425.
- (150) Wirthgen, E., Hoeflich, A., Rebl, A., and Gunther, J. (2018). Kynurenic Acid: The Janus-Faced Role of an Immunomodulatory Tryptophan Metabolite and Its Link to Pathological Conditions. *Frontiers in Immunology* 8, DOI: 10.3389/fimmu.2017.01957.
- (151) MacKenzie, A. E., Lappin, J. E., Taylor, D. L., Nicklin, S. A., and Milligan, G. (2011). GPR35 as a Novel Therapeutic Target. *Frontiers in Endocrinology* 2, DOI: 10.3389/fendo.2011.00068.
- (152) Deng, H., Hu, H., Ling, S., Ferrie, A. M., and Fang, Y. (2012). Discovery of Natural Phenols as G Protein-Coupled Receptor-35 (GPR35) Agonists. *ACS Medicinal Chemistry Letters* 3, 165–169.
- (153) Villar-Cheda, B., Dominguez-Mejide, A., Joglar, B., Rodriguez-Perez, A. I., Guerra, M. J., and Labandeira-Garcia, J. L. (2012). Involvement of microglial RhoA/Rho-Kinase pathway activation in the dopaminergic neuron death. Role of angiotensin via angiotensin type 1 receptors. *Neurobiology of Disease* 47, 268–279.
- (154) Guillard, C., Chrétien, S., Pelus, A.-S., Porteu, F., Muller, O., Mayeux, P., and Duprez, V. (2003). Activation of the Mitogen-activated Protein Kinases Erk1/2 by Erythropoietin Receptor via a GiProtein $\beta\gamma$ -Subunit-initiated Pathway. *Journal of Biological Chemistry* 278, 11050–11056.
- (155) Cha, B. K., Choi, C. H., Kim, B. J., Oh, H.-C., Kim, J. W., Do, J. H., Kim, J. G., and Chang, S. K. (2011). The Effect of Phloroglucinol in Diarrhea-Dominant Irritable Bowel Syndrome: Randomized, Double-Blind, Placebo-Controlled Trial. *Gastroenterology* 140, S-611–S-612.
- (156) CHASSANY, O., BONAZ, B., VARANNES, S. B. D., BUENO, L., CARGILL, G., COFFIN, B., DUCROTTE, P., and GRANGÉ, V. (2007). Acute exacerbation of pain in irritable bowel syndrome: efficacy of phloroglucinol/trimethylphloroglucinol - a randomized, double-blind, placebo-controlled study. *Alimentary Pharmacology & Therapeutics* 25, 1115–1123.

- (157) Kutmon, M., van Iersel, M. P., Bohler, A., Kelder, T., Nunes, N., Pico, A. R., and Evelo, C. T. (2015). PathVisio 3: An Extendable Pathway Analysis Toolbox. *PLoS Computational Biology* 11, ed. by Murphy, R. F., e1004085.
- (158) Malik, R., Mehta, P., Srivastava, S., Choudhary, B. S., and Sharma, M. (2016). Pharmacophore modeling, 3D-QSAR, and in silico ADME prediction of N-pyridyl and pyrimidine benzamides as potent antiepileptic agents. *Journal of Receptors and Signal Transduction* 37, 259–266.
- (159) Ntie-Kang, F., Lifongo, L. L., Mbah, J. A., Owono, L. C. O., Megnassan, E., Mbaze, L., Judson, P. N., Sippl, W., and Efange, S. M. N. (2013). In silico drug metabolism and pharmacokinetic profiles of natural products from medicinal plants in the Congo basin. *In Silico Pharmacology* 1, 12.
- (160) Barcellos, M. P., Santos, C. B. R., Federico, L. B., de Almeida, P. F., de Paula da Silva, C. H. T., and Taft, C. A. (2018). Pharmacophore and structure-based drug design, molecular dynamics and admet/tox studies to design novel potential pad4 inhibitors. *Journal of Biomolecular Structure and Dynamics*, 1–16.
- (161) Welsch, F. (2008). Routes and Modes of Administration of Resorcinol and Their Relationship to Potential Manifestations of Thyroid Gland Toxicity in Animals and Man. *International Journal of Toxicology* 27, 59–63.
- (162) Taskinen, J. (2003). CONJUGATION OF CATECHOLS BY RECOMBINANT HUMAN SULFO-TRANSFERASES, UDP-GLUCURONOSYLTRANSFERASES, AND SOLUBLE CATECHOL O-METHYLTRANSFERASE: STRUCTURE-CONJUGATION RELATIONSHIPS AND PREDICTIVE MODELS. *Drug Metabolism and Disposition* 31, 1187–1197.
- (163) Kristensen, A. S., Andersen, J., Jorgensen, T. N., Sorensen, L., Eriksen, J., Loland, C. J., Stromgaard, K., and Gether, U. (2011). SLC6 Neurotransmitter Transporters: Structure, Function, and Regulation. *Pharmacological Reviews* 63, 585–640.
- (164) Ma, Q. (2013). Role of Nrf2 in Oxidative Stress and Toxicity. *Annual Review of Pharmacology and Toxicology* 53, 401–426.
- (165) Venugopal, R., and Jaiswal, A. K. (1996). Nrf1 and Nrf2 positively and c-Fos and Fra1 negatively regulate the human antioxidant response element-mediated expression of NAD(P)H-quinone oxidoreductase1 gene. *Proceedings of the National Academy of Sciences of the United States of America* 93, 14960–14965.
- (166) Baldessarini, R. J., and Greiner, E. (1973). Inhibition of catechol-o-methyl transferase by catechols and polyphenols. *Biochemical Pharmacology* 22, 247–256.
- (167) Luchtman, D. W., and Song, C. (2010). Why SH-SY5Y cells should be differentiated. *NeuroToxicology* 31, 164–165.
- (168) Kovalevich, J., and Langford, D. In *Neuronal Cell Culture*; Humana Press: 2013, pp 9–21.
- (169) Korecka, J. A., van Kesteren, R. E., Blaas, E., Spitzer, S. O., Kamstra, J. H., Smit, A. B., Swaab, D. F., Verhaagen, J., and Bossers, K. (2013). Phenotypic Characterization of Retinoic Acid Differentiated SH-SY5Y Cells by Transcriptional Profiling. *PLoS ONE* 8, ed. by Lim, K.-L., e63862.

A. *Annex A - Glossary of compounds*

The list of compounds acquired commercially is shown in table A.1, together with the chemical structure, IUPAC nomenclature and purity. The list of synthesized compounds with the respective assigned number, chemical structure, common name and IUPAC nomenclature is also shown below (table A2-A4).

Table A.1 : List of chemical compounds acquired commercially

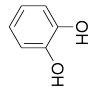
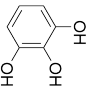
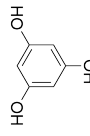
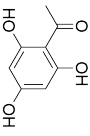
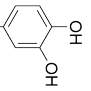
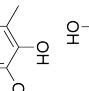
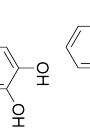
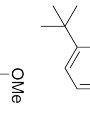
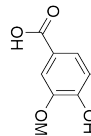
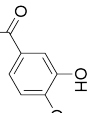
Structure	Nr.	Name	IUPAC	Manufacturer	Purity %
	1	catechol	benzene-1,2-diol	Sigma-Aldrich	>99
	2	pyrogallol	benzene-1,2,3-triol	Sigma-Aldrich	>99
	3	phloroglucinol	benzene-1,3,5-triol	Alfa-aesar	>99
	4	2,4,6-trihydroxy-acetophenone	1-(2,4,6-trihydroxyphenyl)ethan-1-one	Sigma-Aldrich	>99
	6	4-hydroxycatechol	benzene-1,2,4-triol	Carbosynth	>99
	9	3-methylcatechol	3-methylbenzene-1,2-diol	Sigma-Aldrich	>99
	8	4-tert-butylcatechol	4-(tertbutyl)benzene-1,2-diol	Sigma-Aldrich	>99
	10	syringic acid	4-hydroxy-3,5-dimethoxybenzoic acid	Sigma-Aldrich	>99
	16	protocatechuic acid	3,4-dihydroxybenzoic acid	Sigma-Aldrich	>99
	14	-	2,3,4-trihydroxybenzaldehyde	Carbosynth	>99

Table A.2: List of chemical synthesized compounds (compounds are numbered in the order they were evaluated)

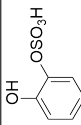
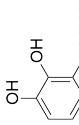
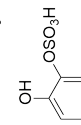
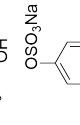
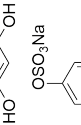
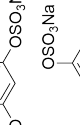
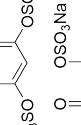
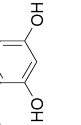
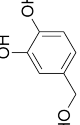
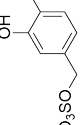
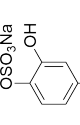
Structure	Nr.	Sub Nu.	Name	IUPAC
	1	1S	catechol-O-sulfate	sodium 2-hydroxyphenyl sulfate
	2	2S1	pyrogallol-O-1-sulfate	Sodium 2,3-dihydroxyphenyl sulfate
	2	2S2	pyrogallol-O-2-sulfate	Sodium 2,6-dihydroxyphenyl sulfate
	3	3SM	phloroglucinol-mono-sulfate	Sodium 3,5-dihydroxyphenyl sulfate
	3	3S2	phloroglucinol-di-sulfate	Sodium 5-hydroxy-1,3-phenylene bi (sulfate)
	3	3S3	phloroglucinol-tri-sulfate	Sodium benzene-1,3,5-triyl tri(sulfate)
	4	4S	2,4,6-trihydroxyacetophenone-O-sulfate	Sodium 4-acetyl-3,5-dihydroxyphenyl sulfate
	5	-	3,4-dihydroxybenzoic acid	4-(hydroxymethyl)-catechol
	5	5S	4-hydroxy-catechol-O-sulfate	4Sodium 3,4-dihydroxyphenyl sulfate
	6	6S	4-hydroxy-catechol-O-sulfate	4Sodium 3,4-dihydroxyphenyl sulfate
	7	-	4-methyl-pyrogallol	4-methylbenzene-1,2,3-triol

Table A.3: List of chemical synthesized compounds (compounds are numbered in the order they were evaluated)

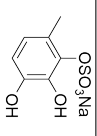
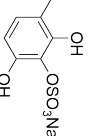
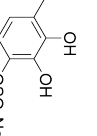
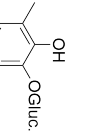
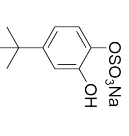
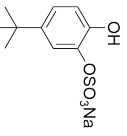
Structure	Nr.	Sub Nr.	Name	IUPAC
	7	7S1	4-methylpyrogallol-O-1-sulfate	Sodium 2,3-dihydroxy-6-methylphenyl sulfate
	7	7S2	4-methylpyrogallol-O-2-sulfate	Sodium 2,6-dihydroxy-3-methylphenyl sulfate
	7	7S3	4-methylpyrogallol-O-3-sulfate	Sodium 2,3-dihydroxy-4-methylphenyl sulfate
	7	7G2	4-methylpyrogallol-O-2-glucuronide	(2S,3S,4S,5R,6S)-6-(2,6-dihydroxy-3-methylphenoxy)-3,4,5-trihydroxytetrahydro-2H-pyran-2-carboxylic acid
	8	8S	4-tertbutylcatechol-O-1-sulfate	Sodium 4-tert-butyl-2-hydroxyphenyl sulfate
	8	8S	4-tertbutylcatechol-O-2-sulfate	Sodium 5-tert-butyl-2-hydroxyphenyl sulfate

Table A.4: List of chemical synthesized compounds (compounds are numbered in the order they were evaluated)

Structure	Nr.	Sub Nr.	Name	IUPAC
	8	8G	4-tert-butylcatechol-O-1-glucuronide	(2S,3S,4S,5R,6S)-6-(5-(tert-butyl)-2-hydroxyphenoxy)-3,4,5-trihydroxytetrahydro-2H-pyran-2-carboxylic acid
	8	8G	4-tert-butylcatechol-O-2-glucuronide	(2S,3S,4S,5R,6S)-6-(4-(tert-butyl)-2-hydroxyphenoxy)-3,4,5-trihydroxytetrahydro-2H-pyran-2-carboxylic acid
	9	9S1	3-methyl-Catechol-O-1-sulfate	Sodium 2-hydroxy-3-methylphenyl sulfate
	9	9S2	3-methyl-Catechol-O-2-sulfate	Sodium 2-hydroxy-6-methylphenyl sulfate
	9	9G1	3-methyl-catechol-O-1-glucuronide	(2S,3S,4S,5R,6S)-3,4,5-trihydroxy-6-(2-hydroxy-6-methylphenoxy)tetrahydro-2H-pyran-2-carboxylic acid
	9	9G2	3-methyl-catechol-O-2-glucuronide	(2S,3S,4S,5R,6S)-3,4,5-trihydroxy-6-(2-hydroxy-3-methylphenoxy)tetrahydro-2H-pyran-2-carboxylic acid
	10	10S	syringic acid-O-sulfate	1-(4-hydroxy-3,5-dimethoxyphenyl)-2-phenylethan-1-one
	10	10G	syringic acid-O-glucuronide	(2S,3S,4S,5R,6S)-6-(4-carboxy-2,6-dimethoxyphenoxy)-3,4,5-trihydroxytetrahydro-2H-pyran-2-carboxylic acid

B. *Annex B- Toxicity effect of second iteration compounds in microglia cells*

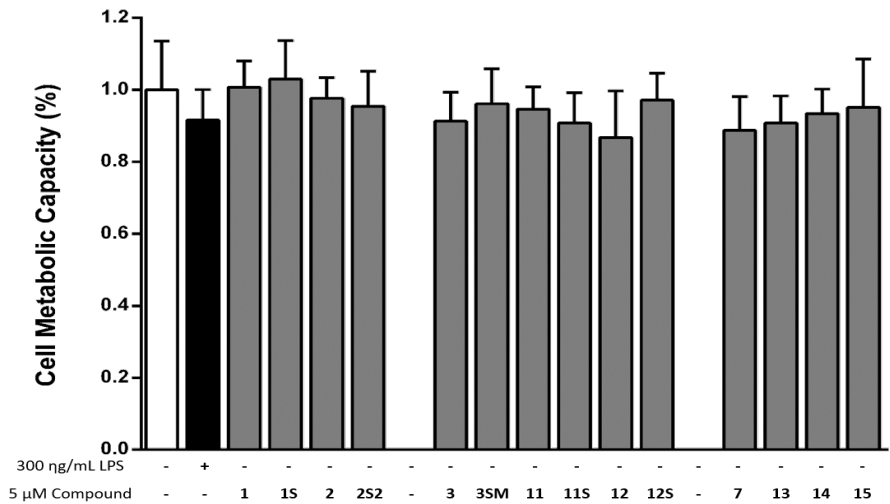


Figure B.1: Cell metabolic capacity was evaluated in microglia cells, in order to verify if toxic effects were evident from compound incubation. No statistical significance was found between the compounds and the control, non-incubated cells.

C. Annex C - Determination of t-BHP LD50 in SH-SY5Y

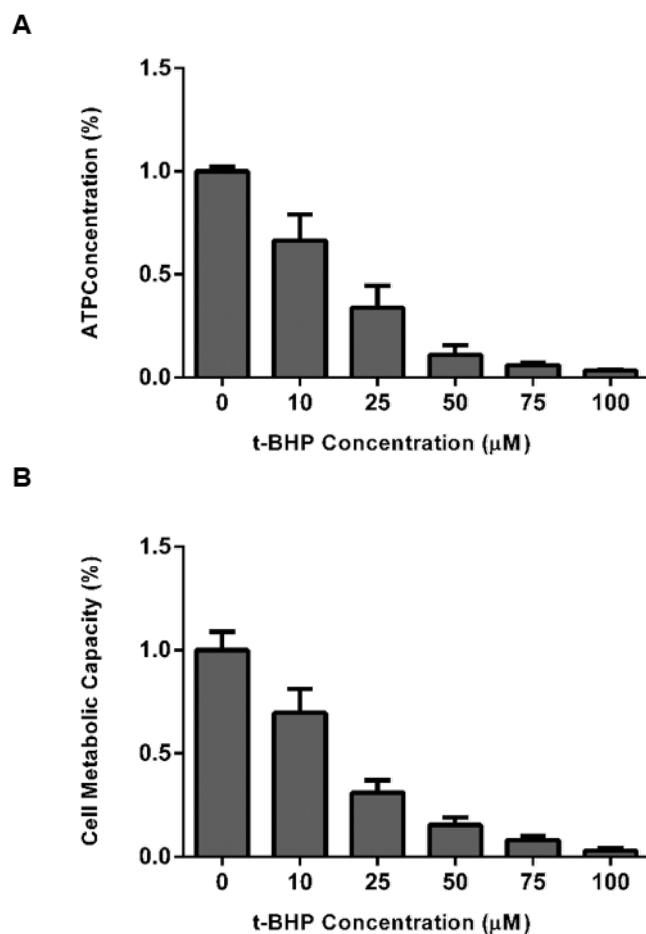


Figure C.1: The LD50 or 50% lethal dose for SH-SY5Y using t-BHP was calculated using celltiter blue and celltiter glo. Dose response curves were created with the same protocol as for the model used for the evaluation of compound neuroprotective capability. For the calculation of LD50, t-BHP logarithmic concentration was plotted vs the measured fluorescence in the case of celltiter blue, and luminescence in case of celltiter glo(in percentage). An exponential curve was plotted and the value of LD50 obtain for a inhibition of 50% relative to control cells. The values of LD50 were 20.38 **A** and 19.80 **B**. A concentration of 20 μM was used as a compromise between both extrapolations.

D. Annex D - Evaluation of compounds in SH-SY5Y

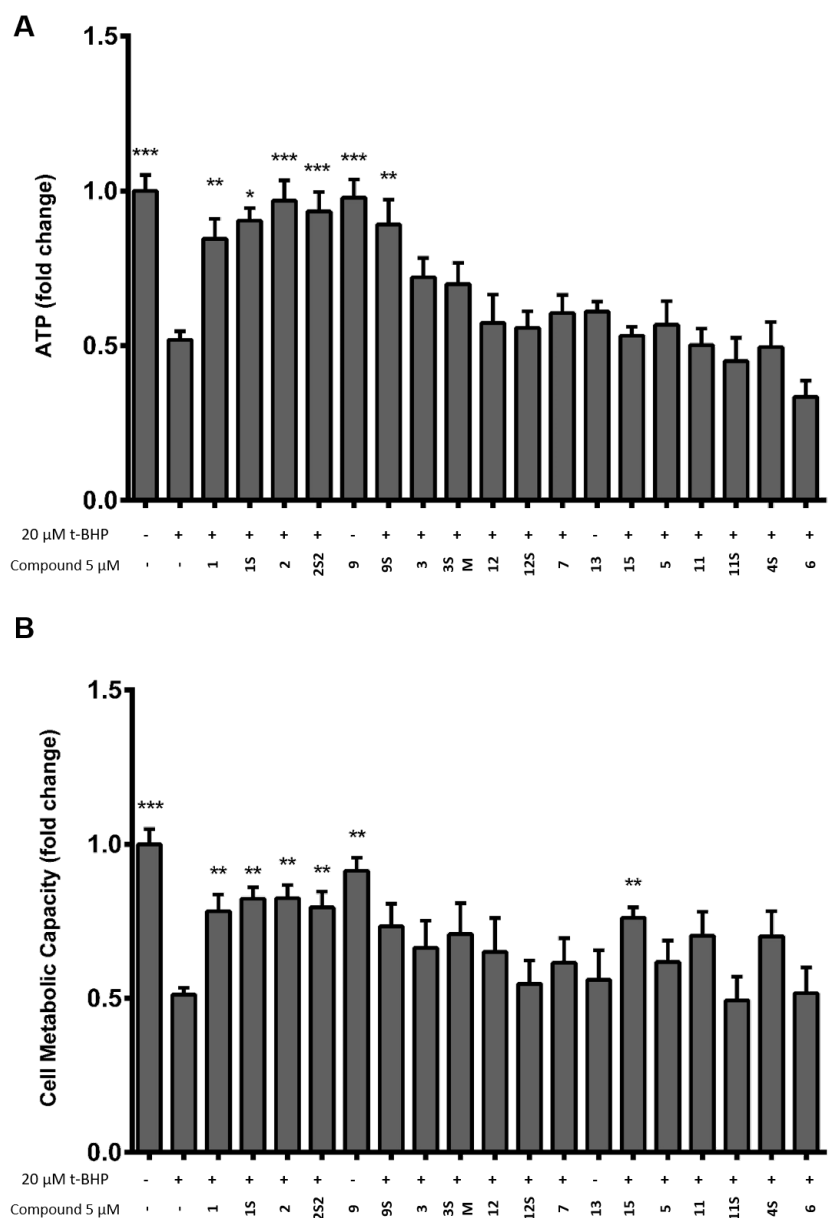


Figure D.1: The toxic effects of eighteen compounds were evaluated in SH-SY5Y neurons using Celltiter Blue (**B**) and celltiter Glo (**A**). Statistical differences are noted as *** p <0.001, ** p <0.01 and * p <0.05 relatively to t-BHP insult

E. Annex E - Evaluation of Neuronal Differentiation

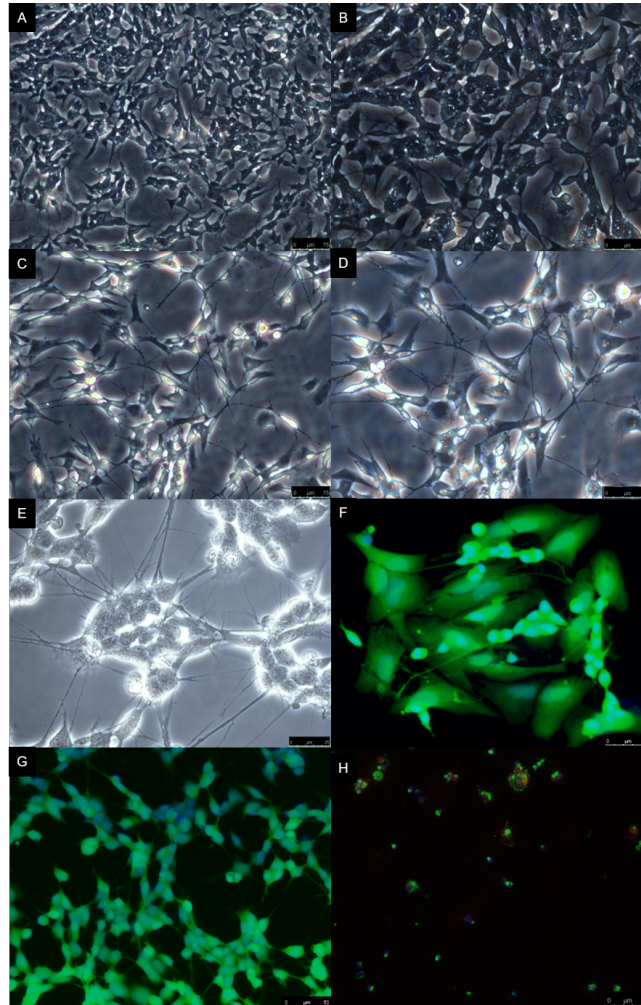


Figure E.1: Microscopy images of SH-SY5Y obtained in a Leica DM6 microscope. Cell morphology and neurite growth were visually inspected along the time of differentiation. **A,B** SH-SY5Y undifferentiated cells at the end of 7 days. **C,D** Differentiated cells at the end of 7 days with all-trans retinoic acid. **E** Live cell imaging of neurons at 7 days of differentiation, the image showed the formation of neuronal networks upon differentiation. **F, G, H** Morphology, neurite growth and viability were verified at the end of 7 days of differentiation using calceunurin, for cell viability, Hoechst 33258 for nucleus stain and propidium iodide for staining dead cells. **F** Live cell imaging of undifferentiated SH-SY5Y, the image showed the presence of epithelial-like population of SH-SY5Y cell line. **G** Differentiated cells showed the formation of long neurites with no signs of dead population. **H** Positive control for dead cells using 20 μ M t-BHP for 16h after cell differentiation.